SOME TRANSPORT PROPERTIES IN SIMPLE METALS

SOME TRANSPORT PROPERTIES

IN

SIMPLE METALS

By

BRUCE EDWARD HAYMAN, M.S.

A Thesis

Submitted to the School of Graduate Studies

in Partial Fulfilment of the Requirements

for the Degree

Doctor of Philosophy

McMaster University

November 1973

DOCTOR OF PHILOSOPHY (1973)
(Physics)

McMASTER UNIVERSITY
Hamilton, Ontario.

TITLE: Some Transport Properties in Simple Metals

AUTHOR: Bruce Edward Hayman, B.Sc. (Agra University)
M.S. (Oklahoma State University)

SUPERVISOR: Dr. J. P. Carbotte

NUMBER OF PAGES: vi, 167

SCOPE AND CONTENTS:

Working within the framework of the conventional first-order variational solutions to the Boltzmann transport equation, a variety of transport properties in the alkali metals (Na, K, Rb, Li) were studied. It was found that a consistent description, in terms of a simple model pseudo-potential and using a spherical Fermi surface, is possible. In particular, it was possible to explain the pressure variation of the ideal electrical resistivities over a wide temperature range and this includes the anomalous (relative to the other metals) behaviour of Li.

Utilizing a scattering time solution to the Boltzmann equation, detailed calculations of the effects of anisotropy in the electron-phonon interaction on the electrical resistivity were carried out. In particular, the temperature dependence of the anisotropy is treated in some detail. The results were also used to discuss the temperature variation of the low field Hall coefficient.

A simple device to eliminate the divergence of the electron-phonon coupling constant (as calculated in the one orthogonalized plane wave approximation) in polyvalent metals is discussed, and its use is

illustrated in the case of Al. The effects of this divergence on the resistivity are pointed out and some conclusions are drawn regarding the effects of anisotropy in polyvalent metals.

ACKNOWLEDGEMENTS

I wish to thank my research supervisor, Dr. J. P. Carbotte, for his patient and yet very enthusiastic guidance throughout this project.

I also wish to acknowledge many extremely useful and stimulating discussions with Dr. C. Leavens, Dr. P. Truant, Dr. F. Kus, Dr. D. Taylor, Dr. R. Bruno, Dr. P. N. Trofimenkoff, Dr. P. Vashishta, Mr. B. White and Mr. K. Leung.

I wish to acknowledge the financial assistance of the National Research Council of Canada and McMaster University.

Finally, I wish to express the greatest thanks and appreciation to my wife, Cheryl, without whom none of this would have been possible.

TABLE OF CONTENTS

CHAPTER I

INTRODUCTION

1.1 Historical Introduction

One of the most fundamental problems in Solid State Physics is to provide a theory which will account for the transport properties of simple metals. In particular, one would like to be able to obtain good agreement between available theory and experiment in dealing with the simplest transport property, the electrical conductivity, in the simplest of metals, the alkalis. The essential features of the problem were first clearly enunciated in the pioneering work of Bloch (1928). The next most important development was the calculation of Bardeen (1937). His was essentially a first principles calculation which was able to give a reasonably good quantitative description of the resistivity of sodium and other monovalent metals in the high temperature region. Due to a lack of detailed information at the time, he was forced to describe the lattice vibrations using the Debye theory and to assume a free electron like behaviour for the conduction electrons. This at once brings to mind the fact that the electrical conductivity, though an apparently simple property, depends in a complicated way on the details of the band structure and the phonon spectrum. A basic problem is to take both these structures into account in describing how the lattice vibrations scatter the conduction electrons. Bailyn (Bailyn 1960) was the first to attempt to include the details of the phonon spectrum in a

calculation of the transport properties of the alkali metals. He calculated the elastic constants and used these in a Born-von Kármán model to determine the phonon frequencies and polarization vectors. For the electronic structure Bailyn assumed a spherical Fermi surface (FS) and used the Bardeen (Bardeen 1937) matrix element to describe the electron-ion scattering. The most significant results of his very detailed and exhaustive calculation were (a) the presence of significant anisotropy in the phonon spectrum which is reflected in the electron-phonon interaction and (b) the crucial role of Umklapp processes even down to the very lowest temperatures. The next significant calculation of the transport properties of the alkalis is that of Collins and Ziman (1961). They employed a modified Debye spectrum for the phonons in which "longitudinal" and "transverse" modes were distinguished by different Debye temperatures θ_L and θ_T. The conduction electrons, however, were treated in some detail through the use of a "twelve cone" model for the FS which in essence assumes that the electron states can be described by a linear combination of two plane waves. Although they were able to obtain reasonably good quantitative agreement with experiment without manipulating too many parameters, they were unable to clearly distinguish between effects due to phonon anisotropy and FS anisotropy.

The advent of the use of neutron spectroscopy to measure in detail the phonon spectrum of metals ushered in a new and much more reliable method of obtaining information about that aspect of the problem. The dispersion curves in Na were first measured and analyzed in terms of a Born-von Kármán force constant fit by Woods et. al. (1962).

Using their published force constants, it immediately became possible to obtain a very accurate and reliable description of the phonons. Since then the same programme has been carried out in K (Cowley et. al. 1966), Rb (Copley 1970) and Li (Smith et. al. 1968). At about the same time the advantages of pseudo-potential theory in describing the electron-ion scattering, along with many other properties of the metallic state, were becoming clearer. This prompted a number of workers to once again undertake calculations of the transport properties of the alkalis, in particular, the electrical resistivity. The most significant calculation is that of Greene and Kohn (1965). While employing a Born-von Kármán description of the phonons using force constants obtained from neutron spectroscopy, they described the electron-ion scattering in terms of a fairly detailed phase shift analysis with the constraint that the phase shifts employed satisfied the Friedel sum rule. While obtaining reasonably good agreement at higher temperatures ($T > 200°K$) their calculations were in serious discrepancy with experiment at lower temperatures. They partially attributed their failure to their neglect of the effects of the change in lattice volume with temperature.

An important facet of the problem which emerged from the many pseudo-potential calculations of the electrical resistivity at this time was the extreme sensitivity of the magnitude of the resistivity to the size of the pseudo-potential form factors for momentum transfers of approximately $2k_f$ (see, for example, Heine 1970). Another noteworthy calculation was that of Hasegawa (1964). In addition to attempting to account for both the magnitude and temperature dependence

of the electrical resistivities in the alkalis, he made the first significant calculations of the effect of pressure on the resistivity. While able to account reasonably well for the behaviour of Na and K using a spherical FS, he found it necessary to resort to a distorted FS to explain the anomalous behaviour of Li under pressure. Also, his calculations of the pressure coefficient were confined to room temperature only. Dickey, Meyer, and Young (1967) performed an interesting calculation of the effect of pressure on the resistivities and thermopowers of the alkalis. Once again, the calculations were confined only to room temperature. A Debye-treatment of the phonons was used whereas the electron-ion interaction was treated in terms of pseudo-atom phase shifts. While the qualitative agreement with experiment was satisfactory the quantitative aspects left much to be desired. One of the major efforts in this thesis will be to account for the behaviour of the resistivities of the alkalis under pressure over a wide temperature range.

As most of the above calculations were concerned with interpreting the overall behaviour of the resistivity (or the other transport coefficients), and since uncertainties in the pseudo-potentials were still of some concern, the very simplest first order variational solutions of the Boltzmann equation were generally employed. By their very nature these solutions ignore the anisotropic nature of the electron-phonon scattering (Collins and Ziman 1961). That this anisotropy is important was pointed out by Bailyn (1960) and Collins and Ziman (1961) and was further emphasized by Deutsch, Paul, and Brooks (1961) (DPB). DPB were engaged in an experimental investigation of the pressure

dependence of the Hall coefficient in the alkali metals. The first significant attempt to calculate the anisotropy in the electron-phonon interaction, as it appears in a consideration of the electrical resistivity and the electron diffusion thermopower, is that of Robinson and Dow (1968)(RD). In view of the difficulty of incorporating anisotropy in a physically transparent way into variational solutions of the Boltzmann equation, RD employed an alternative approach which consisted of setting up a "scattering time" solution in which one obtains an expression for $\tau_{\underline{k}}$, a $\underline{k}$ dependent scattering time. The $\tau_{\underline{k}}$ can be evaluated for different points on the FS and can then be averaged to obtain a total resistivity. One rather interesting feature which RD demonstrated is the fact that the conventional first order variational solution to the Boltzmann equation leads to an expression for the electrical resistivity which amounts to a summing of partial resistivities (a partial resistivity is defined through the corresponding $\tau_{\underline{k}}$) whereas the averaging which they propose results in the much more physical summing of partial conductivities. While demonstrating the existence of significant anisotropy, the calculations of RD were (a) confined to room temperature, (b) carried out for $\underline{k}$ along the three high symmetry directions only and (c) compromised somewhat by the use of the Heine-Abarenkov (Heine and Abarenkov 1964)(HA) pseudo-potential which has since been shown to be clearly inadequate for the alkalis (Hayman and Carbotte 1971a).

In view of the above, it appeared worthwhile to embark on a project which would attempt to accomplish two main objectives:

(a) Working within the framework of the conventional first order variational solutions of the Boltzmann equation one would attempt to obtain a consistent picture of the various transport properties of the alkali metals. One would also attempt to retain the simplest possible description of the electron-ion scattering matrix elements by the use of a spherical FS and the simplest possible model pseudo-potential. In particular, one would like to see whether this rather basic scheme could provide a quantitatively accurate description of the pressure dependence of the ideal (phonon limited) electrical resistivities including the anomalous behaviour of lithium. As a distinct improvement on previous work in this particular area, the calculations would extend over a wide temperature range. In addition, one would hope that after an initial adjustment to obtain a given experimental resistivity (thus eliminating much of the uncertainty involved in the pseudo-potential), relatively sensitive properties such as the electron diffusion and phonon drag contributions to the thermopower could be adequately accounted for with no further change in parameters.

(b) Using a scattering time solution to the Boltzmann equation, one could attempt the first really detailed calculations of the effects of anisotropy in the electron-phonon interaction as it appears in considerations of the electrical resistivity. As a distinct improvement on previous work in this area, the calculations would be carried out over a wide temperature range and thus temperature effects which appear to have been somewhat neglected previously, could be looked at in some detail. Also the details of the anisotropy over the FS could be looked at much more extensively than had been attempted previously.

1.2 Outline Of The Thesis

The two main objectives of this thesis, as outlined in (a) and (b) above, are contained in Chapters II and III respectively.

The contents of Chapter II are as follows. In section 2.1, a broad outline of how the variational principle leads to a formula for the electrical resistivity is given. The conventional formula is recast in terms of a "transport frequency distribution" $\alpha_{tr}^2 F(\omega)$ and the advantages of this reformulation are discussed. The various approximations implicit in the derivation of the formula and in its evaluation are enumerated. Section 2.2 deals with the calculation of the function $\alpha_{tr}^2 F(\omega)$. The Born-von Kármán method for the calculation of the phonons and the pseudo-potential concept for the electron-ion scattering are considered. Also the method employed to calculate changes in the $\alpha_{tr}^2 F(\omega)$ function (and hence the resistivity) with volume is described. In section 2.3 we present the results of our calculations of the constant volume and constant pressure resistivities as a function of temperature. The anomalous behaviour of lithium is discussed and our results are compared with experiment. In section 2.4 the conventional first order variational expression for the ideal thermal resistivity is rearranged in terms of the functions $\alpha_{tr}^2 F(\omega)$ and $\alpha^2 F(\omega)$. The latter function is, of course, rather well known, occurring in the theory of superconductivity. In this section, we later present results in comparison with experiment for the ideal thermal resistivity as a function of temperature. The calculations are carried out using the same potentials as employed in the electrical resistivity. In section 2.5 we turn to the thermopowers and present results for both the electron

diffusion and phonon drag contributions to this quantity. Once again, the calculations use the same potentials as used previously. In the case of the phonon drag contribution the conventional formulae are re-written in terms of two more particular "transport frequency distributions". In section 2.6 the very low temperature behaviour of the ideal electrical and thermal resistivities are considered. The effect of phonon drag on the low temperature electrical resistivity is evaluated.

Chapter III is concerned with the effects of anisotropy in the electron-phonon interaction as it appears in considerations of the electrical resistivity and associated effects. In section 3.1 a scattering time solution to the Boltzmann equation is obtained and is formulated in terms of a directional "transport frequency distribution" $\alpha^2_{tr} F_{\underline{k}}(\omega)$. The calculation of the functions $\alpha^2_{tr} F_{\underline{k}}(\omega)$ is discussed. Section 3.2 deals with the anisotropy in the scattering times $\tau_{\underline{k}}$ over the FS. The reasons for the anisotropy are discussed and results for the variation of the scattering times over the FS, at various temperatures, are presented. The role of the pseudo-potential in determining the degree of anisotropy is also illustrated. In section 3.3 we discuss one of the more striking effects of the anisotropy namely the temperature variation of the low field Hall coefficient and the results of our calculations are compared with experiment. Section 3.4 deals with the effects of anisotropy on the electrical resistivity. The resistivities obtained in the two different solutions of the Boltzmann equation are compared and the particular role of the pseudo-potential is discussed.

Chapter IV contains a short discussion of the results of a calculation which, though strictly not part of the main body of this thesis, is interesting in its own right. We look at the failure of the one orthogonalized plane wave (OPW) approximation in calculating electron-phonon effects in systems where the FS intersects zone boundaries, and we also consider a simple device to overcome this difficulty. The calculations are all performed in Al. Section 4.1 deals with the reasons for the failure of the one OPW approximation and describes the device which is used to correct it. In section 4.2 we illustrate the effects of the failure and its correction. In section 4.3 we discuss the results of our calculations and draw conclusions regarding the dangers of using the one OPW approximation especially in calculations of the low temperature resistivity. We also discuss the fact that when a reasonably correct approach is used in dealing with the one OPW problem in polyvalent metals, the behaviours observed are essentially the same as that in the alkalis.

CHAPTER II

TRANSPORT PROPERTIES IN SOME ALKALIS USING THE STANDARD VARIATIONAL SOLUTIONS TO THE BOLTZMANN EQUATION

2.1 The Formula For The Phonon Limited Resistivity

The simplest approach to the problem of calculating the resistivity of a metal is the Kinetic Method (Ziman 1960). One assumes that the conduction electrons can be treated as independent particles and that the motion of each electron can be monitored separately. Another basic assumption of this method is to assume that the motion of the electrons can be described by a characteristic isotropic relaxation time τ. τ is, of course, the average time spent undergoing acceleration by the applied field before the electron is scattered via a phonon or an impurity or a defect etc. The expression for the electrical conductivity σ obtained is

$$\sigma = \frac{ne^2\tau}{m} \qquad (2.1.1)$$

where n is the number of electrons per unit volume, e is the electronic charge, and m is the free electron mass. If one prefers to think in terms of a mean free path Λ where

$$\Lambda = \tau \bar{v} \qquad (2.1.2)$$

and $\bar{v}$ is the average speed of the electrons one obtains

$$\sigma = \frac{ne^2\Lambda}{m\bar{v}} \qquad (2.1.3)$$

Now since in any real metal we are dealing with electrons governed by the Fermi distribution, it is obvious that only those electrons near the Fermi surface (FS) can be accelerated and hence scattered. Consequently in (2.1.3) we will have to use $\bar{v} = v_f$ and a Λ evaluated for electrons on this surface.

A more rigorous approach is to describe the electrons from a statistical point of view through a distribution function $f_{\underline{k}}(\underline{r})$. This function measures the probability of finding an electron in the $\underline{k}^{th}$ state at $\underline{r}$. One then looks at the change in this function due to the application of external fields etc. This approach was first used by Boltzmann and a detailed treatment is given by Ziman (Ziman 1960). In the ensuing short description of how this approach leads to a formula for the phonon-limited resistivity we will follow Ziman (Ziman 1960) closely.

If the only external field being applied to the specimen is an electric field $\underline{E}$, as would be the case in a measurement of the resistivity and there are no thermal gradients, the rate of change of $f_{\underline{k}}$ can be written as

$$\dot{f}_{\underline{k}} = \dot{f}_{\underline{k}}\Big|_{field} + \dot{f}_{\underline{k}}\Big|_{scatt.} \qquad (2.1.4)$$

where $\dot{f}_{\underline{k}}|_{scatt.}$ is the rate of change due to interactions between the electrons and the phonons (we exclude interactions with defects, impuri-

ties etc. as we are only interested in the phonon-limited resistivity), and $\dot{f}_{\underline{k}}|_{field}$ is self-explanatory. In a steady state situation $\dot{f}_{\underline{k}}$ is zero and for electrons with momentum $\hbar\underline{k}$ we obtain

$$\frac{e}{\hbar}\underline{E}\cdot\frac{\partial f_{\underline{K}}}{\partial \underline{K}} = \dot{f}_{\underline{K}}|_{scatt.} \qquad (2.1.5)$$

Here e is the electron charge and $\hbar$ is Planck's constant. This is the basic Boltzmann equation for the case of an applied electric field and no thermal gradients. If one could obtain $f_{\underline{k}}$ from (2.1.5) the current density $\underline{J}$ would be given by

$$\underline{J} = \sum_{\underline{K}} e\underline{v}_{\underline{K}} f_{\underline{K}} \qquad (2.1.6)$$

where $\underline{v}_{\underline{k}}$ is the velocity of the $\underline{k}^{th}$ state, and the conductivity (resistivity) could be obtained via

$$\underline{J} = \underset{\sim}{\sigma}\,\underline{E} \qquad (2.1.7)$$

$\underset{\sim}{\sigma}$ is the conductivity tensor, which for a cubic system is a scalar.

However, the situation is not straightforward as is obvious if one looks at the scattering term in (2.1.5). It will contain a sum over $\underline{k}$ through the rate at which other states scatter into $\underline{k}$ and will, therefore, contain $f_{\underline{k}}$ itself. One, therefore, has an integro-differential equation of a complicated kind. The standard technique is to "linearize" the equation (Ziman 1960) by writing $f^{\circ}_{\underline{k}}$, the equilibrium distribution (in our case $f^{\circ}_{\underline{k}}$ is the familiar Fermi distribution) for $f_{\underline{k}}$ on the left hand side of (2.1.5) and writing $f_{\underline{k}}$ as

$$f_{\underline{K}} = f^{\circ}_{\underline{K}} - \phi_{\underline{K}}\frac{\partial f^{\circ}_{\underline{K}}}{\partial \varepsilon_{\underline{K}}} \qquad (2.1.8)$$

on the right hand side of (2.1.5). $\Phi_{\underline{k}}$ measures the deviation from equilibrium (presumed small) and $\varepsilon_{\underline{k}}$ is the energy of the $\underline{k}^{th}$ state. However, before doing this, one re-writes $\dot{f}_{\underline{k}}|_{scatt.}$ in (2.1.5) as

$$\dot{f}_{\underline{k}}|_{scatt.} = \sum_{\underline{k}'} \left\{ f_{\underline{k}'}(1-f_{\underline{k}}) - f_{\underline{k}}(1-f_{\underline{k}'}) \right\} P_{\underline{k}}^{\underline{k}'} \qquad (2.1.9)$$

The two factors, of course, measure the inflow and outflow with respect to the state $\underline{k}$ and $P_{\underline{k}}^{\underline{k}'}$ is the transition rate and measures the actual number of transitions per unit time with the system in equilibrium.

Now "linearizing" as indicated above and using (2.1.9) in (2.1.5) and with the assumption that $\dot{f}^{\circ}_{\underline{k}} = \dot{f}^{\circ}_{\underline{k}'}$ (since an average phonon energy is very much smaller than the Fermi energy this is essentially true) we obtain the "linearized Boltzmann equation"

$$e\underline{v}_{\underline{k}} \cdot \underline{E} \frac{\partial f^{\circ}_{\underline{k}}}{\partial \varepsilon_{\underline{k}}} = \beta \sum_{\underline{k}'} (\Phi_{\underline{k}'} - \Phi_{\underline{k}}) P_{\underline{k}}^{\underline{k}'} \qquad (2.1.10)$$

with $\beta = (k_B T)^{-1}$. In deriving (2.1.10) we have also made use of

$$\frac{\partial f^{\circ}_{\underline{k}}}{\partial \varepsilon_{\underline{k}}} = -\beta f^{\circ}_{\underline{k}} (1 - f^{\circ}_{\underline{k}}) \qquad (2.1.11)$$

and

$$\frac{\partial f^{\circ}_{\underline{k}}}{\partial_{\underline{k}}} = \frac{\partial f^{\circ}_{\underline{k}}}{\partial \varepsilon_{\underline{k}}} \cdot \hbar \underline{v}_{\underline{k}} \qquad (2.1.12)$$

At this point we also take note of another important assumption implicit in (2.1.9) and, therefore, in (2.1.10) which is that the phonon distribution is assumed to be in equilibrium. The effects of this will be

considered in section 2.6 of this chapter. In order to assuage doubts about the validity of the linearization process, Ziman (Ziman 1960) points out that this linearized equation (2.1.10) leads to a linear macroscopic transport equation and since this is what is almost invariably observed in practice one has reasonable confidence in it.

In order to derive an expression for the resistivity ρ the variational principle is now invoked and one obtains (Ziman 1960; Kohler 1949)

$$\rho(T) = \frac{\frac{1}{2k_B T} \sum_{\underline{k}} \sum_{\underline{k}'} \left\{ \Phi_{\underline{k}} - \Phi_{\underline{k}'} \right\}^2 P_{\underline{k}}^{\underline{k}'}}{\left| \sum_{\underline{k}} e \underline{v}_{\underline{k}} \Phi_{\underline{k}} \frac{\partial f_{\underline{k}}^{\circ}}{\partial \varepsilon_{\underline{k}}} \right|^2} \qquad (2.1.13)$$

where one notes that the exact solution $\Phi_{\underline{k}}$ to (2.1.10) will minimize (2.1.13) and we are guaranteed that all other trial solutions for $\Phi_{\underline{k}}$ will give a resistivity greater than the true resistivity. Since the exact solution to (2.1.10) is unknown, the standard procedure (Ziman 1960; Kohler 1949; Sondheimer 1950) is to substitute a trial function which is a linear expansion of known functions and then to minimize the resistivity through the coefficients in the expansion.

Before considering this we will now introduce the details of the electron-phonon interaction into (2.1.13) following the procedure outlined by Greene and Kohn (1965) (GK) . We once again note that we are only considering electron-phonon scattering processes and no others.

Using time dependent perturbation theory GK write $P_{\underline{k}}^{\underline{k}'}$ as

$$P_{\underline{k}}^{\underline{k}'} = \frac{2\pi}{\hbar} \left| M_{\underline{k}}^{\underline{k}'} \right|^2 f_{\underline{k}}^{\circ} \left(1 - f_{\underline{k}'}^{\circ}\right) \delta\left(\varepsilon_{\underline{k}} - \varepsilon_{\underline{k}'} + \hbar\omega\right) \qquad (2.1.14)$$

$M_{\underline{k}}^{\underline{k}'}$ is the matrix element for the transition $\underline{k} - \underline{k}'$ and ω is the energy of the phonon involved.

Following Van Hove (Van Hove 1954) in the weak scattering or Born approximation limit (we will discuss the validity of this in section 2.2) GK write $P_{\underline{k}}^{\underline{k}'}$ as

$$P_{\underline{k}}^{\underline{k}'} = \frac{2\pi}{\hbar} \left| W(\underline{q}) \right|^2 f_{\underline{k}}^{\circ} (1 - f_{\underline{k}'}^{\circ}) S(\underline{q}, \omega) \qquad (2.1.15)$$

where $\underline{q} = \underline{k}' - \underline{k}$ is the momentum transfer, $W(\underline{q})$ is the scattering amplitude and is essentially $\langle \underline{k}+\underline{q} | W_{ion} | \underline{k} \rangle$ where W_{ion} is the rigid potential (it is assumed to be carried along with the ion as it vibrates) due to a single ion, and $S(\underline{q},\omega)$ is the dynamical structure factor which contains all the dynamics of the ion system.

The advantage of Van Hove's formulation is this separation of $P_{\underline{k}}^{\underline{k}'}$ into two parts one of which depends only on the scattering amplitude for a single ion and the other containing the dynamics of the vibrating system. Van Hove's original considerations were with regard to neutrons scattering off a crystal; however, as pointed out by Baym (Baym 1964) the basic idea is just as valid in the case of electron-ion scattering.

After some considerable mathematical manipulations which include substituting (2.1.15) into (2.1.13), transforming the sums in (2.1.13) to volume integrals, introducing double surface integrals over a spherical FS, and then further re-transforming back to a volume integral and a line integral GK obtain for the resistivity ρ

$$\rho(T)=\frac{(\hbar^2 32\pi^5 v_f^2)^{-1}\int_{q<2k_f}\frac{d^3q}{q}\left[\Phi_{\underline{k}}-\Phi_{\underline{k}'}\right]^2|W(\underline{q})|^2 S(\underline{q})}{\left[\frac{1}{4\pi^3}\int e\underline{v}_{\underline{k}}\,\Phi_{\underline{k}}\frac{\partial f_{\underline{k}}}{\partial\epsilon_{\underline{k}}}\,d^3\underline{k}\right]^2} \qquad .....(2.1.16)$$

where

$$S(\underline{q})=\frac{\hbar}{k_B T}\int_0^\infty d\omega\, S(\underline{q},\omega)\frac{\omega}{1-e^{-\beta\omega}} \qquad (2.1.17)$$

For $\Phi_{\underline{k}}$ GK now use the standard (Ziman 1960; Kohler 1949) function

$$\Phi_{\underline{k}} \propto \underline{k}\cdot\underline{u} \qquad (2.1.18)$$

($\underline{u}$ is a unit vector in the direction of the electric field $\underline{E}$), and use the one-phonon approximation (only contributions of second order in the ionic displacements are considered) for $S(\underline{q})$ to obtain finally

$$\rho(T)=\frac{3\pi\Omega_0}{16Me^2v_f^2k_f^4}\int d^3q\, q|W(\underline{q})|^2\sum_\lambda\frac{(\epsilon_{\underline{q}\lambda}\cdot\underline{q})^2/k_BT}{(e^{\beta\omega_{\underline{q}\lambda}}-1)(1-e^{-\beta\omega_{\underline{q}\lambda}})} \qquad .....(2.1.19)$$

Here Ω_0 is the volume per ion. We note also that cubic symmetry has been used to average $\underline{q}\cdot\underline{u}$ as $\frac{1}{3}q^2$ in (2.1.19). For details of the one-phonon approximation to $S(\underline{q})$ the reader is referred to the work of Dynes and Carbotte (1968). In (2.1.9) M is the ionic mass.

In this work we will only be considering the resistivity as given by (2.1.19) and, therefore, involving (2.1.18). However, GK indicate that if one wishes to try a more complex trial function $\Phi_{\underline{k}}$ can be written as a linear combination of known functions and ρ can be minimized with respect to the coefficients.

Since (2.1.19) is the expression that we will eventually evaluate to obtain ρ let us summarize below the most important approximations inplicit in its derivation.

(a) The simplest trial function $\Phi_{\underline{k}} \alpha \underline{k} \cdot \underline{u}$ is used for the solution of the Boltzmann equation.

(b) The phonons are assumed to be in their equilibrium distribution.

(c) The Fermi surface is assumed spherical.

(d) The electron-phonon interaction is treated in the weak scattering limit where electrons in plane wave states scatter off a weak ionic potential (an ionic pseudo-potential as it turns out).

(e) The scattering amplitude $W(\underline{q})$ is assumed to depend only on $\underline{q}$ and not on $\underline{k}$ and $\underline{k}'$.

(f) The ionic system is treated in the one-phonon approximation which means that since only second order terms in the ionic displacements are considered, Debye-Waller factor and other multi-phonon terms are neglected. (However, GK point out that a cancellation effect between the Debye-Waller factor and the other higher order terms occurs and thus this approximation is probably quite good.)

If these approximations can be used with any validity at all, it is unquestionably true that the alkali metals would be the best system. In particular one notes that the assumption of a spherical FS and a description of the electron states as single plane waves are most applicable to these metals.

The standard procedure (Greene and Kohn 1965; Ziman 1961; Ostrom 1965; Animalu 1965; Ashcroft and Guild 1965; Ashcroft and

Lekner 1966; Ashcroft and Langreth 1967; Dynes and Carbotte 1968; Kaveh and Wiser 1972a; Bross and Holz 1963; Ziman 1964a) in most calculations of the resistivity of solid or liquid metals is to use a form of (2.1.19) which can be written as

$$\rho(T) = C \int_{<2k_f} d^3q\, q \left|W(q)\right|^2 \langle S(q)\rangle_{av} \qquad (2.1.20)$$

where C is the appropriate constant and $\langle S(q)\rangle_{av}$ is given by

$$\langle S(\underline{q})\rangle_{av} = \int \frac{d\Omega_q}{4\pi} S(\underline{q}) \qquad (2.1.21)$$

and is the angular average of

$$S(\underline{q}) = \frac{\hbar}{MNk_BT} \sum_{\lambda} \frac{(\epsilon_{q\lambda}\cdot \underline{q})^2}{(e^{\beta\omega_{\underline{q}\lambda}}-1)(1-e^{-\beta\omega_{\underline{q}\lambda}})} \qquad (2.1.22)$$

In order to calculate the resistivity at various temperatures, it is, then, obvious that $\langle S(q)\rangle_{av}$ has to be calculated at each temperature and the overlap integral (2.1.20) performed to obtain $\rho(T)$. To avoid this recalculation at each temperature we will reformulate the resistivity in terms of a "transport frequency distribution" and once this function is obtained the resistivity at any temperature can be obtained trivially (Hayman and Carbotte 1971a).

The procedure is quite simple and goes as follows. One introduces a fictitious integration over all frequencies ω and rewrites (2.1.19) thus

$$\rho(T) = C' \int_0^\infty d\omega \sum_{\lambda} \int_{<2k_f} \frac{d^3q\, q \left|W(\underline{q})\right|^2 \beta \left|\underline{q}\cdot\underline{\epsilon}_{q\lambda}\right|^2}{(e^{\beta\omega_{\underline{q}\lambda}}-1)(1-e^{-\beta\omega_{\underline{q}\lambda}})} \delta(\omega-\omega_{\underline{q}\lambda}) \qquad (2.1.23)$$

However, now using the fact that the δ-function on the right hand side of (2.1.23) operates only when $\omega = \omega_{\underline{q}\lambda}$ we can rewrite (2.1.23) as

$$\rho(T) = C' \int_0^\infty \frac{\beta\omega \, d\omega}{(e^{\beta\omega}-1)(1-e^{-\beta\omega})} \sum_\lambda \int_{<2k_f} d^3q \, q \, \frac{|W(\underline{q})|^2 |\underline{q}\cdot\underline{\varepsilon}_{\underline{q}\lambda}|^2}{\omega_{\underline{q}\lambda}} \delta(\omega-\omega_{\underline{q}\lambda}) \quad (2.1.24)$$

which further reduces to

$$\rho(T) = C'' \int_0^\infty \frac{\beta\omega \, d\omega}{(e^{\beta\omega}-1)(1-e^{-\beta\omega})} \cdot \alpha_{tr}^2 F(\omega) \quad (2.1.25)$$

where

$$C'' = \frac{12\pi^3}{e^2 v_f k_f^2}, \quad \beta = \frac{1}{k_B T}, \text{ and } \alpha_{tr}^2 F(\omega)$$

is given by

$$\alpha_{tr}^2 F(\omega) = \frac{1}{N} \sum_\lambda \int_{<2k_f} \frac{d^3q}{(2\pi)^3} \left[\frac{q|\underline{q}\cdot\underline{\varepsilon}_{\underline{q}\lambda}|^2 |W(\underline{q})|^2}{\omega_{\underline{q}\lambda}} \cdot \frac{m}{8Mk_f^3} \right] \delta(\omega-\omega_{\underline{q}\lambda}) \quad (2.1.26)$$

The calculation of ρ(T) is thus reduced to a calculation of the function $\alpha_{tr}^2 F(\omega)$. We have written $\alpha_{tr}^2 F(\omega)$ in the form (2.1.26) in order to show its close connection with the $\alpha^2 F(\omega)$ function which occurs in superconductivity and also to make it dimensionless. When this work was first published (Hayman and Carbotte 1971a) instead of using $\alpha_{tr}^2 F(\omega)$ as written in (2.1.26) a function $\overline{\alpha^2 F(\omega)}$ was used instead, and one notes that $\overline{\alpha^2 F(\omega)}$ and $\alpha_{tr}^2 F(\omega)$ are identical to within a constant and a frequency factor. However, $\alpha_{tr}^2 F(\omega)$ has the advantage of being dimensionless. The expression for $\alpha^2 F(\omega)$ is given below

$$\alpha^2 F(\omega) = \frac{1}{N} \sum_\lambda \int_{q<2k_f} \frac{d^3q}{(2\pi)^3} \left[\frac{|\underline{q}\cdot\underline{\varepsilon}_{\underline{q}\lambda}|^2 |W(\underline{q})|^2}{q\omega_{\underline{q}\lambda}} \cdot \frac{m}{4Mk_f} \right] \delta(\omega-\omega_{\underline{q}\lambda}) \quad \ldots\ldots (2.1.27)$$

and we note that $\alpha^2_{tr}F(\omega)$ is identical to $\alpha^2F(\omega)$ except the integral contains an extra factor of $\frac{q^2}{2k_f^2}$ which is merely the extra $1 - \cos(\theta)$ term which occurs in electron scattering as it appears in transport theory (Ziman 1960). θ is, of course, the angle between $\underline{k}$ and $\underline{k}'$, the initial and final states.

The important point to note here is that the resistivity as given by (2.1.25) can now be calculated at any temperature T (for a fixed lattice volume) once $\alpha^2_{tr}F(\omega)$ is known, and that all details of phonon frequencies, polarization vectors, and pseudo-potential form factors are included in $\alpha^2_{tr}F(\omega)$ — the temperature dependence is fully taken care of in the frequency integration. However, if one wishes to calculate a resistivity at a different lattice volume, a new $\alpha^2_{tr}F(\omega)$ will have to be obtained. How this is done will be discussed later.

To conclude this section then we note that to calculate $\rho(T)$ we need the function $\alpha^2_{tr}F(\omega)$ and in order to obtain $\alpha^2_{tr}F(\omega)$ we need:

(a) A description of the phonons (phonon frequencies and polarization vectors).

(b) A description of the electron-ion scattering amplitudes.

In the next section we will discuss how (a) and (b) are obtained and how, using them, the $\alpha^2_{tr}F(\omega)$ function is calculated.

2.2 Calculation Of The Function $\alpha^2_{tr}F(\omega)$

As noted in the last section, to calculate $\alpha^2_{tr}F(\omega)$ and thus the resistivity, one needs a description of (a) the phonons and (b) the electron-ion scattering amplitudes. We obtain these as follows.

The phonon polarization vectors and frequencies are taken from Born-von Kármán force constant models for the lattice vibrations. Briefly what occurs is the phonon dispersion curves (usually in high symmetry directions) are measured experimentally, using the techniques of inelastic neutron scattering, and are then fitted, using a least squares fit, by a force constant model for the lattice vibrations. In these models one assumes that the ions are attached to each other via a system of springs and that the inter-ionic forces extend out to a specified number of nearest neighbour shells. Beyond a certain distance the forces are assumed to be zero. Once the inter-ionic force constants are obtained by fitting the ω vs. q curves in the symmetry directions the polarization vectors and frequencies for a point anywhere in the Brillouin zone can be determined by diagonalizing the appropriate dynamical matrix. Specifically, one writes

$$\omega_{\underline{q}\lambda}^2 \epsilon_{\underline{q}\lambda} = \sum_{\beta} D_{\alpha\beta}(\underline{q}) \epsilon_{\beta \underline{q}\lambda} \qquad (2.2.1)$$

where $\omega_{\underline{q}\lambda}$ and $\epsilon_{\underline{q}\lambda}$ are the frequency and polarization vector of the phonon with branch index λ and wave vector q, and the dynamical matrix $D_{\alpha\beta}(q)$ is given by

$$D_{\alpha\beta}(\underline{q}) = \frac{1}{M} \sum_{m} e^{-i \underline{q} \cdot \underline{R}_m^{\circ}} \Phi_{\alpha\beta m} \qquad (2.2.2)$$

where M is the ionic mass, $\underline{R}_m^{\circ}$ is the equilibrium position of the m^{th} ion relative to the ion at the origin, and $\Phi_{\alpha\beta m}$ is the force on the ion at the origin in the α direction due to a unit displacement of the m^{th} ion in the β direction. α and β represent the x, y and z directions. $\Phi_{\alpha\beta m}$ are the force-constants which are obtained from the fit to the experimentally determined dispersion curves. Thus to determine $\omega_{\underline{q}\lambda}$

and $\epsilon_{q\lambda}$ all that is necessary is to diagonalize $D_{\alpha\beta}(q)$. The dispersion curves in the alkali metals have been measured and fitted with the appropriate force constants by the following workers. In sodium at 90°K by Woods, Brockhouse, March, Stewart and Bowers (1962), in potassium at 9°K by Cowley, Woods and Dolling (1966), in rubidium at 120°K by Copley (1970), and in lithium at 98°K by Smith et. al. (1968).

The other ingredient necessary for a calculation of the resistivity is the electron-ion scattering amplitudes. These we take from pseudo-potential theory. Pseudo-potential theory and its application to metals is discussed in great detail by Harrison (1966), and Heine (1970). Briefly what it states, in the context of our work, is that in a simple metal the electron states can be separated into two distinct groups — core states and conduction band states. The former are localized around an ion, the latter are non-local. The effect of the Pauli exclusion principle on the conduction band states is to state that they must be orthogonal to the core states and in the pseudo-potential method one describes this orthogonalization by introducing a repulsive term into the potential seen by the conduction electrons. So, in addition to the strong attractive ionic potential, the electrons experience this repulsive term and the net potential is a weak one. This is quite important as it allows one to treat the electron-ion scattering in perturbation theory and this is one of the major assumptions made in section 2.1 where we outlined how the resistivity formula we use is obtained. The conduction electrons are then assumed to be in plane wave states and scatter off a weak ionic pseudo-potential. In general

one considers the electron states as expansions in terms of plane waves. However, for the alkali metals we will consider only one plane wave to be sufficient and thus our calculations are done in the one OPW (orthogonalized plane wave) approximation as opposed to a multiple OPW approximation.

For the actual pseudo-potential form factors (electron-ion scattering amplitudes) one can take these from empirical calculations which tabulate the $W(q)$ for values of q from 0 to $2k_f$ and beyond (Harrison 1966; Shaw and Pynn 1969; Appapillai and Williams 1973) or one may assume a model parametrized potential such as the Ashcroft (1966) form. We choose the latter for its simplicity and, more importantly, it is easily corrected for volume changes. Also, the extreme sensitivity of the resistivity to the value of the form factors around $2k_f$ (Heine 1970) prompts us to use a potential that can be easily fitted to a given resistivity so that other effects can be looked at with some degree of confidence.

The Ashcroft model potential is obtained in real space as follows

$$V(r) = 0 \qquad r \leq R_c$$
$$V(r) = \frac{Ze^2}{r} \qquad r > R_c \tag{2.2.3}$$

Inside a "core radius" R_c the orthogonalization terms cancel the ionic potential and beyond R_c the potential is Coulombic. Z is the ionic charge. The value of R_c is then a parameter to be obtained from experiment or, as in our case, by fitting to a particular physical property.

This potential leads to a bare form factor for the isolated ion of the form

$$W^{\circ}(q) = \frac{4\pi e^2}{q^2} \cos(q R_c) \cdot \frac{1}{\Omega_o} \qquad (2.2.4)$$

However, inside the metal, the conduction electrons screen $W^{\circ}(q)$ and the effective form factor $W(q)$ is then

$$W(q) = \frac{W^{\circ}(q)}{\varepsilon(q)} \qquad (2.2.5)$$

where $\varepsilon(q)$ is the dielectric function. Various fairly sophisticated forms for $\varepsilon(q)$ are available (Price, Singwi, and Tosi 1970); however, we choose to use the familiar Lindhard expression for $\varepsilon(q)$ since variations of R_c will produce a much stronger effect on the shape of $W(q)$ than variations in any parameters in $\varepsilon(q)$ and that should be quite sufficient for our purposes. Consequently we write $\varepsilon(q)$ as

$$\varepsilon(q) = 1 + \frac{K_f e^2}{q^2 \pi} \left\{ 1 + \frac{1}{q K_f} \cdot \left[K_f^2 - \frac{q^2}{4} \right] \ln \left| \frac{q + 2K_f}{q - 2K_f} \right| \right\} \qquad .....(2.2.6)$$

We turn now to the actual calculation of the function $\alpha^2_{tr}F(\omega)$. We start by noting the standard expression for the phonon density of states $F(\omega)$. $F(\omega)$ is written as

$$F(\omega) = \frac{1}{N} \sum_{\lambda} \int_{FBZ} \frac{d^3q}{(2\pi)^3} \delta(\omega - \omega_{q\lambda}) \qquad (2.2.7)$$

FBZ indicates that the integration is carried out over the First Brillouin Zone (FBZ).

Gilat and Raubenheimer (1966) (GR) have developed sophisticated computer techniques for calculating $F(\omega)$ from force constant fits to

dispersion curves. Their method consists essentially of dividing up reciprocal space into a dense set of cubes and then diagonalizing the dynamical matrix for the $\underline{q}$ value at the centre of the cube to obtain the appropriate frequencies. $F(\omega)$ is then built up by adding to the appropriate frequency bin a factor proportional to the volume of the original cube. Points on boundaries or corners of the zone are weighted accordingly. Cubic symmetry is used insomuch that the operations are only performed over the irreducible $1/48^{th}$ of the FBZ. One notes that the GR method for calculating $F(\omega)$ is accurate enough that Van Hove singularities are clearly resolved and in addition special care is taken to ensure that the distributions obtained are particularly accurate near the origin.

The GR method was adapted by Carbotte and Dynes (1968) to calculate the function $\alpha^2F(\omega)$. The calculation of $\alpha^2_{tr}F(\omega)$ proceeds in much the same way as for $\alpha^2F(\omega)$ and briefly what is done is (a) the integration in (2.2.7) is extended to a sphere of radius $2k_f$, and (b) each $\underline{q}$ point is further weighted according to the factor $L_{\underline{q}\lambda}$ given by

$$L_{\underline{q}\lambda} = \frac{q\,|\underline{q}\cdot\underline{\epsilon}_{\underline{q}\lambda}|^2\,|W(\underline{q})|^2}{\omega_{\underline{q}\lambda}} \cdot \frac{m}{8Mk_f^3} \qquad (2.2.8)$$

In extending the integration out to $2k_f$ a great saving in computational time is achieved by mapping out the $1/48^{th}$ into the solid cone subtended by it, using appropriate reciprocal lattice vectors. Thus, diagonalizations etc. are confined only to the irreducible $1/48^{th}$. Also, one takes note of one important fact. The computations properly include all Umklapp processes that occur in a calculation of the resis-

tivity, (or in $\alpha^2F(\omega)$) this occurs in the mapping out process mentioned above. For a more detailed description of the techniques involved the reader is referred to the work of Dynes (1968) and Carbotte, Dynes and Trofimenkoff (1969).

Since we will be calculating resistivities as a function of volume, it would be appropriate here to describe how we intend to incorporate volume changes into the calculation of $\alpha^2_{tr}F(\omega)$. The changes in the phonon frequencies are introduced using the Grüneisen constant γ which is defined as follows

$$\frac{d\ln\omega}{d\ln V} = -\gamma \qquad (2.2.9)$$

In general γ is mode and q dependent; however, we will assume that it is important to include the average shift with volume and that deviations from this average are of secondary importance. We will take this average γ from experiment. Using (2.2.9) we can write the phonon frequency $\omega(V)$ as a function of volume V as follows

$$\omega(V) = \omega(V_0)\left[1-\left(\frac{V-V_0}{V_0}\right)\gamma\right] \qquad (2.2.10)$$

where V_0 is a reference volume, which will turn out to be the lattice volume at which the phonons are measured. We note here that this procedure includes volume changes due to temperature and/or pressure changes.

The changes in the form factors — given by (2.2.4), (2.2.5), and (2.2.6) — will be considered only insomuch that the values of k_f and Ω_0 change in those expressions. We will assume that R_c, once fixed, is an intrinsic property of the ion-core and is independent of its immediate surroundings and does not change with volume. The two effects

of a volume change (other than the direct scaling through Ω_0) are (a) to alter the screening through an altered k_f and (b) to change the position of the first node in the potential, through $\cos(qR_c)$ (in the form factors q is measured in units of $2k_f$). This second effect is quite important as it alters the Umklapp contribution to the resistivity in a significant way.

To recalculate the resistivity at a new lattice volume would appear to necessitate a detailed recalculation of $\alpha_{tr}^2 F(\omega)$ at the new volume, properly including the changes in phonon frequencies and form factors in (2.1.26). However, a simple scaling technique, which we describe below, enables us to derive the new $\alpha_{tr}^2 F_V(\omega)$ (at volume V) from an original $\alpha_{tr}^2 F_{V_0}(\omega)$ (at volume V_0). The method is completely analogous to the one employed by Trofimenkoff and Carbotte (1970) in calculating changes in the super-conductivity function $\alpha^2 F(\omega)$ with volume.

If the expression for $\alpha_{tr}^2 F(\omega)$ given by (2.1.26) is multiplied by ω and integrated over all frequencies, one obtains

$$\int_0^\infty \omega\, \alpha_{tr}^2 F(\omega)\, d\omega = C \int_0^\infty \omega \frac{d\omega}{N} \sum_\lambda \int_{<2k_f} d^3q \, \frac{q|W(\underline{q})|^2 |\underline{q}\cdot\underline{\varepsilon}_{\underline{q}\lambda}|^2}{\omega_{\underline{q}\lambda}} \delta(\omega - \omega_{\underline{q}\lambda}) \qquad \text{..... (2.2.11)}$$

where $C = \frac{m}{8Mk_f^3}$

Using the δ-function on the right hand side we have

$$\int_0^\infty \omega\, \alpha_{tr}^2 F(\omega)\, d\omega = \frac{C}{N} \sum_\lambda \int_{<2k_f} d^3q \, q\, |W(\underline{q})|^2 |\underline{q}\cdot\underline{\varepsilon}_{\underline{q}\lambda}|^2 \qquad (2.2.12)$$

The closure relation for the polarization vectors

$$\sum_\lambda \underline{\varepsilon}_{\alpha \underline{q}\lambda}\, \underline{\varepsilon}^*_{\beta \underline{q}\lambda} = \delta_{\alpha\beta}$$

is used on the right hand side of (2.2.12) to give

$$\int_0^\infty \omega \alpha_{tr}^2 F(\omega) = \frac{C}{N} \int_{<2k_f} d^3q\, q^3 \left|W(\underline{q})\right|^2 \qquad (2.2.13)$$

performing the angular integration one obtains

$$\int_0^\infty \omega \alpha_{tr}^2 F(\omega) = \frac{4\pi C}{N} \int_{<2k_f} q^5 \left|W_\omega(\underline{q})\right|^2 dq \qquad (2.2.14)$$

If we now make the assumption that under a small volume change the shape of the function remains the same, and if we use the well-known property of the δ-function namely

$$\delta(An) = \frac{1}{A}\,\delta(n)$$

We can write

$$\alpha_{tr}^2 F_V(A\omega) = \frac{S}{A^2}\,\alpha_{tr}^2 F_{V_0}(\omega) \qquad (2.2.15)$$

where $A = \omega(V)/\omega(V_0)$; and S is given by

$$S = \frac{\int_0^1 t^5 dt \left|W_V(t)\right|^2}{\int_0^1 t^5 dt \left|W_{V_0}(t)\right|^2} \qquad (2.2.16)$$

t is $q/2k_f$, (the reader should note here that the k_f^6 which comes from the transformation to the variable t cancels the volume factors from the k_f^3 in C and the k_f^{-3} in N) and $W_V(t)$ and $W_{V_0}(t)$ are the form factors for volumes V and V_0. It is then clear that S describes the change in $\alpha_{tr}^2 F(\omega)$ due to the change in form factors and A^2 the change due to altered phonon frequencies.

Using (2.2.15) we can, quite simply, generate the required $\alpha_{tr}^2 F_V$ from a basic $\alpha_{tr}^2 F_{V_0}$ and this will suffice to calculate the resis-

tivity at the new volume, for all temperatures. In the results we will demonstrate that the method of scaling outlined above is sufficiently accurate, relative to the method of a detailed recalculation, to justify its exclusive use in all our calculations. In addition, it has the advantage of clearly indicating how the different mechanisms affect the resistivity when the volume is changed.

We are now ready to proceed to actual results and calculations and these will be presented in the next section.

2.3 The Resistivities At Constant Pressure And Constant Volume

One of the main objectives of this work was to determine whether the resistivities of the alkali metals, both at constant (zero-temperature) volume and constant (atmospheric) pressure, could be accounted for using as simple an approach as possible. This effort and the results obtained will be discussed in this section.

Before we begin let us recount previous efforts in this direction and their results. In the recent past, two significant efforts stand out. Hasegawa (1964) attempted to calculate the constant volume resistivity $\rho_V(T)$ as a function of temperature and, in addition, calculated the volume derivative of the resistivity $d\ln\rho/d\ln V$ at room temperature, in Na, K, and Li. For the phonons Hasegawa used neutron data in Na, and specific heat data in K and Li. For the electron-ion scattering he used the Bardeen matrix element (Bardeen 1937). He obtained reasonable agreement with experiment for $\rho_V(T)$ and $d\ln\rho/d\ln V$. However, to explain the anomalous value of $d\ln\rho/d\ln V$ in Li, he had to resort to a distorted Fermi surface for Li (Na and K were considered to have

spherical Fermi surfaces). More recently Dickey, Meyer and Young (1967) calculated the volume derivatives of the resistivities and thermopowers of all the alkali metals, at room temperature. A Debye model was used for the phonons and pseudo-atom phase shifts for the electron-ion scattering. The agreement obtained with experiment was qualitatively good; however, significant quantitative discrepancies were obtained.

The present work is a definite improvement on the above inasmuch that we will attempt to calculate volume effects over a wide range of temperature (not only at room temperature as above) and, in addition, we will show that it is not necessary to resort to comparatively sophisticated techniques (distorted Fermi surfaces, electron-ion phase shifts etc.) to explain the relevant data.

The first step in our calculations is to fit the electrical resistivity at a particular temperature and lattice volume to determine the parameter R_c in the Ashcroft potential, and to thus determine the reference distribution $\alpha_{tr}^2 F_{V_0}(\omega)$ which will then be scaled in order to determine ρ as a function of volume, at various temperatures. It was decided that the best temperature to do this would be the temperature (lattice volume) at which the phonon dispersion curves are measured experimentally as this would eliminate any need to change the phonons or form factors at this initial stage. Accordingly, then, we fit the constant (atmospheric) pressure resistivity in Na, Li, and Rb at 90°K, 100°K, and 120°K respectively, and in the case of K, in view of the negligible difference in lattice volume at 0 and 9°K, we fit the constant (zero temperature and atmospheric pressure) volume resistivity at 90°K.

TABLE 2.3.1

ZERO TEMPERATURE LATTICE PARAMETER AND FERMI MOMENTUM, THE VALUES OF THE GRÜNEISEN PARAMETER γ, AND THE VARIATION OF THE LATTICE VOLUME WITH TEMPERATURE FOR Na, K, Rb, AND Li

Metal	Lattice Parameter At T = 0°K (In Å)	Fermi Momentum, k_f, At T = 0°K (In $Å^{-1}$)	$\frac{V(30°K)}{V(0°K)}$	$\frac{V_{50}}{V_0}$	$\frac{V_{100}}{V_0}$	$\frac{V_{150}}{V_0}$	$\frac{V_{200}}{V_0}$	$\frac{V_{250}}{V_0}$	$\frac{V_{300}}{V_0}$	Grüneisen Constant γ
Na	4.2268	0.9222	—	1.0014	1.0062	1.0149	1.0243	1.0342	1.0442	1.3
K	5.2275	0.7456	1.0010	1.0028	1.0125	1.0234	1.0347	1.0460	1.0573	1.3
Rb	5.5855	0.6978	1.0030	1.0070	1.0183	1.0300	1.0417	1.0543	1.0660	1.0
Li	3.4812	1.1196	—	1.0009	1.0035	1.0077	1.0131	1.0194	1.0267	0.78

Since we are interested in volume effects, it is necessary to use the appropriate values of lattice parameter and Fermi momentum at this stage. The experimental data used is summarized in Table (2.3.1) and is taken from Dugdale and Gugan (1962), Dugdale and Phillips (1965), and Martin (1965). Also included are the values of the Grüneisen parameter γ which is later used to scale the phonons with volume. We also take note here that all experimental data on the electrical resistivities used here and later for purposes of comparison are taken from Dugdale and Philips, Dugdale and Gugan, and Dugdale and Gugan (1960).

We find that in each case the experimental resistivity is reproduced by two different values of R_c. The values for each metal are Na, ~ 1.05 and ~ 0.83Å; K, ~ 1.28 and ~ 1.03Å; Rb, ~ 1.44 and ~ 1.04Å; and Li, ~ 1.0 and ~ 0.52Å. This is a characteristic property of the Ashcroft form of potential and has appeared in the calculation of various properties in various systems (Cohen and Heine, 1970). In our context this can be easily understood — the different shapes of the potentials give different amounts of Normal and Umklapp contributions to the resistivity; however, the sum is the same. In our case it is relatively easy to make a clear cut choice in favour of one of the two values. In Rb, Na, and K, we make the choice on the basis of which value gives a better overall fit to the constant volume resistivity, and in the case of Li, since reliable data, especially at low temperatures, is not available, we choose the potential which approximates best the available empirical potentials. In Figures (2.3.1) and (2.3.2) we show plots of the various potentials together with the best available

Fig. 2.3.1 Pseudo-potential form factors in Li and Rb.

—— Ashcroft; ● Shaw (Li), Heine-Abarenkov (Rb); x Appapillai and Williams.

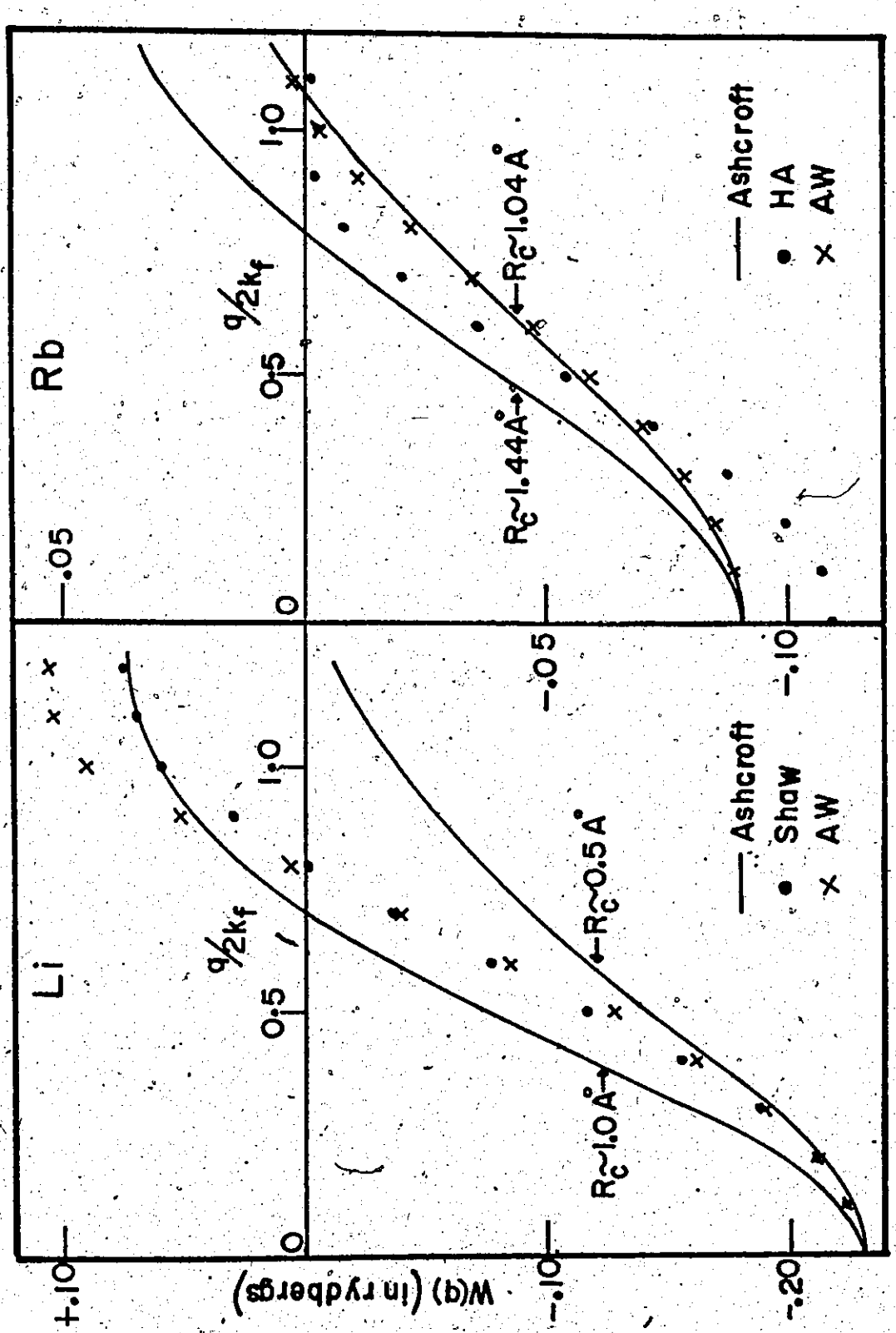
Li
Rb
W(q) (in rydbergs)
+.10
0
-.10
-.20
-.05
0
.05
.10
-.05
-.10
q/2k_f
0.5
1.0
R_c~0.5 A°
R_c~1.0 A°
R_c~1.04 A°
R_c~1.44 A°
Ashcroft
Shaw
HA
AW

Fig. 2.3.2 Pseudo-potential form factors in Na and K.
—— Ashcroft; ● Shaw; x Appapillai and Williams.

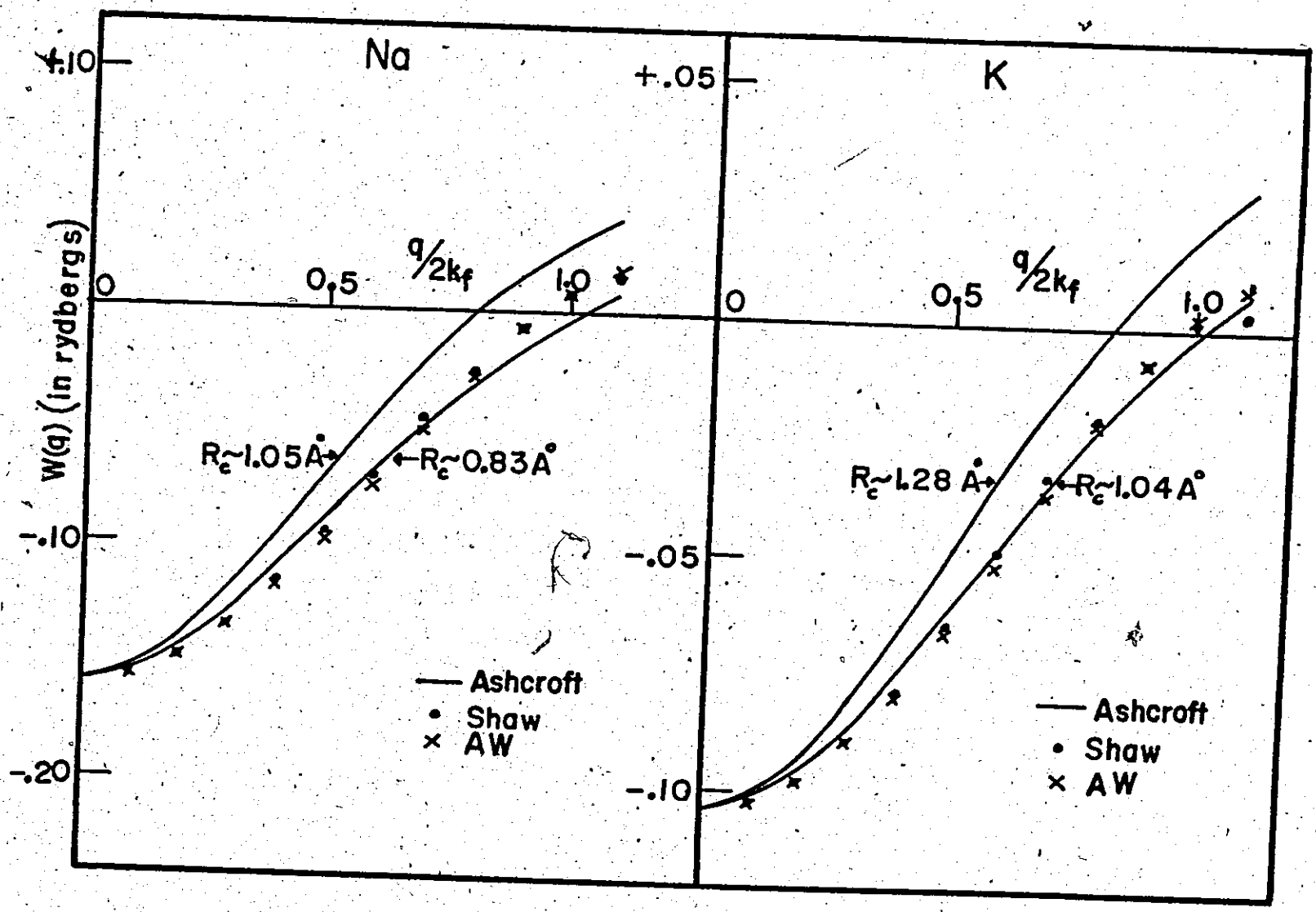
Na
K
+.10
-.10
-.20
+.05
-.05
-.10
W(q) (in rydbergs)
0
0.5
q/2k_f
1.0
R_c~1.05Å
R_c~0.83Å
R_c~1.28 Å
R_c~1.04 Å
Ashcroft
Shaw
AW

Fig. 2.3.3 $\alpha_{tr}^2 F(\omega)$ for zero lattice volume in Na and K using selected R_c's. Frequency units are 10^{12} cps. $\alpha_{tr}^2 F$ is dimensionless.

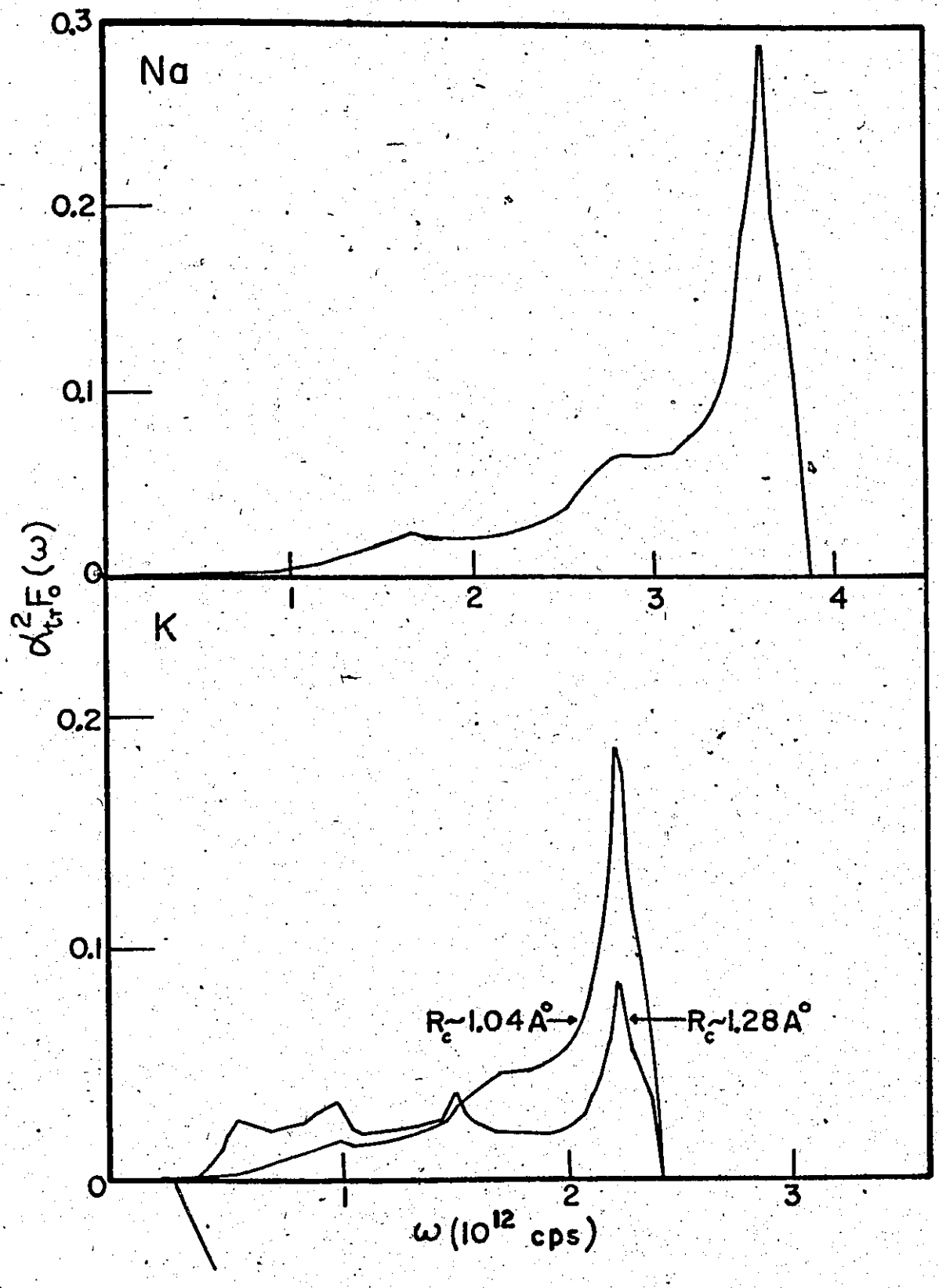
Na
K
0.3
0.2
0.1
0
1
2
3
4
$\alpha^2_{tr}F_0(\omega)$
$R_c \sim 1.04 A^\circ$
$R_c \sim 1.28 A^\circ$
$\omega\ (10^{12}\ cps)$

Fig. 2.3.4 $\alpha_{tr}^2 F(\omega)$ for zero lattice volume in Li and Rb using selected R_c's. Frequency units are 10^{12} cps. $\alpha_{tr}^2 F$ is dimensionless.

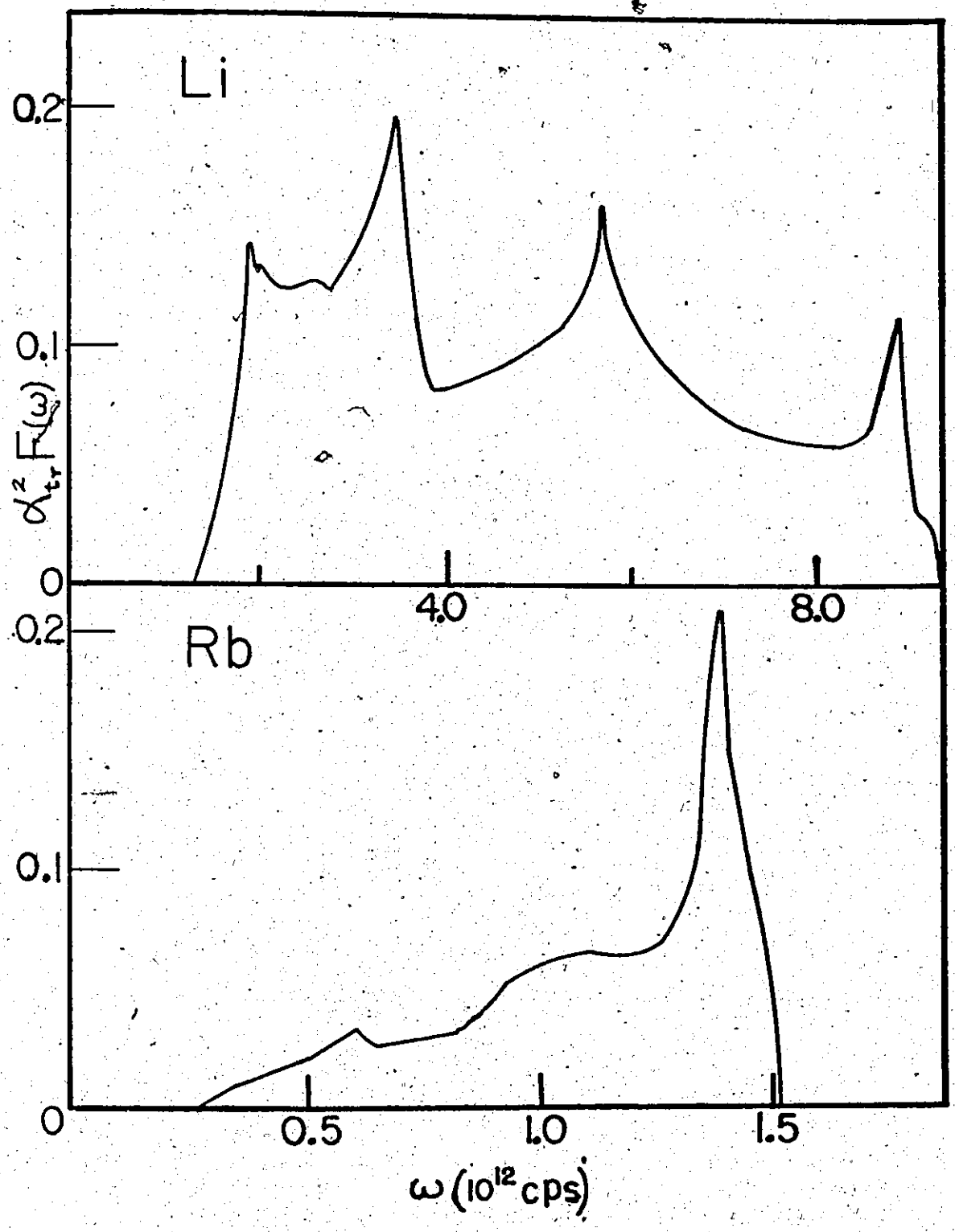
Li
0.2
0.1
0
$\alpha^2_{tr} F(\omega)$
4.0
8.0
Rb
0.2
0.1
0
0.5
1.0
1.5
ω (10^{12} cps)

empirical potentials (Shaw and Pynn 1969; Appapillai and Williams 1973 (AW); Heine and Abarenkov 1964 (HA)). It is quite clear that in each case one of our potentials approximates the empirical potentials much better than the other (we note that in Rb, the HA potential is clearly in serious error). In Na, Rb, and K, it also turns out that the potentials which fit the constant volume resistivity are the same ones which approximate the empirical potentials best. Accordingly, then, a completely unambiguous choice is possible and the values of R_c selected in each case are Na, 0.8282Å; K, 1.0353Å; Rb, 1.0422Å; and Li, 1.0005Å.

In Figures (2.3.3) and (2.3.4) we show plots of the $\alpha^2_{tr}F_{V_0}(\omega)$ functions for each metal using the chosen value of R_c. We note here that in each case the functions shown are for zero temperature lattice volume. In the case of K the zero volume functions are, of course, immediately available from the fitting procedure but in the cases of Na, Rb, and Li, we have scaled the original $\alpha^2_{tr}F$ functions down to zero volume according to (2.2.15). The validity of the scaling procedure is discussed shortly. Also for K we have shown the $\alpha^2_{tr}F$ functions which result from both values of R_c — as can be seen the distributions are distinctly different and this, of course, leads to the very different temperature dependence for the constant volume resistivity.

We can now present our first set of results and these are shown in Table (2.3.2) and Figure (2.3.5). Table (2.3.2) consists of a comparison of the constant volume resistivities for the various potentials with experiment, at various select temperatures. We note that in general the best results are obtained with our potentials (this is not

TABLE 2.3.2

A COMPARISON OF THE EXPERIMENTAL VALUES AT VARIOUS TEMPERATURES OF THE CONSTANT (ZERO) VOLUME RESISTIVITIES OF Na, K, Rb, AND Li WITH THE VALUES GENERATED USING VARIOUS PSEUDO-POTENTIALS

Metal	Resistivity in μΩ-cms	Temperature (°K)						
		30	50	100	150	200	250	295
Na	Expt.	.074	.314	1.108	1.857	2.566	3.262	3.882
	Shaw	.069	.267	.858	1.420	1.961	2.498	2.981
	AW	.083	.316	1.006	1.662	2.294	2.914	3.466
	Ashcroft (R_c ~ 0.83Å)	.101	.357	1.093	1.792	2.467	3.137	3.730
K	Expt.	.283	.705	1.716	2.643	3.543	4.445	5.272
	Shaw	.251	.619	1.492	2.323	3.130	3.951	4.676
	AW	.259	.650	1.582	2.465	3.332	4.191	4.961
	Ashcroft (R_c ~ 1.035Å)	.301	.725	1.721	2.688	3.620	4.562	5.398
Rb	Expt.	.798	1.527	3.203	4.842	6.570	--	--
	HA	.236	.472	1.023	1.559	2.090	--	--
	AW	.668	1.295	2.770	4.207	5.635	--	--
	Ashcroft (R_c ~ 1.04)	.780	1.493	3.177	4.822	6.455	--	--
Li	Expt.	--	--	1.710	3.688	5.710	7.680	9.456
	Shaw	--	--	1.322	2.355	3.368	4.360	5.535
	AW	--	--	3.130	5.476	7.770	10.016	12.009
	Ashcroft (R_c ~ 1.0Å)	--	--	1.707	2.994	4.251	5.479	6.569

Fig. 2.3.5 Ideal resistivities, at zero lattice volume, in Na, K, and Rb. The dotted line in Na represents the resistivity of the bcc component of the two phase mixture.

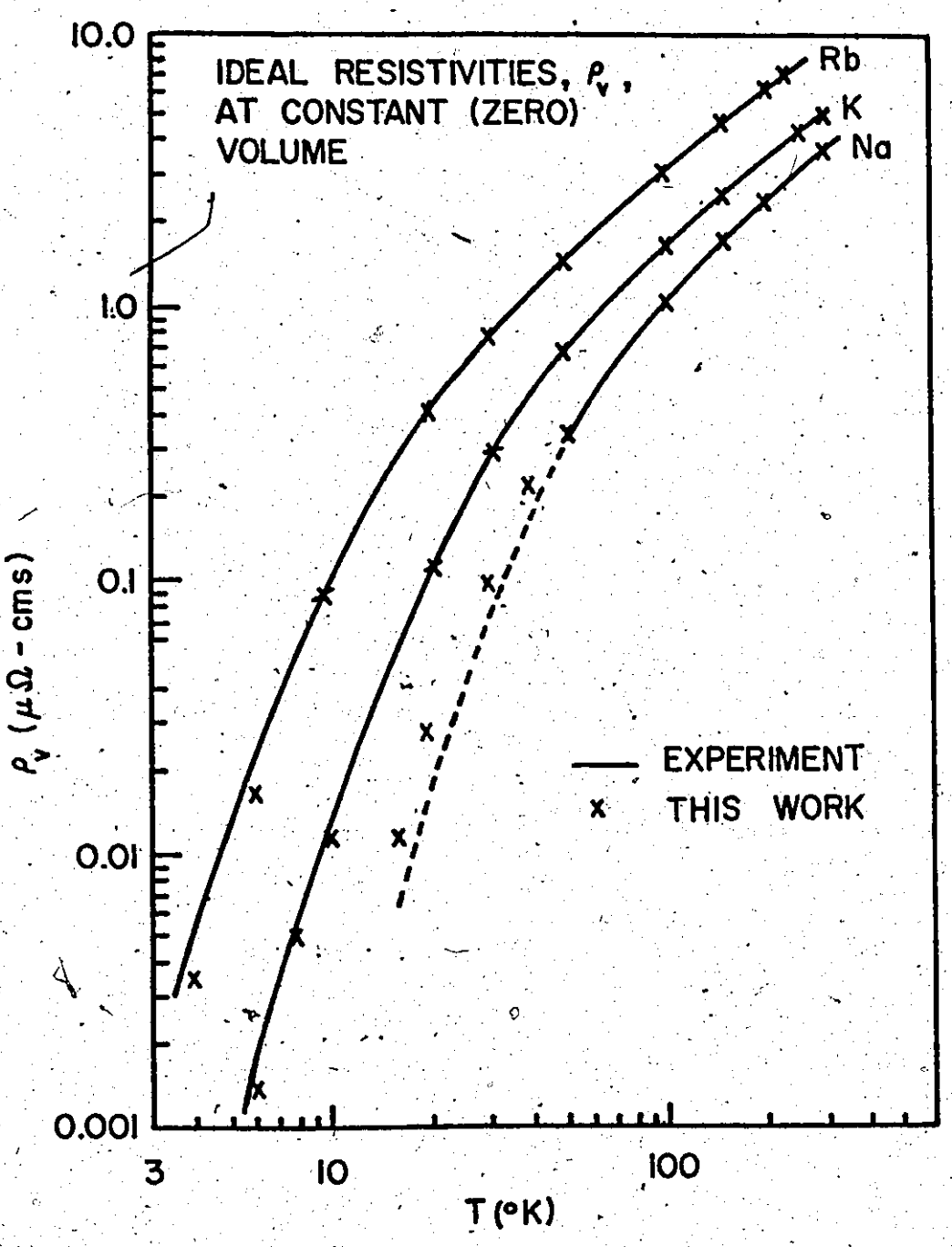
IDEAL RESISTIVITIES, ρ_v, AT CONSTANT (ZERO) VOLUME
Rb
K
Na
EXPERIMENT
THIS WORK
10.0
1.0
0.1
0.01
0.001
ρ_v ($\mu\Omega$ - cms)
3
10
100
T (°K)

surprising since we fit to a given resistivity). In K and Na the Shaw and AW potentials yield resistivities that are not in too serious disagreement with experiment and one notes that the AW potential is a definite improvement on the Shaw potential in this respect. In Rb, the HA potential hopelessly underestimates the resistivity and the AW potential is again obviously a considerable improvement in this metal. Finally in Li, we note that all the potentials, including ours, yield rather poor agreement with experiment either overestimating (AW) or underestimating (Shaw, Ashcroft) the experimental values. This is disappointing and is perhaps due to the fact that the pseudo-potential concept is somewhat inadequate in Li since the "core" states are considerably less well defined than in the other alkalis. In Figure (2.3.5) we show the constant volume resistivities generated using the Ashcroft form with the selected R_c's, in comparison with experiment. We have left out Li as reliable low temperature (<80°K) experimental data is not available and, in addition, Na and Li undergo martensitic transformations below 40°K and 80°K respectively. In the case of Na in Figure (2.3.5) the dotted line represents the resistivity of the bcc part of the two phase mixture — this has been extracted from the total resistivity by Dugdale and Gugan (1960). Apparently this is not yet available in a quantitative form in Li.

As can be seen from the Figure the agreement with experiment is very satisfactory over a wide temperature range.

Our major effort, however, is to account for the differences in $\rho_V(T)$ and $\rho_p(T)$ and we proceed next to discuss the calculation of $\rho_p(T)$ and these differences. We begin by attempting to justify the scaling

Fig. 2.3.6 A comparison of the $\alpha^2_{tr}F(\omega)$ function obtained, for an arbitrary volume change of 10%, using the scaling technique (the crosses) as opposed to a detailed recalculation (the dashed curve). The $\alpha^2_{tr}F_{V_0}$ (zero volume) is also shown (the solid curve).

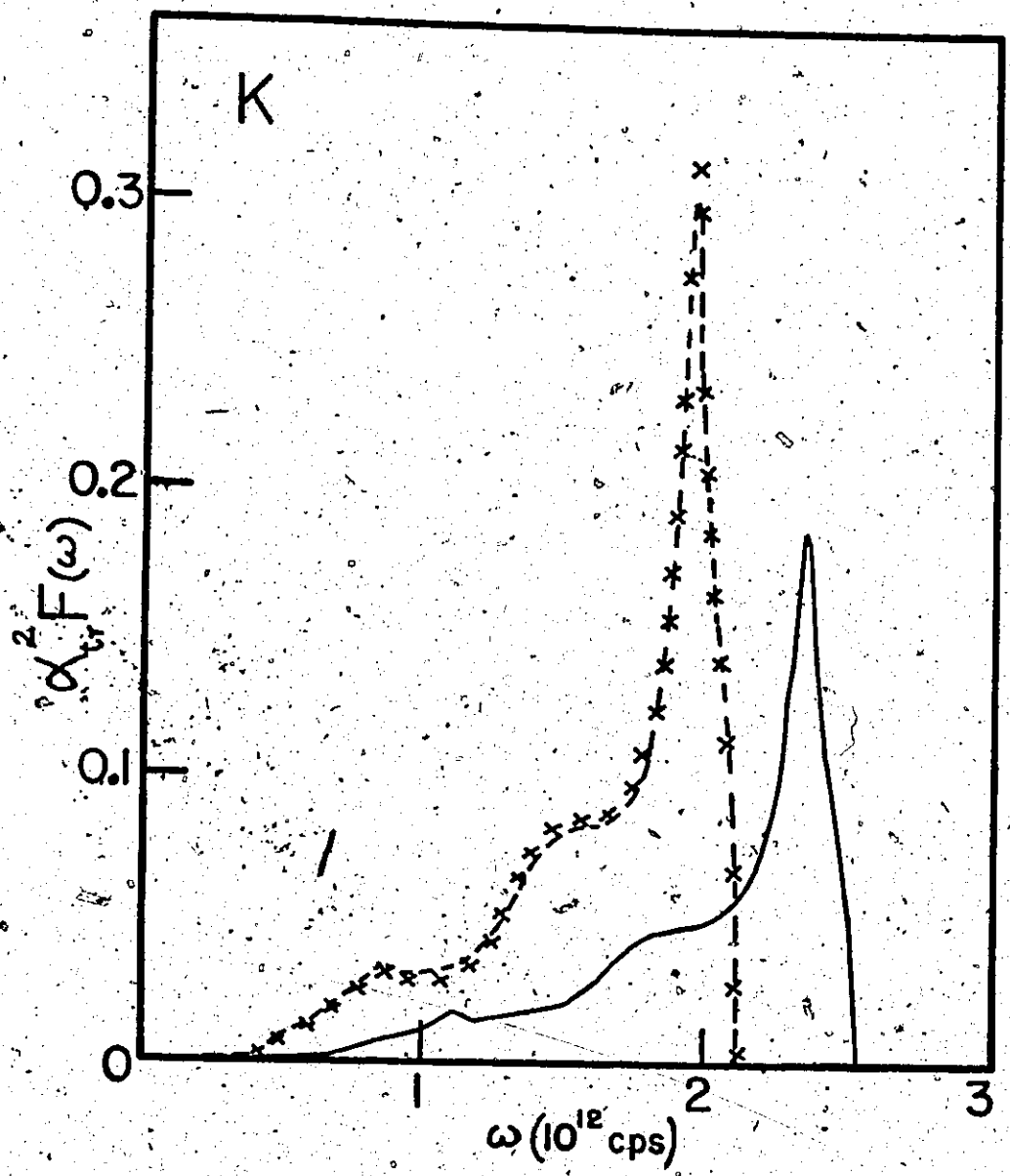
K
0.3
0.2
0.1
0
$\alpha^2 F(\omega)$
1
2
3
$\omega\,(10^{12}\,\mathrm{cps})$

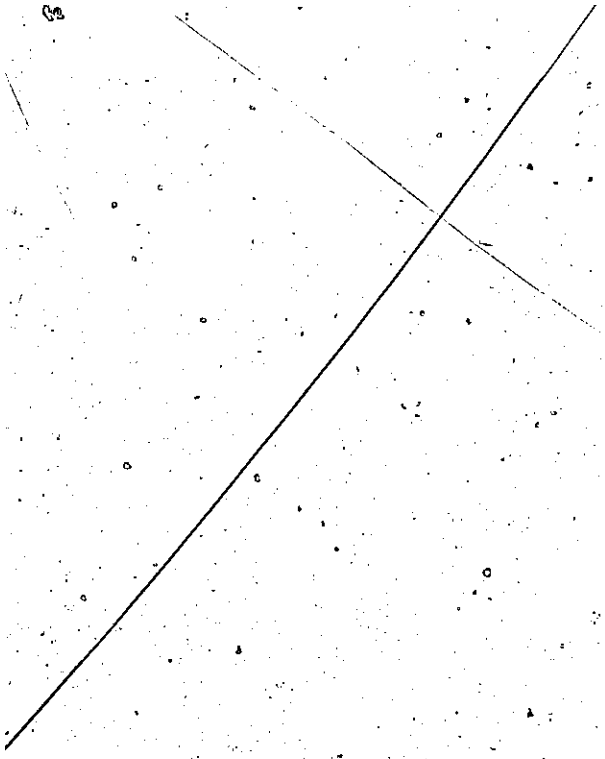

Fig. 2.3.7 The temperature variation of the constant (atmospheric) pressure resistivity in Na, K, and Rb. —— Experiment; x our calculated values using the scaling technique outlined in the text.

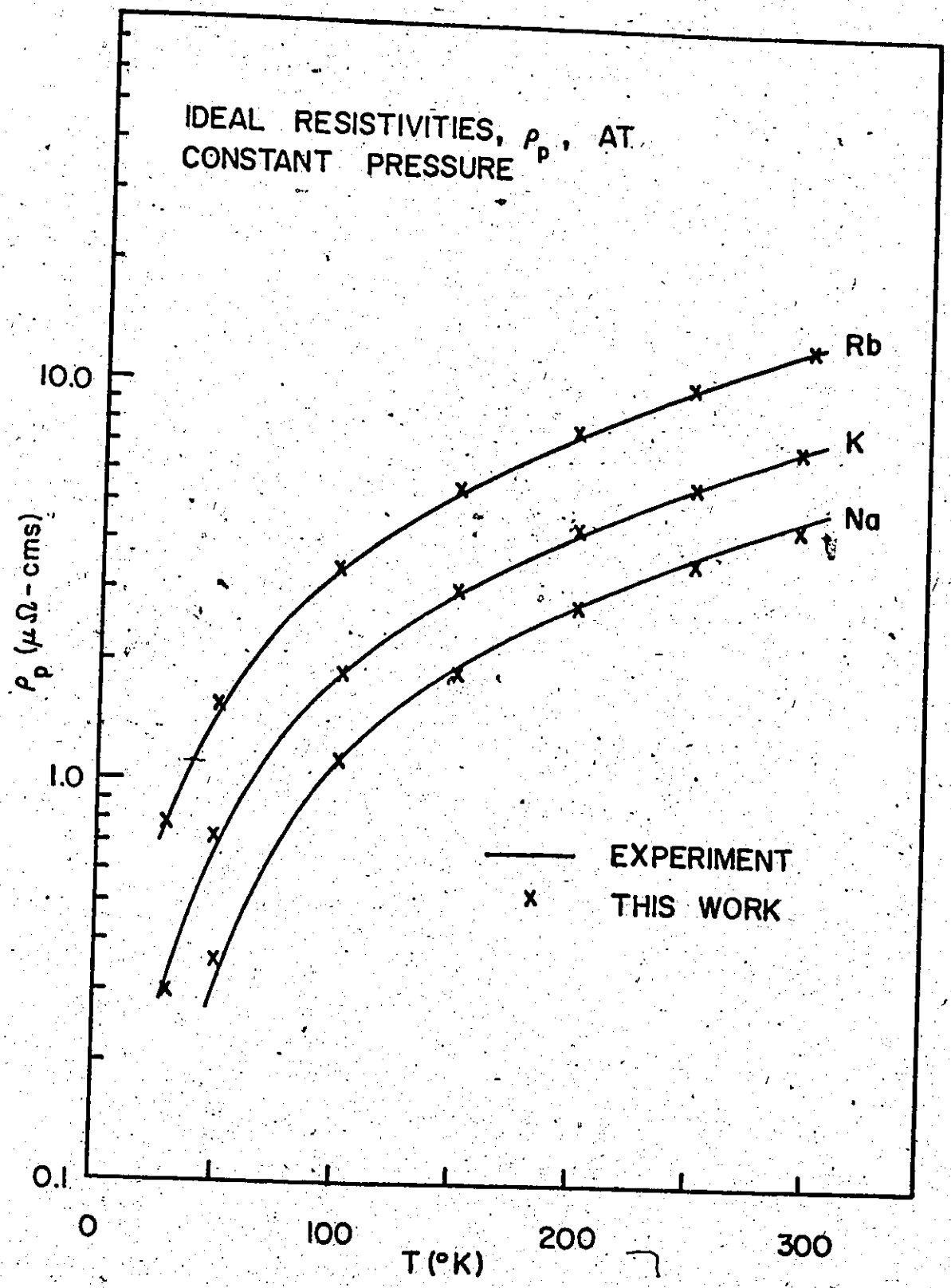
IDEAL RESISTIVITIES, ρ_p, AT CONSTANT PRESSURE
Rb
K
Na
EXPERIMENT
THIS WORK
10.0
1.0
0.1
ρ_p ($\mu\Omega$-cms)
0
100
200
300
T (°K)

technique (described in section 2.2), as opposed to a detailed recalculation used to obtain $\alpha_{tr}^2 F$, and hence the resistivity, at an altered volume.

In order to do this we show in Figure (2.3.6) $\alpha_{tr}^2 F_{V_0}$ in K corresponding to the lattice volume at 0°K and atmospheric pressure and $\alpha_{tr}^2 F_V$ corresponding to a lattice volume 10% larger than at 0°K. In one case the latter function is recalculated in detail (the dashed curve) and in the other (the crosses) is generated by scaling $\alpha_{tr}^2 F_{V_0}$ using (2.2.15). We have purposely used an increase in volume larger than any which occurs in the actual calculations (a maximum of ~ 8%). As can be seen the agreement is very good. If one calculates resistivities at 300°K using the two functions the values obtained differ by ~ 1.5%, whereas the change in resistivity at 300°K due to a volume change of that magnitude is of the order of 40%. One notes, however, that if very much larger volume changes are considered, one would undoubtedly question the accuracy of this method.

For the sake of consistency and, of course, economy, we have, therefore, used the scaling technique to obtain the resistivities at all other volumes and temperatures of interest from our original $\alpha_{tr}^2 F$'s obtained from the fitting procedure.

In Figure (2.3.7) we compare the constant (atmospheric) pressure resistivities as a function of temperature in Na, K, and Rb, with experiment. One notes that the agreement is again very satisfactory over the same wide temperature range.

In Figure (2.3.8) we compare our values for the differences

Fig. 2.3.8 The temperature variation of the difference between the constant volume and constant pressure resistivities in Na, K, and Rb. —— Experiment; x the results of our calculations.

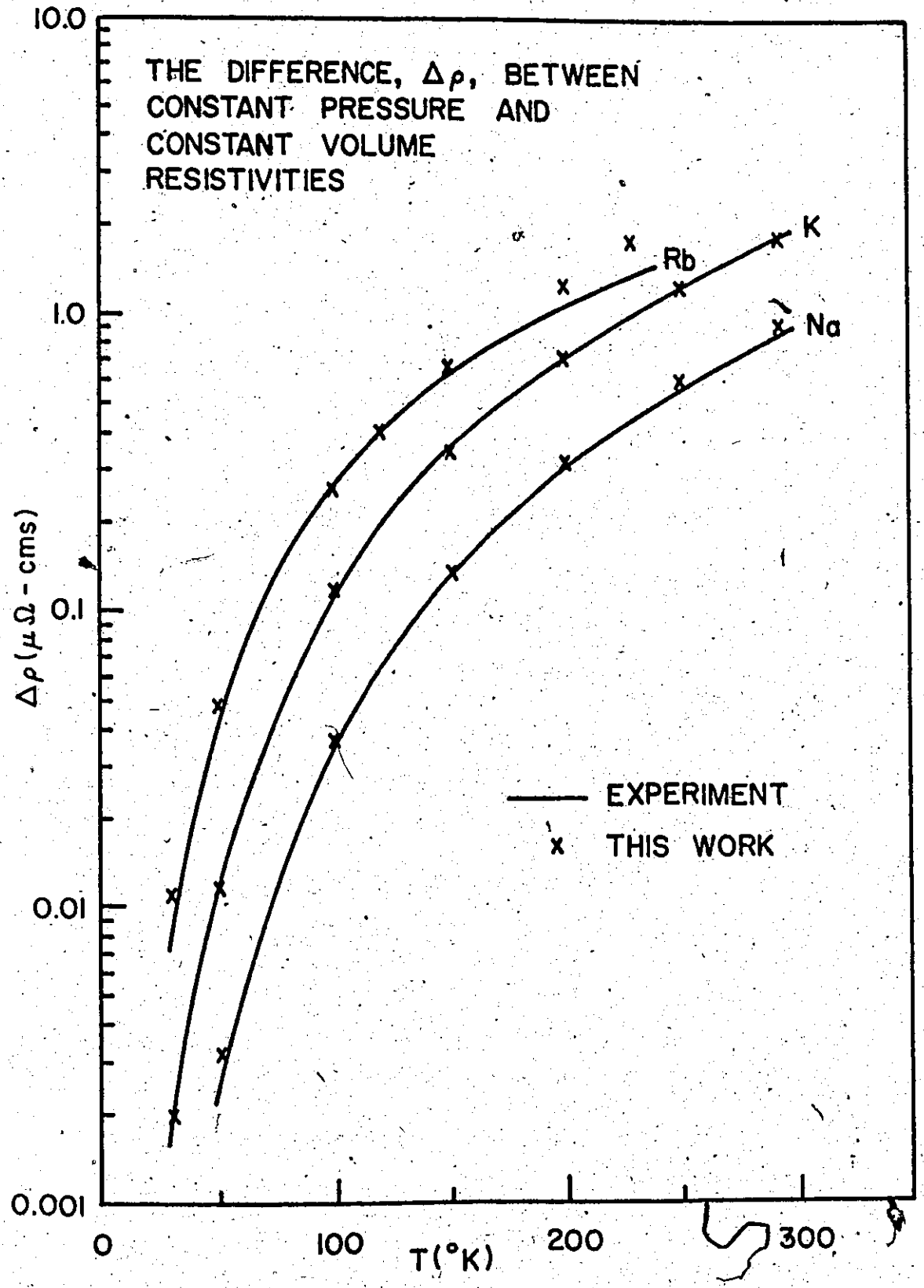
THE DIFFERENCE, Δρ, BETWEEN
CONSTANT PRESSURE AND
CONSTANT VOLUME
RESISTIVITIES
Rb
K
Na
EXPERIMENT
THIS WORK
Δρ (μΩ - cms)
10.0
1.0
0.1
0.01
0.001
0
100
200
300
T(°K)

between the constant pressure and constant volume resistivities as a function of temperature, with experiment, noting that this should provide a somewhat more stringent test for our calculations. The agreement is again surprisingly good.

We have excluded Li from the above plots as the behaviour of the resistivity of Li under pressure is anomalous in comparison with the other alkalis and we will consider it separately in somewhat more detail below.

In the alkalis Na, K, and Rb the resistivities inevitably decrease under pressure (for small pressure changes), which means that the constant (zero) volume resistivity is always less than the constant (atmospheric) pressure resistivity. However, in Li, this is not true. What is observed (Dugdale and Gugan 1962) is that for temperatures $> \sim 180°K$ the resistivity <u>increases</u> with pressure, at $T \sim 180°K$ there is essentially no change, and for $T < 180°K$ the resistivity <u>decreases</u> with pressure. Since two separate mechanisms operate to change the resistivity with pressure, namely, the change in the lattice frequencies and the change in the pseudo-potential form factors and since the effect of pressure on the lattice is always to make it stiffer and hence less polarizable (consequently lowering the resistivity) the different behaviour of Li must be due to the different way in which its form factors change with volume relative to the other alkalis. Also the effect must be such that the two mechanisms oppose each other in Li, whereas they reinforce each other in Na, K, and Rb.

To demonstrate this difference in behaviour of the form factors (which is crucial to an explanation of the anomalous behaviour of Li),

in Figure (2.3.9) we have shown plots of the form factors in Rb and Li at zero volume and at 90% zero volume. The form factors have been normalized to the long wave-length limit of $\frac{2}{3} E_f$ to exclude the effect of the direct change in Fermi energy which, of course, always takes place with a volume change. On the q axis we have shown the regions of exclusively Normal process, exclusively Umklapp processes, and where both occur. One notes the following important difference in the behaviour of Li and Rb. In Rb, under pressure the form factors everywhere decrease, consequently the quantity S (which describes the effect of the changed electron-ion scattering on the resistivity) given by (2.2.16) decreases under pressure. However, for Li for $q/2k_f < \sim 0.7$ the form factors decrease but for the region $1.0 > q/2k_f > \sim 0.7$ they actually increase. If one remembers that in the expression for S there is a q^5 appearing in the integrands it is obvious that in Li S will increase under pressure. Physically this corresponds to an increase in the probability of Umklapp processes under pressure. Hasegawa (1964) incorporated this in his calculations by assuming an increase in distortion of the Fermi surface under pressure. However, as one can see from the above argument a much simpler explanation involving a spherical Fermi surface is possible.

To momentarily summarize, then, in Na, K, and Rb, the effect of pressure on the form factors is to decrease the resistivity (a reduction in the probability of Umklapp processes) whereas in Li the effect is to increase the resistivity. Thus in Na, K, and Rb, the net effect of this and the change in the lattice vibrations is to always decrease ρ whereas in Li depending on the volume change involved the net effect is

Fig. 2.3.9 Pseudo-potential form factors in Li and Rb for zero volume (-.-.-) and 90% zero volume (——). The form factors have been normalized to $\frac{2}{3} E_f$. On the q-axis is indicated the regions of exclusively Normal (N) processes, exclusively Umklapp (U) processes, and a mixture of the two (N+U).

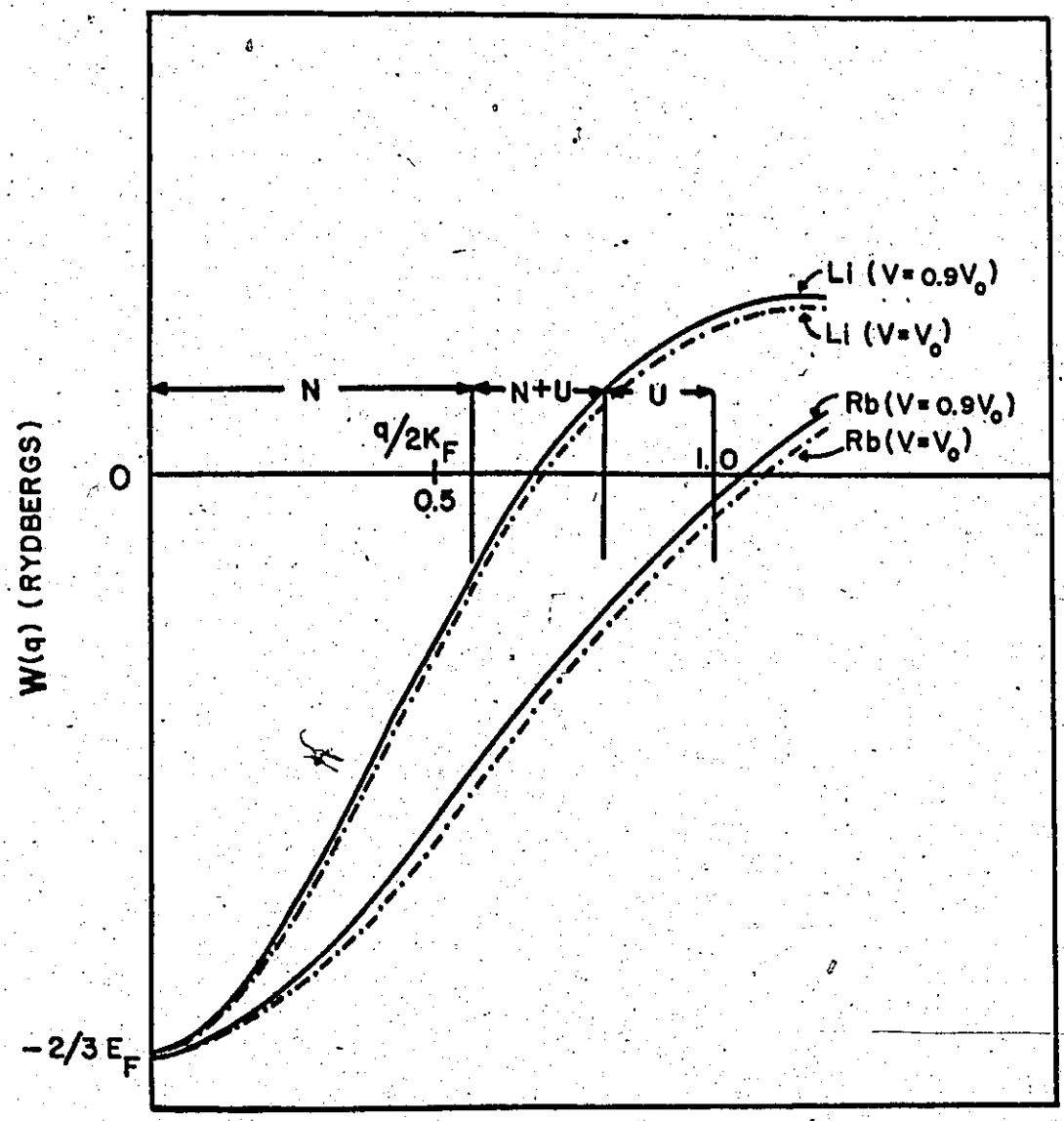
Li (V=0.9V$_0$)
Li (V=V$_0$)
N
N+U
U
Rb(V=0.9V$_0$)
Rb(V=V$_0$)
q/2K$_F$
0.5
1.0
0
W(q) (RYDBERGS)
-2/3 E$_F$

TABLE 2.3.3

A COMPARISON OF THE EXPERIMENTAL VALUES OF $\Delta\rho(T)(\equiv \rho_p(T) - \rho_V(T))$ WITH OUR CALCULATED VALUES, IN Na, K, Rb, AND Li

Metal	Temp. (°K)	$\Delta\rho \equiv \rho_p - \rho_V$ (μΩ-cms.)	
		Experiment	Calculated
K	30	0.0021	0.0020
	50	0.0135	0.0118
	100	0.1187	0.1198
	150	0.3621	0.3527
	200	0.7380	0.7237
	250	1.2750	1.2410
	295	1.9166	1.8426
Na	50	0.0027	0.0032
	100	0.0375	0.0379
	150	0.1370	0.1376
	200	0.3080	0.3284
	250	0.5598	0.6059
	295	0.8679	0.9288
Rb	30	0.0890	0.0113
	50	0.0465	0.0481
	100	0.2580	0.2777
	120	0.3912	0.4087
	150	0.6240	0.6777
	200	1.0780	1.2895
	230	1.3777	1.7826
Li	80	0.0024	0.0001
	100	0.0040	0.0007
	150	0.0090	- 0.0063
	200	- 0.0060	- 0.0196
	250	- 0.0700	- 0.0413
	275	- 0.0956	- 0.0560

TABLE 2.3.4

A TABULATION OF THE CALCULATED CONTRIBUTIONS OF THE VARIOUS MECHANISMS TO $\Delta\rho(T)$ AT VARIOUS TEMPERATURES; IN Na, K, Rb, AND Li

Metal	Temp. (°K)	$(\Delta\rho/\rho_o)$% Change In Lattice Volume	$(\Delta\rho/\rho_o)$% Change In Pseudo-Potential Form Factors	$(\Delta\rho/\rho_o)$% Change In Phonon Frequencies	$(\Delta\rho/\rho_o)$% Total
	50	+ .28	+ .17	+ 1.19	+ 1.64
K	150	+2.34	+1.37	+ 9.40	+13.11
	250	+4.60	+2.65	+19.95	+27.20
	50	+ .14	+ .07	+ .69	+ .90
Na	150	+1.49	+ .78	+ 5.41	+ 7.68
	250	+3.42	+1.77	+14.17	+19.36
	50	+ .70	+ .33	+ 2.19	+ 3.22
Rb	120	+1.83	+ .85	+ 7.97	+10.65
	200	+4.17	+1.88	+13.93	+19.98
	80	+ .255	- .655	+ .530	+ .010
Li	160	+ .878	-2.524	+ 1.369	- .277
	260	+2.086	-5.865	+ 2.948	- .831

either an increase or a decrease or no change at all.

We have been able to demonstrate these features in our calculations for Li and this is shown in Table (2.3.3) where we have tabulated our values for $\Delta\rho(T)(\equiv \rho_p(T)-\rho_v(T))$ and the corresponding experimental values for all four metals. We note that the actual quantitative agreement in the case of Li is not as good as the other alkalis; however, we do not consider that important as the changes in resistivity with pressure are very small and thus difficult to measure. What is important is that the main features are present. We believe this to be the first calculation which demonstrates this. Previous work (Hasegawa 1964; Dickey, Meyer and Young 1967) only considered effects at one temperature (~ 295°K).

In Table (2.3.4) we have tabulated the contributions from the various sources to the change in resistivity with volume (pressure) at various temperatures. In Na, K, and Rb the main contribution is from the change in phonons (~ $2/3^{rds}$ in most cases), whereas in Li the changes in the form factors are the largest contribution. This is, of course, due to the fact that the pseudo-potential in Li is large at $q \sim 2k_f$.

At high temperatures (larger than the Debye temperature of the metal) the resistivity may be approximately expressed as (Dugdale and Gugan 1962; Hasegawa 1964)

$$\rho_T = KT/M\theta^2 \qquad (2.3.1)$$

where M is the ionic mass, θ is a characteristic temperature which measures the intensity of the lattice vibrations, and K is an interaction constant which depends chiefly on the electron-ion interaction.

Fig. 2.3.10 A plot of S/S_0 vs V/V_0 (2.3.10a) in Na, K, Rb and Li, and a plot of the experimental values of K/K_0 vs V/V_0 (2.3.10b) for the same metals. The insert contains a comparison of the values of $d\ln K/d\ln V$ obtained theoretically and observed experimentally.

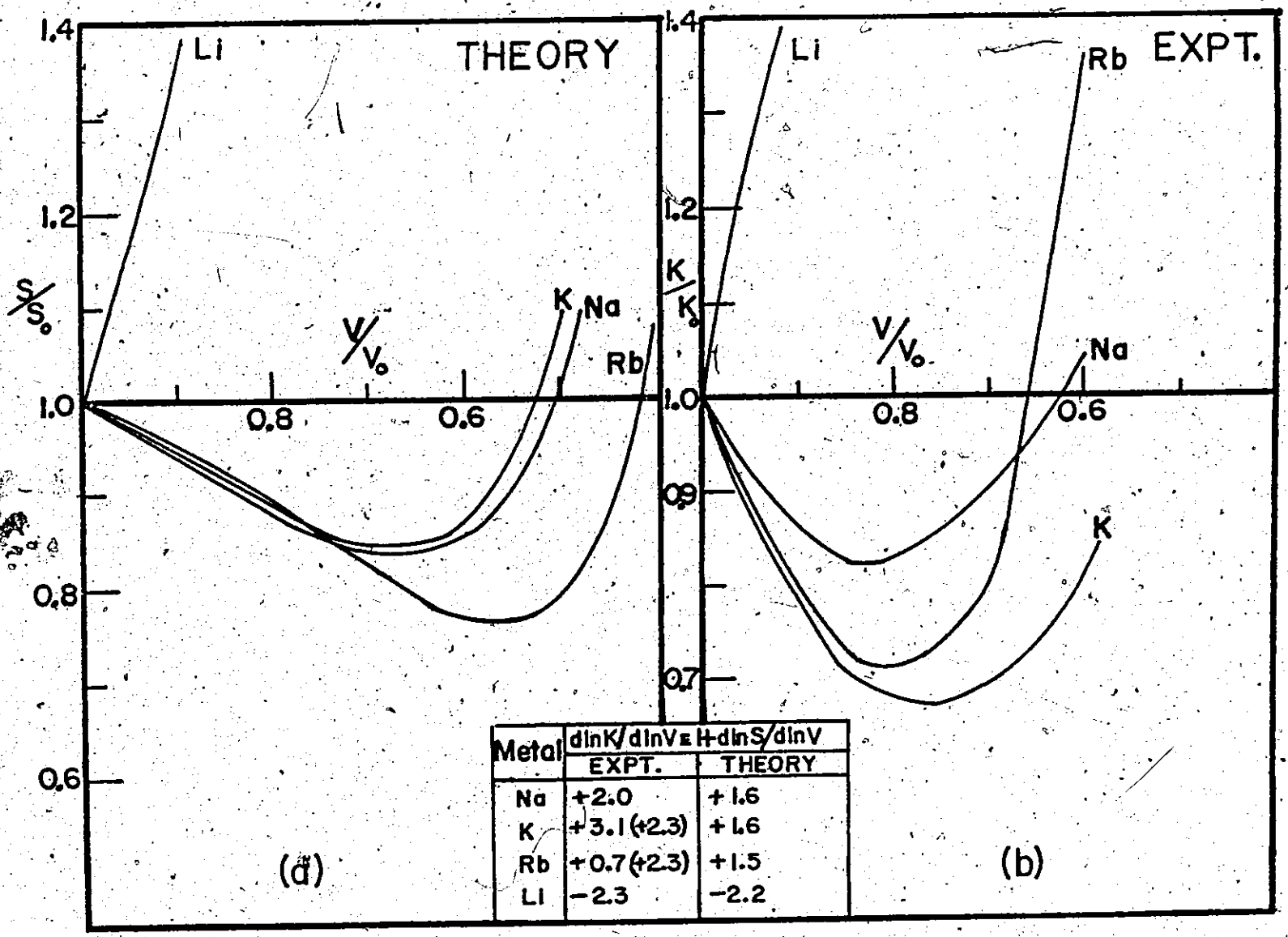

Metal	dlnK/dlnV ≡ H-dlnS/dlnV	
	EXPT.	THEORY
Na	+2.0	+1.6
K	+3.1 (+2.3)	+1.6
Rb	+0.7 (+2.3)	+1.5
Li	−2.3	−2.2

We should stress that this is only a very approximate way of describing $\rho(T)$; however, it has the effect of allowing the volume coefficient of the resistivity to be separated out according to

$$\frac{d\ln\rho}{d\ln V} = \frac{d\ln K}{d\ln V} + 2\gamma \qquad (2.3.2)$$

where $\gamma = -\, d\ln\theta/d\ln V$ is the familiar Grüneisen parameter. With some simple mathematical manipulations our formula (2.1.25), in the limit $\hbar\omega \ll k_B T$, can be made to yield the following formula

$$\frac{d\ln\rho}{d\ln V} = 1 + \frac{d\ln S}{d\ln V} + 2\gamma \qquad (2.3.3)$$

where S is given by (2.2.16).

Consequently, we can compare $\frac{d\ln K}{d\ln V}$ as obtained experimentally with our calculated values of $1 + \frac{d\ln S}{d\ln V}$. To do this we refer to Figure (2.3.10) where we have plotted S/S_0 vs. V/V_0 alongside an experimentally determined plot of K/K_0 vs. V/V_0 (Dugdale 1961). $d\ln S/d\ln V$ and $d\ln K/d\ln V$ are, of course, the slopes of the various curves taken at the origin. S_0 and K_0 refer to the values of S and K at some reference volume, in this case at 0°C. We are pleased to see that our rather simple theory again displays all the essential features of experiment and as shown in the insert in the Figure we obtain values of $d\ln K/d\ln V$ in reasonably good agreement with experiment. In particular, once again, the quite different behaviour of Li is well accounted for.

We have also calculated the pressure variation of the resistivity in Rb at two temperatures, 20.5°K and 78.9°K. Here we need the compressibility of the solid to compute the volume change corresponding to the applied pressure. One can assume that the compressibility is indepen-

TABLE 2.3.5

THE PRESSURE VARIATION OF THE RESISTIVITY OF Rb AT TWO SELECT TEMPERATURES, 20.5°K AND 78.9°K

Pressure (In Atm.)	$\frac{\rho(P)}{\rho(P=0)}$ At 78.9°K			Pressure (In Atm.)	$\frac{\rho(P)}{\rho(P=0)}$ At 20.5°K		
	Expt.	Calc. With Constant β	Calc. With $\beta = \beta(V)$		Expt.	Calc. With Constant β	Calc. With $\beta = \beta(V)$
0	1.000	1.000	1.000	0	1.000	1.000	1.000
500	0.929	0.917	0.922	250	0.959	0.955	0.957
1000	0.864	0.840	0.858	500	0.922	0.912	0.919
1500	0.810	0.768	0.805	750	0.885	0.870	0.886
2000	0.759	0.703	0.761	1000	0.852	0.831	0.856
2500	0.703	0.642	0.724	1250	0.820	0.793	0.830
				1500	0.790	0.756	0.806

dent of volume, but this is somewhat misleading for the alkalis where it is fairly volume dependent. A lattice volume change of 2.3% at 120°K in Rb changes the compressibility by 15.7% (Dugdale and Phillips 1965). Accordingly, we have performed these calculations assuming (a) that the compressibility is independent of volume and (b) that as a first approximation, it varies linearly with volume. Even for the small volume changes considered here the differences in the results are quite marked. The results are given in Table (2.3.5) and one notes that the agreement with experiment, when the compressibility is considered volume dependent, is very satisfactory. All compressibility data were taken from Dugdale and Phillips (1965).

We would like to conclude this section by noting that since the publication of the above work (Hayman and Carbotte 1971a; Hayman and Carbotte 1971b), a paper by Kaveh and Wiser (1972a) has appeared in which they calculate the resistivities of Na and K at constant volume and constant pressure. They consider phonon effects in much more detail than we do, specifically, they also include anharmonic effects in the polarization vectors and calculate the changes in phonon frequencies in detail throughout the zone and not in an average way as we do. They also consider amplitude effects in the calculation of the constant volume resistivity. However, judging from their published results, these additional corrections are rather small. We would also like to point out that their claim that our treatment of anharmonic effects, through an average γ, leads to contributions to the change in resistivity that amount to only 50% of what they obtain with a more detailed

treatment, is incorrect. As shown in Table (2.3.4) we find that changes in phonon frequencies account for about 72% of the change in the resistivity in K at 250°K. In their work for a similar volume change the more detailed anharmonic effects account for ~ 80% of the difference. It appears then that our method is quite good and, of course, has the advantage of being very much simpler.

2.4 The Ideal Thermal Resistivities

Having had some success in calculating the absolute value and volume dependence of the electrical resistivities in K, Na, Rb and Li, we would like to see whether, with the same potentials, one is able to reproduce the magnitude and temperature dependence of the ideal thermal resistivities $W_{th}(T)$.

The basic variationally derived expression for $W_{th}(T)$ is (Ziman 1960; Baym 1964)

$$W_{th}(T)=\frac{1}{L_0 T}\,C'\sum_{\lambda}\int_{<2k_f}\frac{d^3q\,|W(q)|^2\beta|\underline{q}\cdot\underline{\varepsilon}_{q\lambda}|^2}{\left[e^{\beta\omega_{q\lambda}}-1\right]\left[1-e^{-\beta\omega_{q\lambda}}\right]}\cdot\left[q+\left(\frac{\beta\omega_{q\lambda}}{\pi}\right)^2\times\left(\frac{3k_f^2}{q}-\frac{q}{2}\right)\right] \qquad .....(2.4.1)$$

where $C'=\dfrac{3k}{MNe^2 16 v_f^2 k_f^4}$

In writing down (2.4.1) we have made use of the fact that in limit that $T>>T_{DEBYE}$ the $\omega_{q\lambda}^2$ term is negligible so that the Wiedmann-Franz law applies. L_0 in (2.4.1) is the familiar Lorentz constant.

In a manner completely analogous to that employed in section 2.1 in rewriting the resistivity in terms of $\alpha_{tr}^2 F(\omega)$, (2.4.1) can be

rewritten in terms of $\alpha_{tr}^2 F(\omega)$ and $\alpha^2 F(\omega)$ (see 2.1.26 and 2.1.27) as follows

$$W_{th}(T) = \frac{12\pi^3}{e^2 v_f k_f^2 L_o T} \int_o^\infty \frac{\omega\, d\omega}{(e^{\beta\omega}-1)(1-e^{-\beta\omega})} \left[\left(\beta - \frac{\beta^3\omega^2}{2\pi^2}\right) \cdot \alpha_{tr}^2 F(\omega) + \frac{3}{2}\frac{\beta^3\omega^2}{\pi^2} \cdot \alpha^2 F(\omega) \right] \qquad (2.4.2)$$

We again note the same economy as achieved in the electrical resistivity. All details of phonon frequencies, polarization vectors, and pseudopotential form factors are included in the $\alpha_{tr}^2 F(\omega)$ and $\alpha^2 F(\omega)$ functions, the determination of $W_{th}(T)$ is reduced to a simple integration which properly includes the temperature dependence.

To calculate $W_{th}(T)$, then, we need the $\alpha_{tr}^2 F(\omega)$ functions and, in addition, the $\alpha^2 F(\omega)$ function given by (2.1.27). It is obvious that a trivial modification of the programme to calculate $\alpha_{tr}^2 F(\omega)$ will give $\alpha^2 F(\omega)$ and in Figures (2.4.1) and (2.4.2) we show the $\alpha^2 F(\omega)$ functions for zero volume in the four metals. We have, of course, used the values of R_c already fixed from the electrical resistivity.

Since the temperature range of genuine interest in $W_{th}(T)$ is the low T region (MacDonald, White, and Woods 1956), we have ignored all volume effects in the calculation of $W_{th}(T)$ and all calculations shown are for zero lattice volume. In Figures (2.4.3), (2.4.4), (2.4.5), and (2.4.6) we compare our values with experiment. The experimental values are taken from MacDonald et. al. (1956). In each metal we have also plotted $W_{th}(T)$ obtained using the AW (Appapillai and Williams 1973) potential which is considered to be the best empirical potential available at the time of writing.

Fig. 2.4.1 The $\alpha^2F(\omega)$ functions in Nb and K, for zero lattice volume. $\alpha^2F(\omega)$ is dimensionless.

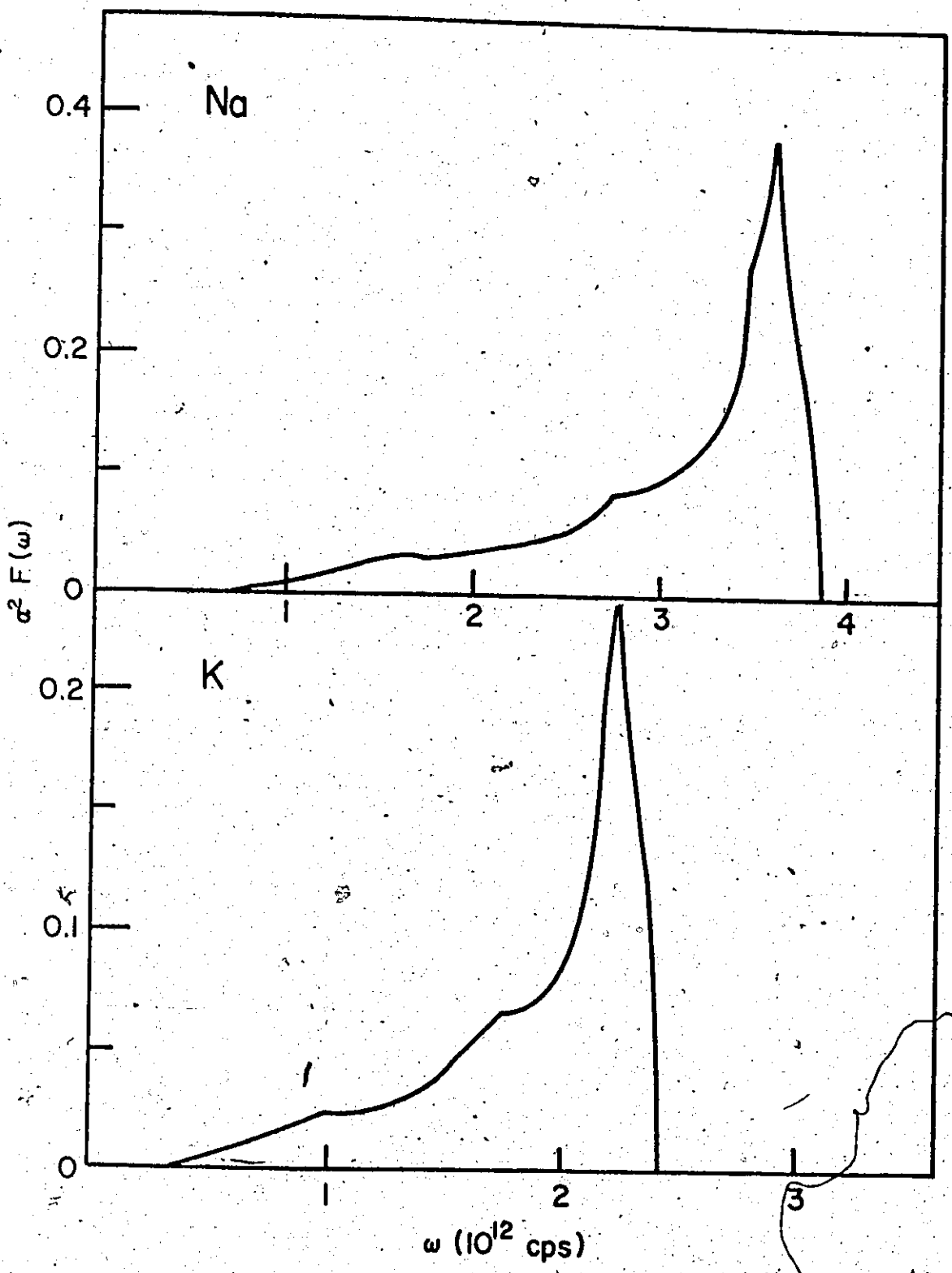
Na
K
0.4
0.2
0
0.2
0.1
0
1
2
3
4
1
2
3
$\alpha^2 F(\omega)$
ω (10^{12} cps)

Fig. 2.4.2 The $\alpha^2F(\omega)$ functions in Li and Rb, for zero lattice volume. $\alpha^2F(\omega)$ is dimensionless.

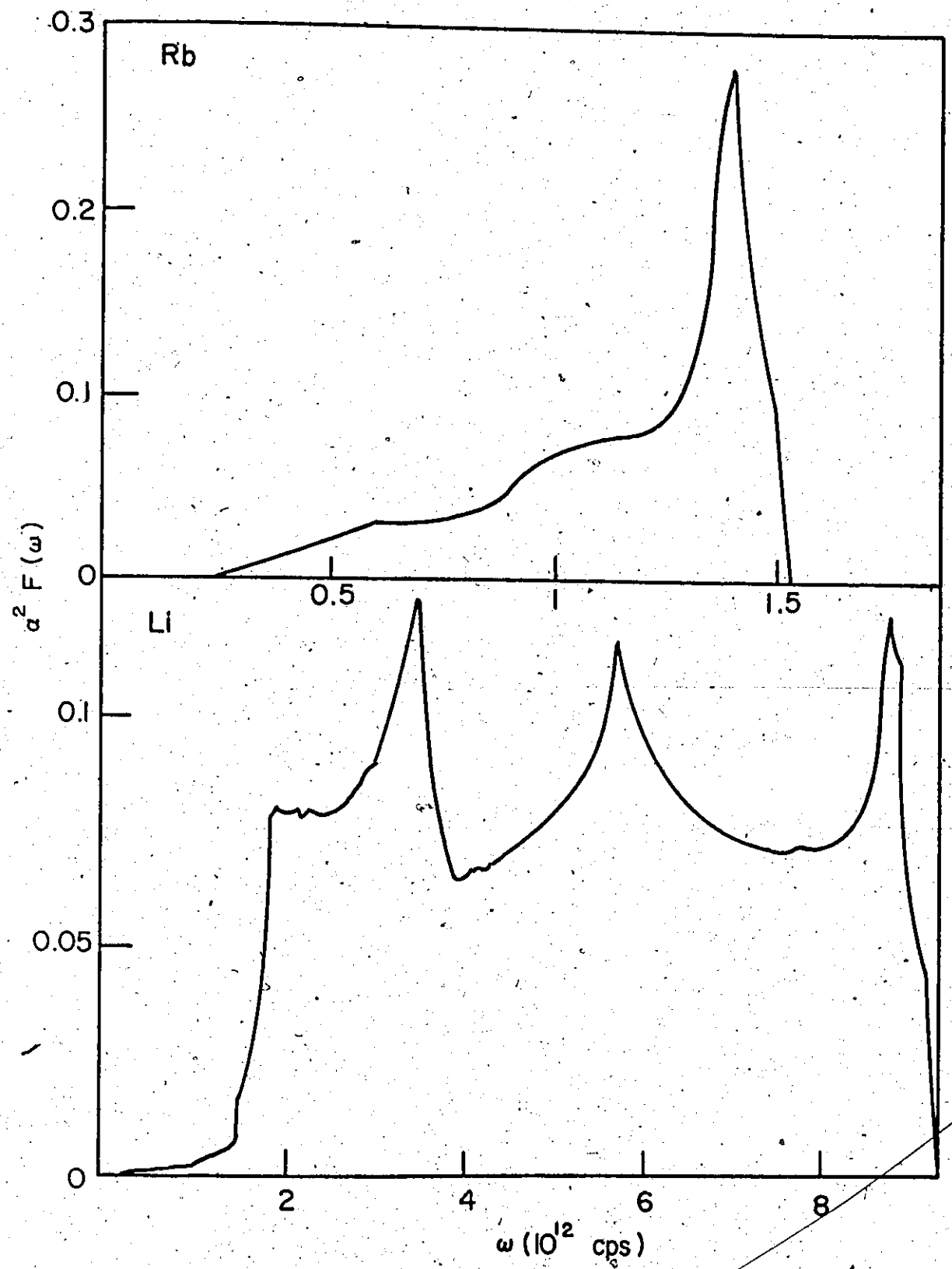
Rb
Li
0.3
0.2
0.1
0
0.5
1
1.5
0.1
0.05
0
2
4
6
8
$\alpha^2 F(\omega)$
ω (10^{12} cps)

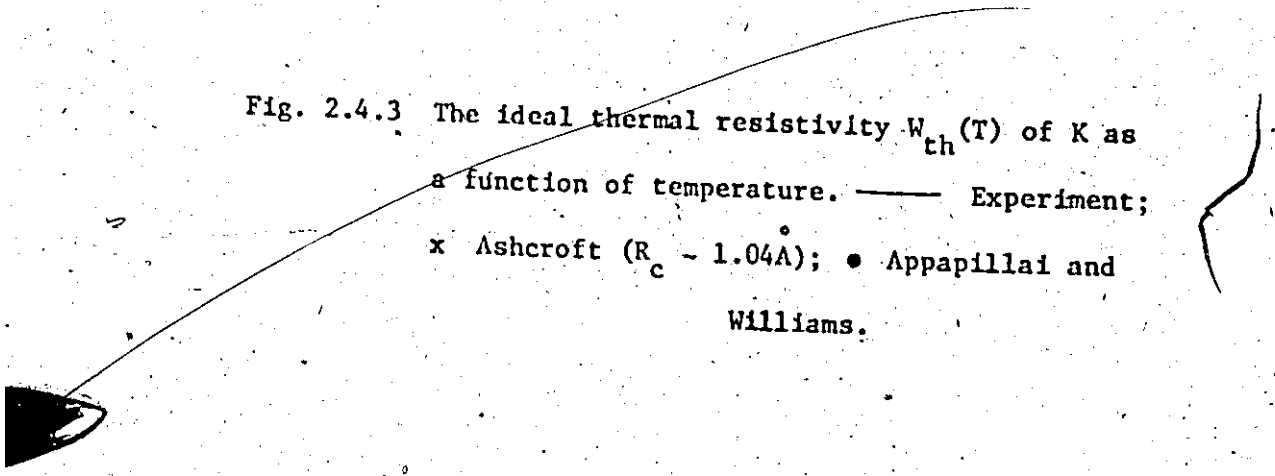

Fig. 2.4.3 The ideal thermal resistivity $W_{th}(T)$ of K as a function of temperature. ——— Experiment; x Ashcroft ($R_c \sim 1.04\text{Å}$); • Appapillai and Williams.

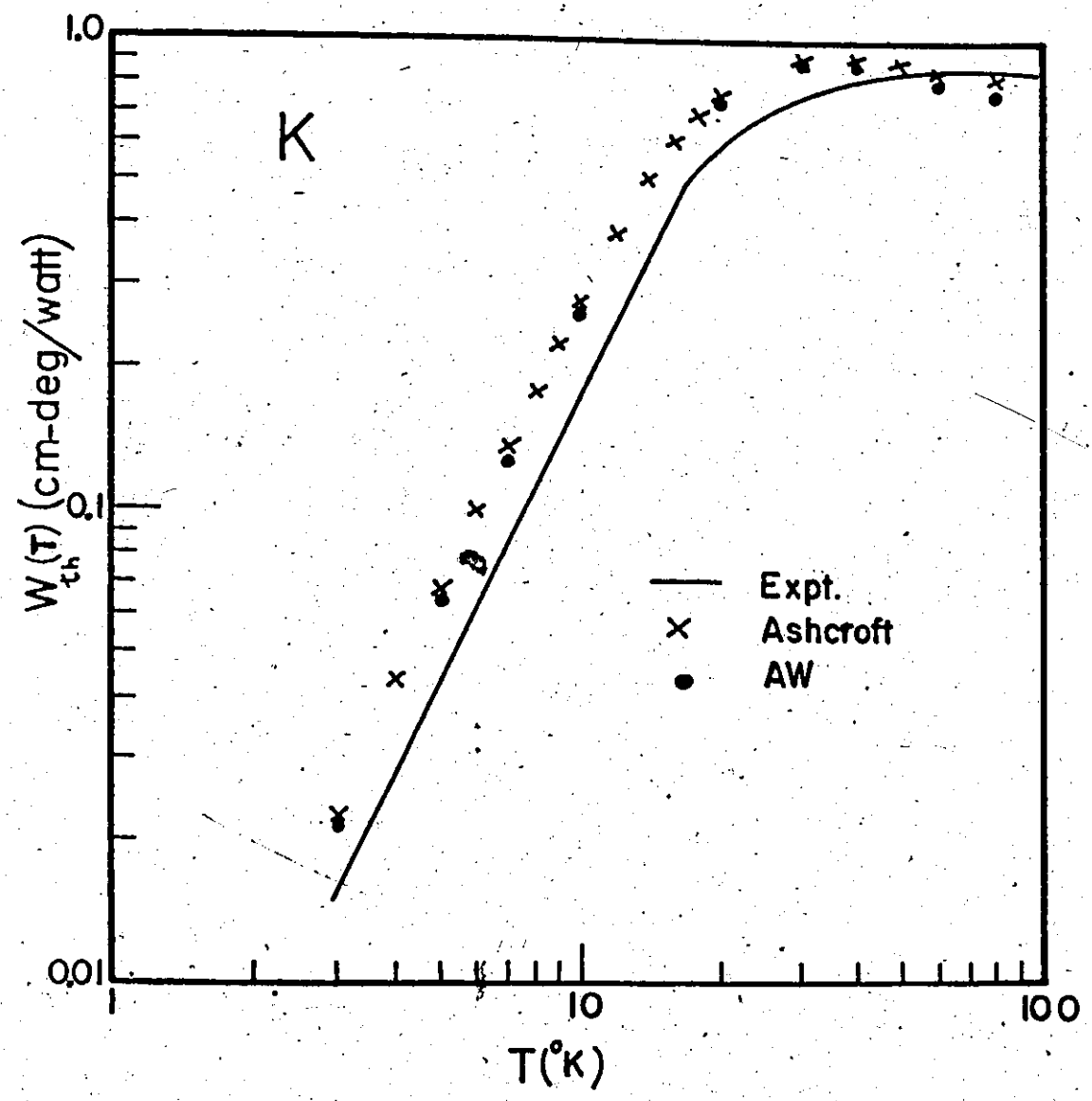
K
1.0
0.1
0.01
$W_{th}(T)$ (cm-deg/watt)
1
10
100
T(°K)
Expt.
Ashcroft
AW

Fig. 2.4.4 The ideal thermal resistivity $W_{th}(T)$ of Na as a function of temperature. ——— Experiment; x Ashcroft ($R_c \sim 0.83\text{Å}$); • Appapillai and Williams.

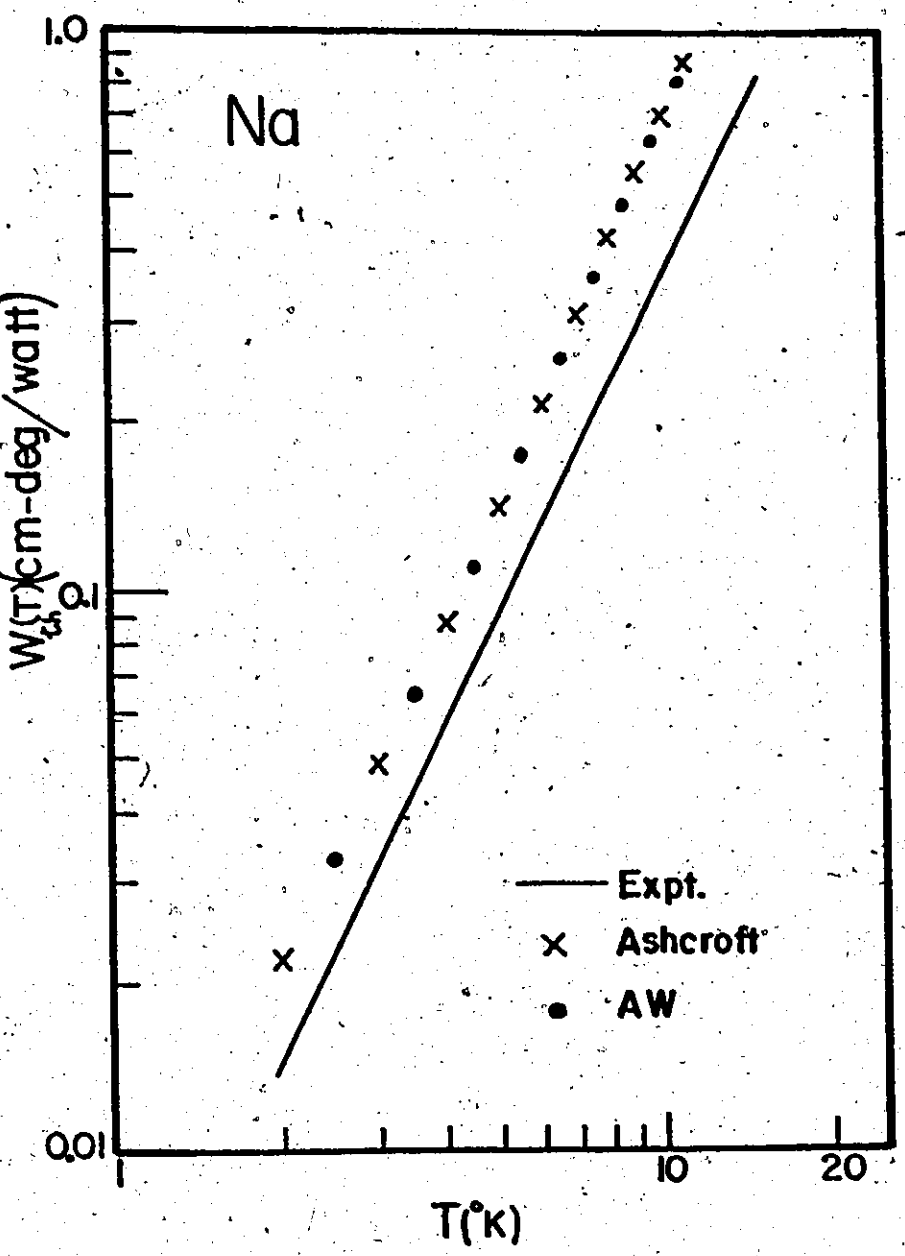
Na
1.0
0.1
0.01
W(T) (cm-deg/watt)
10
20
T(°K)
Expt.
Ashcroft
AW

Fig. 2.4.5 The ideal thermal resistivity $W_{th}(T)$ of Rb as a function of temperature. —— Experiment; x Ashcroft ($R_c \sim 1.04\text{Å}$); • Appapillai and Williams.

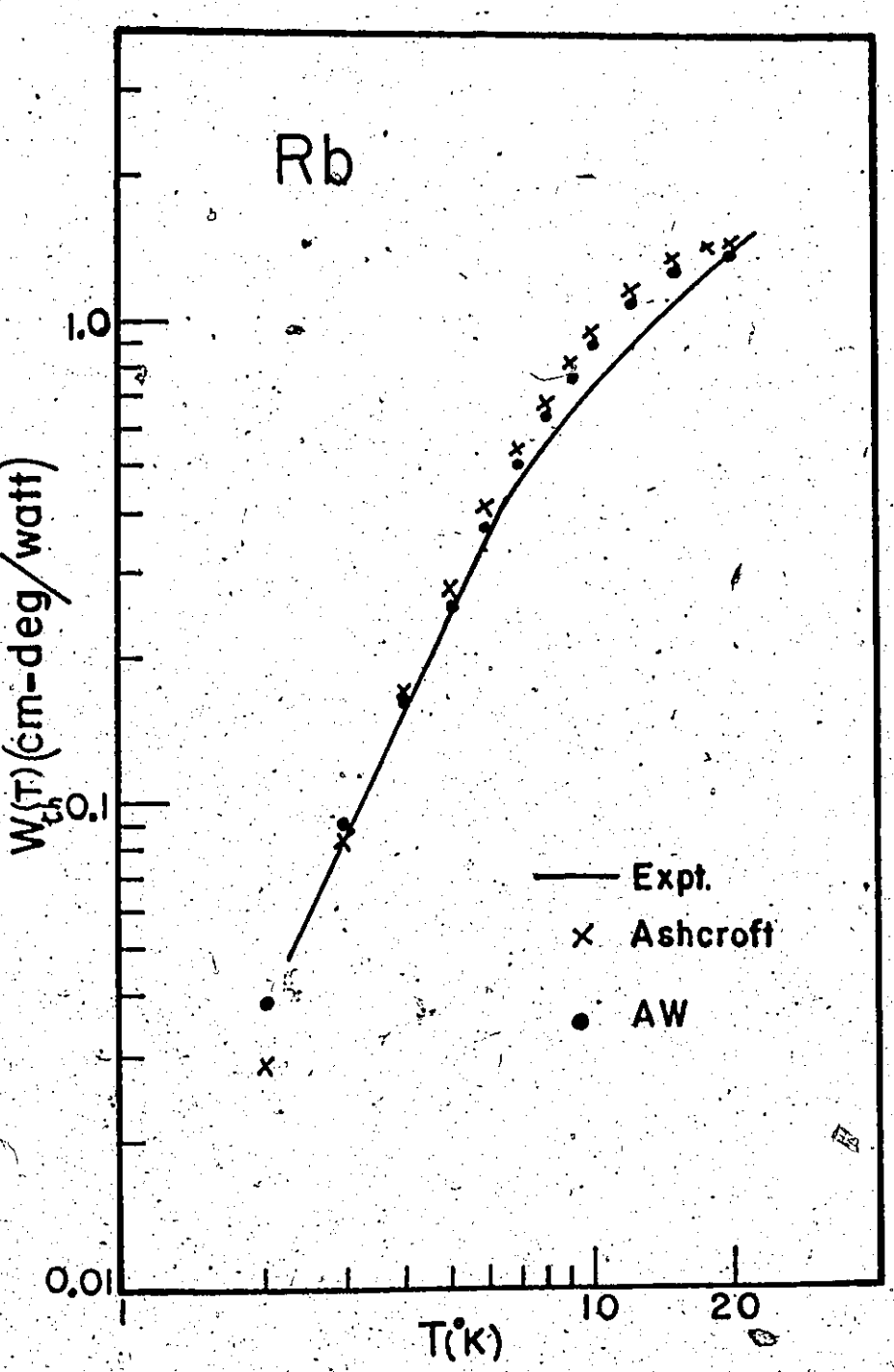
Rb
1.0
0.1
0.01
$W_c(T)$ (cm-deg/watt)
Expt.
Ashcroft
AW
10
20
T(°K)

Fig. 2.4.6 The ideal thermal resistivity $W_{th}(T)$ of Li as a function of temperature. —— Experiment; x Ashcroft ($R_c \sim 1.0\text{Å}$); • Appapillai and Williams.

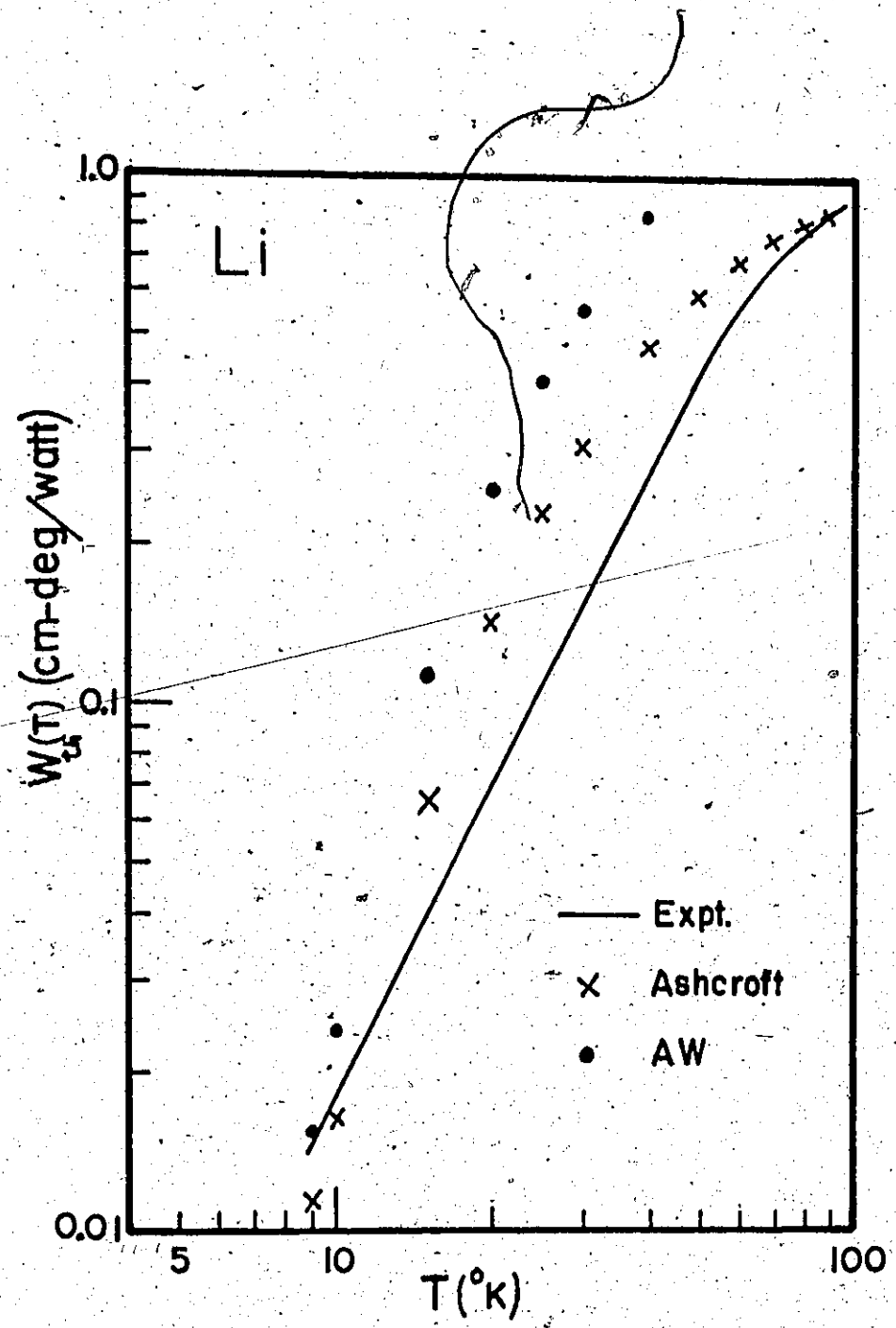
Li
1.0
0.1
0.01
$W_{ZS}(T)$ (cm-deg/watt)
5
10
100
T(°K)
Expt.
Ashcroft
AW

We notice that in the cases of K, Na, and Rb, the AW potential and our Ashcroft form give essentially the same values. This is in contrast to the electrical resistivity where the results of the two potentials differed more markedly. In Li, however, our potential gives a somewhat better description though neither agrees particularly well with experiment.

For our potentials the quantitative agreement is not quite as good as in the case of the electrical resistivity; however, it is still quite reasonable. A possible reason for the discrepancy could be that the first order variational expression for $W_{th}(T)$ is known to be less satisfactory compared to higher order expressions in the case of the thermal resistivity than for the corresponding situation in the electrical resistivity (Ziman 1960). One notes that our calculations are consistently higher than experiment and the use of higher order expressions is known to bring the numbers down. This stems, of course, from the essence of the variational principle.

We also note that in Na and Li, as mentioned before, a martensitic transformation takes place below ~ 40°K and ~ 80°K respectively and the experimental numbers used here are for the two phase mixture whereas our calculations are, of course, only for the bcc phase.

2.5 The Thermopowers

In this section we turn to an evaluation of the thermopowers of the four metals considered previously. If one writes the electrical current $\underline{J}$ and the thermal current $\underline{U}$ in terms of the applied electric field $\underline{E}$ and the temperature gradient $\underline{\nabla T}$ in the specimen, the following relations hold true (Ziman 1960)

$$\underline{J} = L_{EE}\underline{E} + L_{ET}\underline{\nabla T}$$
$$\underline{U} = L_{TE}\underline{E} + L_{TT}\underline{\nabla T} \qquad (2.5.1)$$

The L's are the macroscopic transport coefficients, and are properly speaking tensors. However, in cubic systems, they are simply scalars. The resistivity ρ is simply the reciprocal of L_{EE}, the thermal conductivity is $-\left(L_{TT} - \frac{L_{TE}\cdot L_{ET}}{L_{EE}}\right)$ and the thermopower Q, which is directly related to an electric field in a specimen subjected to a thermal gradient through $\underline{E} = Q\underline{\nabla T}$ is given by

$$Q = -\frac{L_{ET}}{L_{EE}} \qquad (2.5.2)$$

At high temperatures, using the standard variational solutions to the Boltzmann equation, Q can be written as (Ziman 1960; Dickey, Meyer, and Young 1967)

$$Q = -\left(\pi^2 k_B^2 T/3|e|E_F\right)\xi \qquad (2.5.3)$$

where ξ is a dimensionless parameter related to the electron-ion interaction and is given by

$$\xi = 3 - 2q - \tfrac{1}{2}r \qquad (2.5.4)$$

ξ essentially measures the rate of change of the resistivity with a change in the Fermi energy, all other quantities remaining the same. In the limit of a local energy independent pseudo-potential, as we are using here, the third term in (2.5.4) drops out (it measures the explicit rate of change of the form factors with energy—the energy of the sphere on which the electrons are scattering) and ξ reduces to

$$\xi = 3 - 2q = 3 - \frac{4|W(2k_F)|^2 S(2k_F)}{\int_0^2 |W(k_F r)|^2 S(k_F r) r^3 dr} \qquad (2.5.5)$$

TABLE 2.5.1

A COMPARISON OF EXPERIMENTAL AND CALCULATED VALUES OF ξ, THE PARAMETER WHICH APPEARS IN THE HIGH TEMPERATURE ELECTRON DIFFUSION THERMOPOWER, AND $d\ln Q/d\ln V$, THE VOLUME COEFFICIENT OF THE ELECTRON DIFFUSION THERMOPOWER

Metal	ξ		$d\ln Q/d\ln V$	
	Expt.	Theory	Expt.	Theory
Na	+2.7(+2.7)	+ 2.7	+ 2.10	- 0.58
K	+3.8(+4.7)	+ 2.7	- 0.36	- 0.52
Rb	+2.3	+ 1.8	+ 0.39	- 1.9
Li	-6.7(-5.2)	- 4.4	+ 0.43	+ 1.10

where $n = q/k_f$ and $S(q)$ is the angular average of the structure factor $S(q)$ and is given by (2.1.21) and (2.1.22). One can see from (2.5.5) that ξ is closely related to the size of the pseudo-potential at $2k_f$.

We have evaluated ξ and the volume dependence of Q for the four alkalis using our Ashcroft potentials and the results are tabulated and compared with experiment in Table (2.5.1).

If we first consider the values of ξ we note that the qualitative agreement is good. We predict the correct sign in all four cases and the magnitudes are reasonably good; whatever quantitative differences exist can perhaps be attributed to the neglect of the non-local contribution to ξ. One can understand the anomalous behaviour of Li quite simply. For the other three alkalis the pseudo-potential at $2k_f$ is quite small as can be seen from Figures (2.3.1) and (2.3.2). Thus q in (2.5.5) is small, and ξ is near 3. In Rb $W(2k_f)$ is larger than in the other two and this is reflected in the value of ξ. However, in Li, $W(2k_f)$ is very large and thus q is large and ξ turns out negative, in agreement with experiment.

The values of dlnQ/dlnV are in somewhat poorer agreement with experiment, in fact in Rb and Na we predict the wrong sign. This can perhaps be understood from two points of view (a) the neglect of the non-local part of ξ and (b) one notes that the sign of dlnQ/dlnV is determined (in our model) by the position of the node in W(q) relative to $2k_f$. This second point is explained further.

Under pressure the node moves to the left on the q-axis. Thus, if the node occurs to the right of $2k_f$, $W(2k_f)$ decreases and dlnQ/dlnV is negative. If it occurs to the left of $2k_f$, dlnQ/dlnV is positive.

Thus, any slight adjustment in the pseudo-potential around $2k_f$ (due, perhaps, to a better treatment of screening) could change the position of the node relative to $2k_f$, and thus affect the sign of dlnQ/dlnV. This is especially true if the node is very close to $2k_f$ as in the case of Na.

We might, therefore, suggest that explaining both the magnitude and sign of ζ and dlnQ/dlnV simultaneously would be a very stringent test for a pseudo-potential, especially in the region around $2k_f$.

We would also like to note that a more sophisticated treatment of this problem using phase-shifts and incorporating the non-local part of the electron-ion scattering has been attempted by Dickey, Meyer, and Young (1967) and one finds that their quantitative agreement is not much better than ours and besides, they also fail to predict the correct sign of dlnQ/dlnV in two of the alkalis (K and Rb). So perhaps our simple theory has worked as well as can be expected.

At low temperatures the dominant contribution to the thermopowers comes from a phenomenon which we have as yet not considered. The effect being referred to is known as "phonon drag" (Ziman 1960; MacDonald, Pearson and Templeton 1958). Fundamentally it arises as follows. In all our considerations above, we have assumed that, though the electron distribution is perturbed as a result of electron-phonon interactions which give rise to the resistivity etc., the phonon distribution is in its equilibrium configuration. This, of course, cannot be true — the phonons must be influenced to some extent by any change in the electron distribution. The assumption that the

phonon distribution is in equilibrium is sometimes referred to as the "Bloch assumption" since it was first made by Bloch (1928) in his pioneering treatment of the resistivities of simple metals. The assumption is equivalent to saying that $\phi_{\underline{q}}$, which measures the non-equilibrium part of the phonon distribution, is zero. The usual treatment of the problem (Ziman 1960) is to assume that $\phi_{\underline{q}}$ is not zero but is given by

$$\phi_{\underline{q}} \propto \underline{q} \cdot \underline{u} \tag{2.5.6}$$

where $\underline{u}$ is again a unit vector in the direction of the applied field. If this is incorporated into the solutions of the Boltzmann equation the following two formulae for the ideal electrical resistivity and the thermopower are obtained (Ziman 1960) (we are here using Ziman's notation)

$$\rho(T) = \rho_i(T)\left(1 - \frac{P_{IL}^2}{P_{II} P_{LL}}\right) \tag{2.5.7}$$

$$S(T) = \frac{k_B}{|e|} \cdot \frac{1}{n_\alpha} \cdot \left(\frac{C_L}{3Nk_B}\right) \cdot \frac{P_{IL}}{P_{LL}} \tag{2.5.8}$$

Here, $\rho_i(T)$ is the resistivity obtained without the phonon drag correction and is given by (2.1.25), S(T) is the phonon drag contribution to the thermopower, n_α is the number of free electrons per atom, C_L is the lattice specific heat and P_{II}, P_{IL}, and P_{LL} are integrals given by

$$P_{II} = C\beta \int_0^\infty \frac{\hbar\omega \cdot \alpha_{tr}^2 F(\omega)}{(e^{\beta\omega} - 1)(1 - e^{-\beta\omega})} d\omega \tag{2.5.9}$$

$$P_{IL} = C\beta \int_0^\infty \frac{\hbar\omega \cdot \alpha_{IL}^2 F(\omega)}{(e^{\beta\omega}-1)(1-e^{-\beta\omega})}\, d\omega$$

$$P_{LL} = C\beta \int_0^\infty \frac{\hbar\omega \cdot \alpha_{LL}^2 F(\omega)}{(e^{\beta\omega}-1)(1-e^{-\beta\omega})}\, d\omega \qquad (2.5.9)\ \text{(cont'd)}$$

where $C = \frac{4\pi}{e v_f \hbar}$, $\beta = (k_B T)^{-1}$, and $\alpha_{II}^2 F(\omega)$, $\alpha_{IL}^2 F(\omega)$, and $\alpha_{LL}^2 F(\omega)$ are the following

$$\alpha_{II}^2 F(\omega) = \alpha_{tr}^2 F(\omega) = \frac{1}{N}\sum_\lambda \int_{<2k_f} \frac{d^3q}{(2\pi)^3}\left[\frac{q\,|\underline{q}\cdot\underline{\epsilon}_{q\lambda}|^2 |W(q)|^2}{\omega_{q\lambda}} \cdot \frac{m}{8Mk_f^3}\right]\delta(\omega-\omega_{q\lambda})$$

$$\alpha_{IL}^2 F(\omega) = \frac{1}{N}\sum_\lambda \int_{<2k_f} \frac{d^3q}{(2\pi)^3}\left[\frac{(q\cdot q_{red.})\,|\underline{q}\cdot\underline{\epsilon}_{q\lambda}|^2 |W(q)|^2}{q^2\ \omega_{q\lambda}} \cdot \frac{m}{8Mk_f^3}\right]\delta(\omega-\omega_{q\lambda})$$

$$\alpha_{LL}^2 F(\omega) = \frac{1}{N}\sum_\lambda \int_{<2k_f} \frac{d^3q}{(2\pi)^3}\left[\frac{q_{red.}^2\,|\underline{q}\cdot\underline{\epsilon}_{q\lambda}|^2 |W(q)|^2}{q^2\ \omega_{q\lambda}} \cdot \frac{m}{8Mk_f^3}\right]\delta(\omega-\omega_{q\lambda}) \qquad .....(2.5.10)$$

We note that $\alpha_{II}^2 F(\omega)$ is identical to $\alpha_{tr}^2 F(\omega)$, and this arises due to the fact that P_{II} is directly related to the resistivity ρ_i through

$$\rho_i(T) = P_{II} \cdot \frac{3\pi^2\hbar}{e k_f^3} \qquad (2.5.11)$$

and that $\alpha_{IL}^2 F(\omega)$ and $\alpha_{LL}^2 F(\omega)$ are similar to $\alpha_{tr}^2 F(\omega)$ except that the q^2 factor which appears in $\alpha_{tr}^2 F(\omega)$ ($\underline{q} = \underline{k} - \underline{k}'$, $\underline{k}$ and $\underline{k}'$ are the electron wave vectors) is replaced by $\underline{q}\cdot\underline{q}_{red}$ ($\underline{q}_{red}$ being $\underline{q}$ reduced to the FBZ) and q_{red}^2, in $\alpha_{IL}^2 F$ and $\alpha_{LL}^2 F$ respectively.

We note here that in writing down (2.5.9) and (2.5.10) we have

proceeded in exactly the same fashion as when rewriting the resistivity in terms of $\alpha_{tr}^2 F(\omega)$.

It is clear, then, that to evaluate (2.5.7) and (2.5.8) one merely has to determine the additional functions $\alpha_{IL}^2 F(\omega)$ and $\alpha_{LL}^2 F(\omega)$. It is also clear that only a trivial modification of the programme to calculate $\alpha_{tr}^2 F(\omega)$ will suffice to produce these two functions. In addition, in (2.5.8) we need the lattice specific heat C_L. Though this can be obtained from experiment we prefer, for the sake of consistency, to evaluate it using the following expression (Ziman 1960)

$$C_L(T) = N k_B \int_0^\infty \frac{(\hbar\omega\beta)^2 e^{\hbar\omega\beta}}{(e^{\hbar\omega\beta}-1)^2} F(\omega) d\omega \qquad (2.5.12)$$

where $F(\omega)$ is the phonon density of states.

Accordingly, then, we have determined the distributions $\alpha_{IL}^2 F(\omega)$ and $\alpha_{LL}^2 F(\omega)$ in the four metals being considered here and have used them to evaluate the effects of phonon drag on the resistivity and the thermopower according to (2.5.7) and (2.5.8).

We start by showing the three distributions, for zero lattice volume, in each of the four metals in Figures (2.5.1), (2.5.2), (2.5.3), and (2.5.4). One notes in particular that in each case $\alpha_{IL}^2 F(\omega)$ has regions which are negative. This is discussed below.

The expression for $\alpha_{IL}^2 F(\omega)$ contains a factor $q \cdot q_{red}$ which, for most Umklapp processes, is negative since q and q_{red} will in general be in essentially opposite directions. Thus the shape of $\alpha_{IL}^2 F(\omega)$ is sensitive to the geometry of the scattering processes and, in particular, to the weighting given to the Umklapp contributions.

Fig. 2.5.1 The $\alpha^2_{II}F(\omega)$, $\alpha^2_{IL}F(\omega)$, and $\alpha^2_{LL}F(\omega)$ functions in Na.

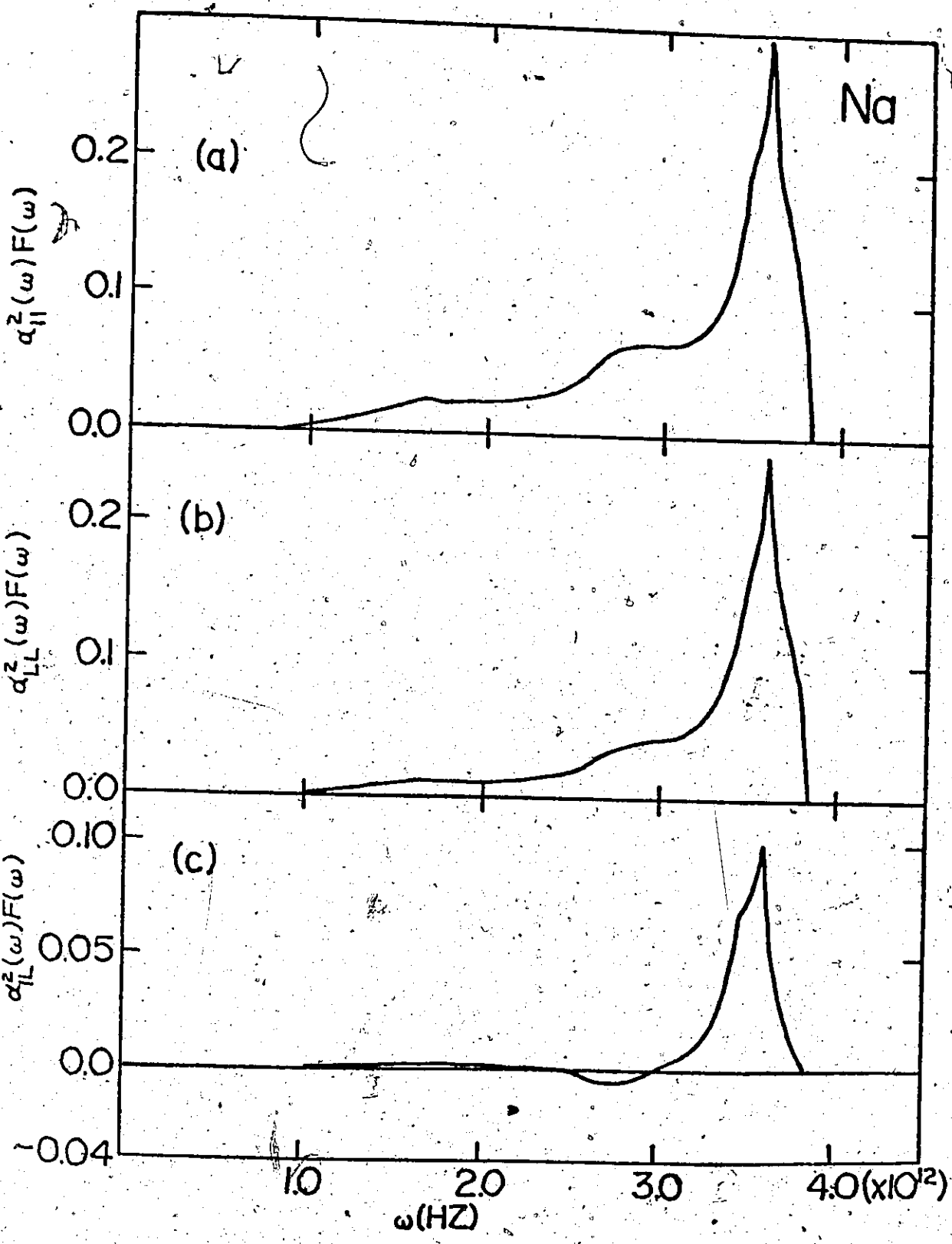
Na
(a)
(b)
(c)
$\alpha_{11}^2(\omega)F(\omega)$
$\alpha_{LL}^2(\omega)F(\omega)$
$\alpha_{TL}^2(\omega)F(\omega)$
0.2
0.1
0.0
0.2
0.1
0.0
0.10
0.05
0.0
-0.04
1.0
2.0
3.0
4.0(x10^{12})
ω(HZ)

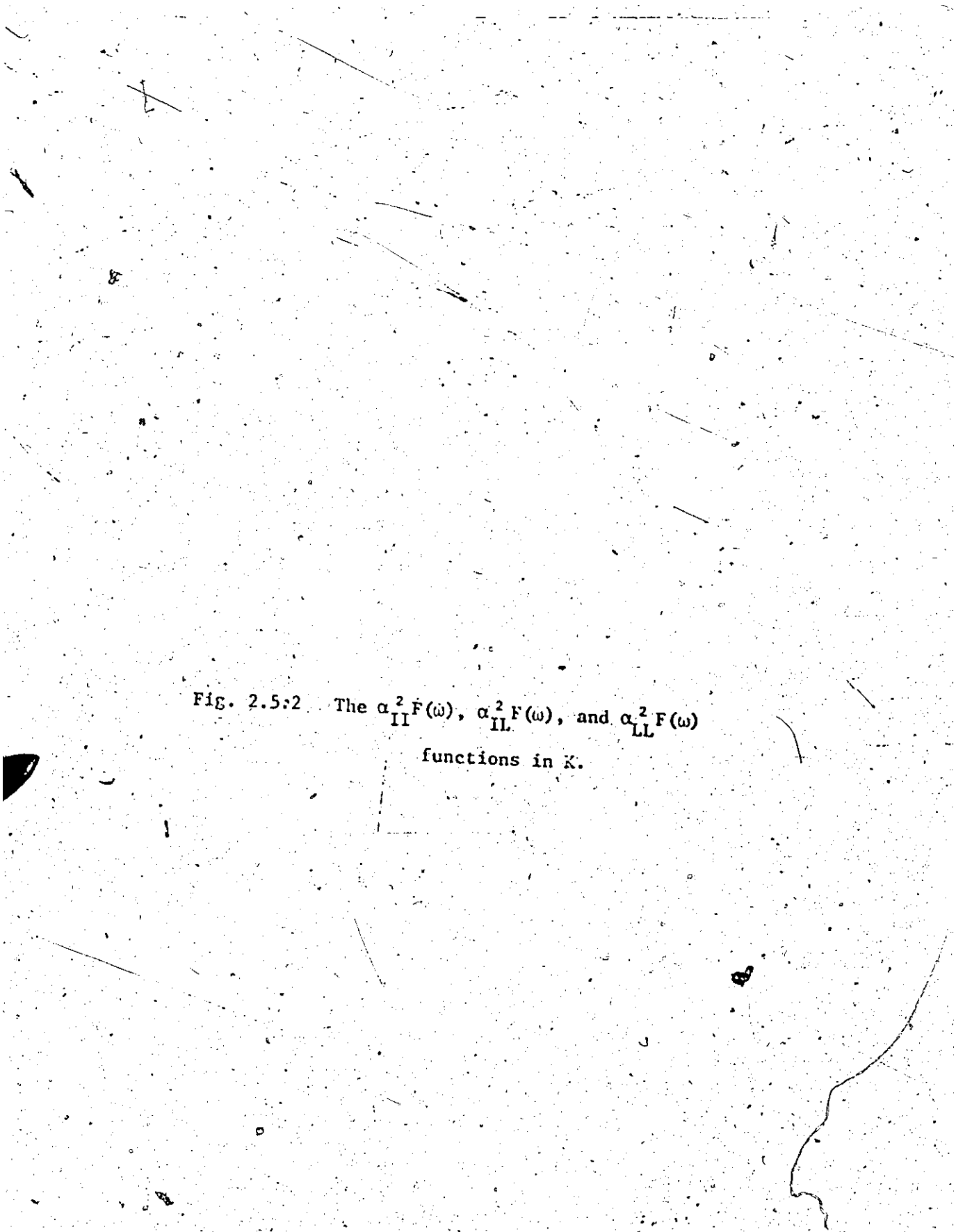

Fig. 2.5.2 The $\alpha^2_{II}F(\omega)$, $\alpha^2_{IL}F(\omega)$, and $\alpha^2_{LL}F(\omega)$ functions in K.

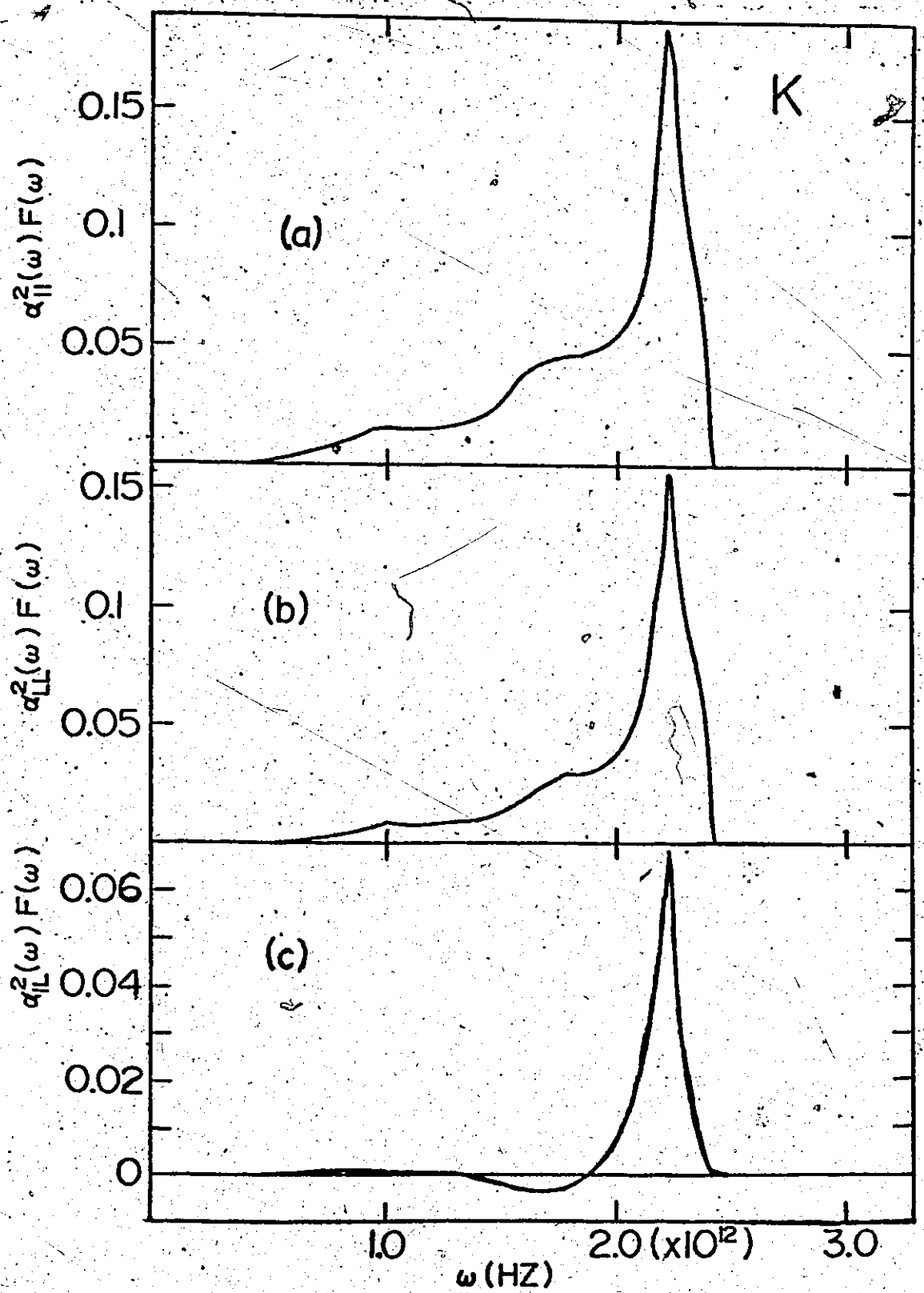
K
(a)
(b)
(c)
$\alpha^2_{11}(\omega)F(\omega)$
$\alpha^2_{LL}(\omega)F(\omega)$
$\alpha^2_{1L}(\omega)F(\omega)$
0.15
0.1
0.05
0.06
0.04
0.02
0
1.0
2.0 (x10^{12})
3.0
ω (HZ)

Fig. 2.5.3 The $\alpha_{II}^2 F(\omega)$, $\alpha_{IL}^2 F(\omega)$, and $\alpha_{LL}^2 F(\omega)$ functions in Rb.

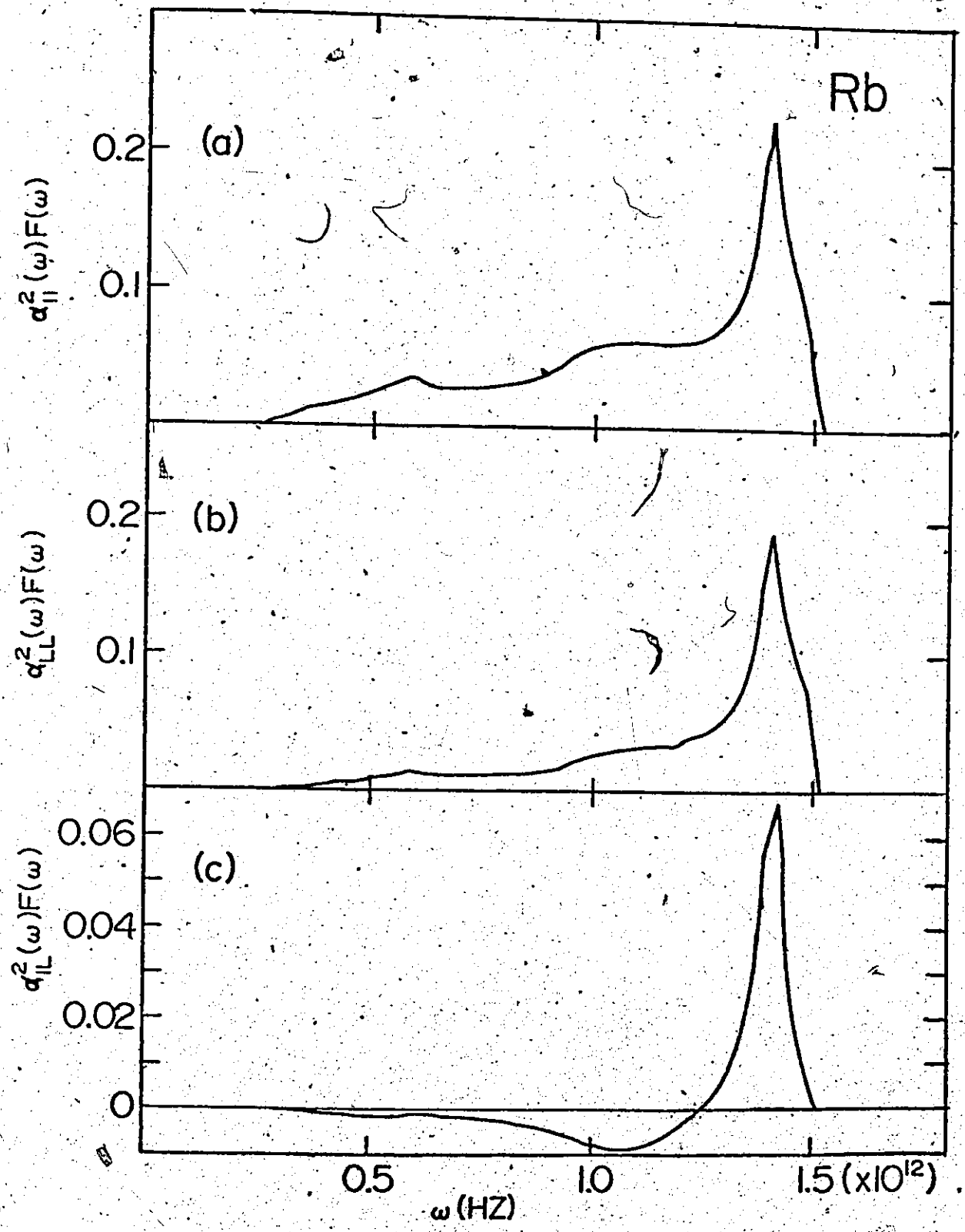
Rb
(a)
(b)
(c)
0.2
0.1
0.2
0.1
0.06
0.04
0.02
0
$\alpha_{11}^2(\omega)F(\omega)$
$\alpha_{LL}^2(\omega)F(\omega)$
$\alpha_{IL}^2(\omega)F(\omega)$
0.5
1.0
1.5 (x10¹²)
ω (HZ)

Fig. 2.5.4 The $\alpha^2_{II}F(\omega)$, $\alpha^2_{IL}F(\omega)$, and $\alpha^2_{LL}F(\omega)$ functions in Li.

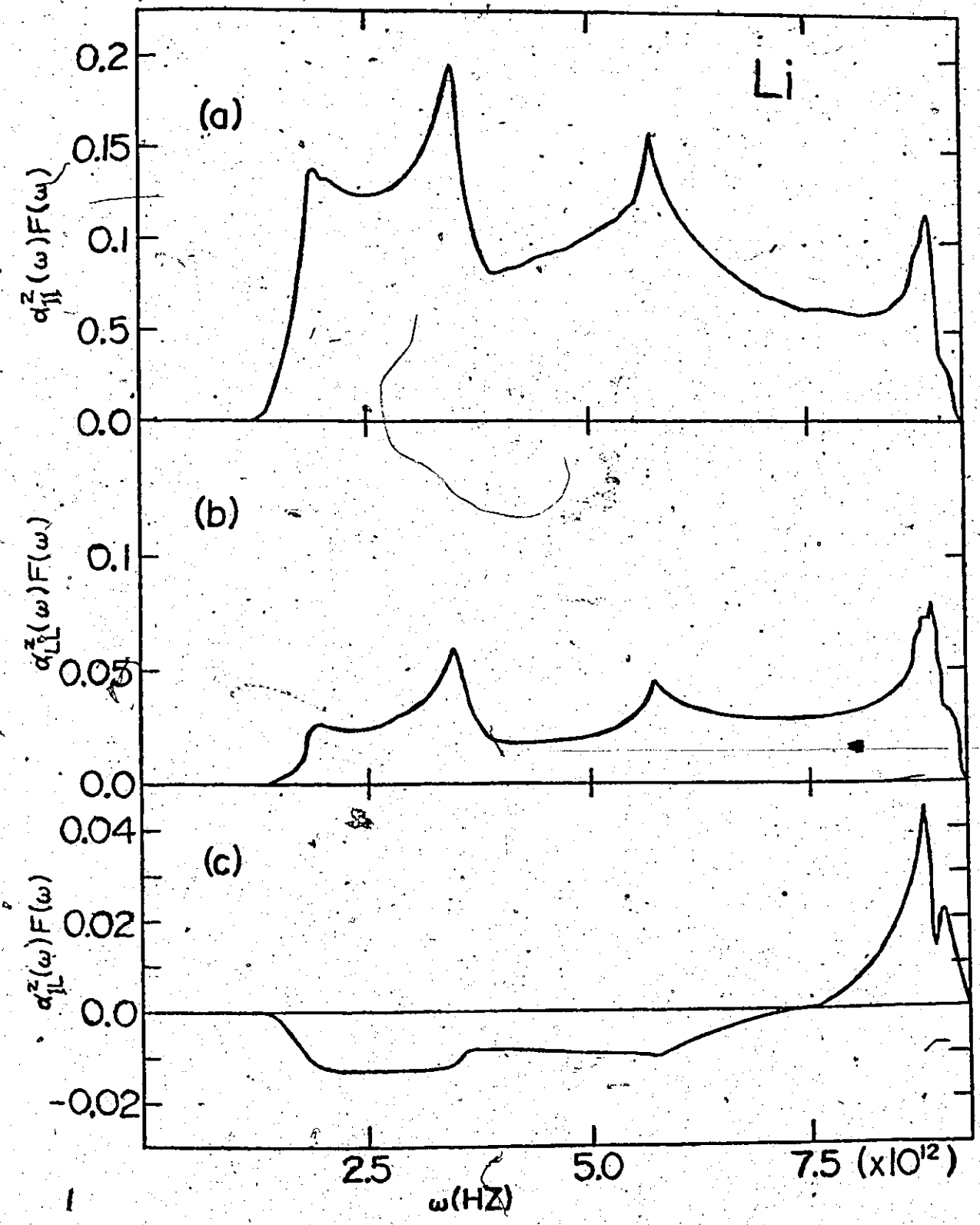
Li
(a)
(b)
(c)
0.2
0.15
0.1
0.5
0.0
0.1
0.05
0.0
0.04
0.02
0.0
-0.02
$\alpha^2_{11}(\omega)F(\omega)$
$\alpha^2_{LL}(\omega)F(\omega)$
$\alpha^2_{1L}(\omega)F(\omega)$
2.5
5.0
7.5 (x10^{12})
ω(HZ)

it will be very sensitive to the shape of the pseudo-potential employed. If Umklapp processes are heavily weighted (W(q) large around $2k_f$), as in the case of Li and to a somewhat lesser extent in Rb, the $\alpha^2_{IL}F(\omega)$ distributions for these two metals will be more extensively negative than in the cases of Na and K where W(q) for $q \sim 2k_f$ is definitely smaller. This is clearly seen in the plots of $\alpha^2_{IL}F(\omega)$, the most negative of the distributions being in Li, followed by Rb, and the least negative being K and Na.

The $\alpha^2_{LL}F(\omega)$ distributions are essentially similar in shape to the $\alpha^2_{II}F(\omega)$ except that the low ω regions are relatively smaller. This is quite simply due to the fact that the Umklapp processes (which contribute in the low ω region) are now weighted by a q^2_{red} instead of a q^2.

Thus the shape of the thermopower vs. temperature curve will be sensitively determined by the shape of the $\alpha^2_{IL}F(\omega)$ distribution (through P_{IL} which appears in (2.5.8)) which is in turn very dependent on the shape of the pseudo-potential. We would, therefore, expect this effect to be a stringent test of the pseudo-potentials employed here.

In Figure (2.5.5) we show the thermopower vs. temperature curves obtained. One notes the quite different behaviours observed. For the lowest temperatures all four metals have S negative. This is due to the fact that since the Fermi surface does not intersect zone boundaries in the alkalis of (at least in our model) the lowest regions ($\omega < \sim 0.9\ \omega_{max}$) all the distributions considered here are completely determined by Normal processes only—this is the familiar "freezing out of

Fig. 2.5.5 A plot of the calculated values of the phonon drag component of the thermo-power as a function of temperature in Na, K, Rb and Li.

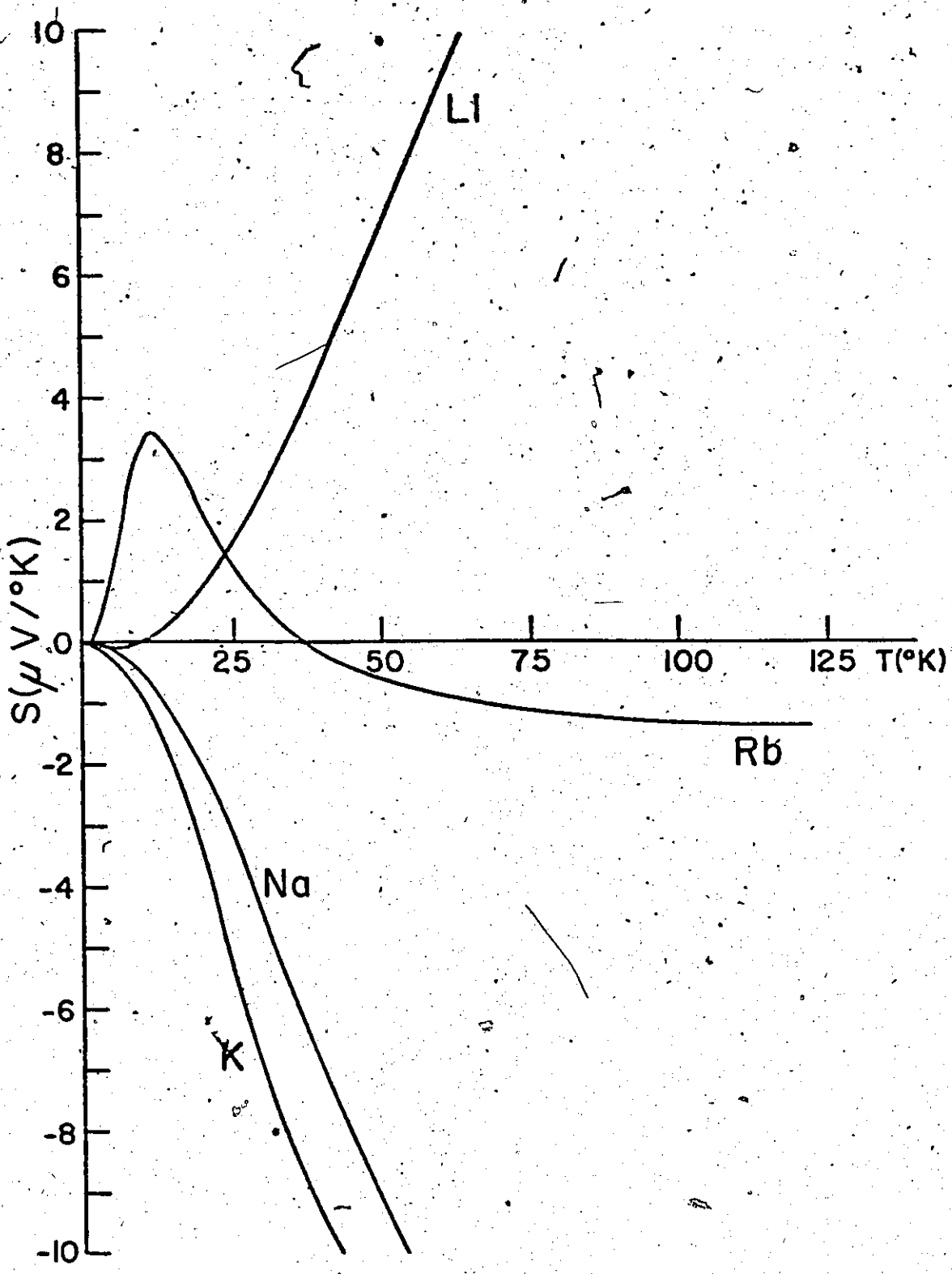
10
8
6
4
2
0
-2
-4
-6
-8
-10
S(μV/°K)
25
50
75
100
125
T(°K)
Li
Rb
Na
K

Fig. 2.5.6 A plot of the experimental values of the phonon drag component of the thermopower as a function of T/θ_D (θ_D is the Debye temperature) in Na, K, Rb and Li. The insert contains θ_D for the four metals.

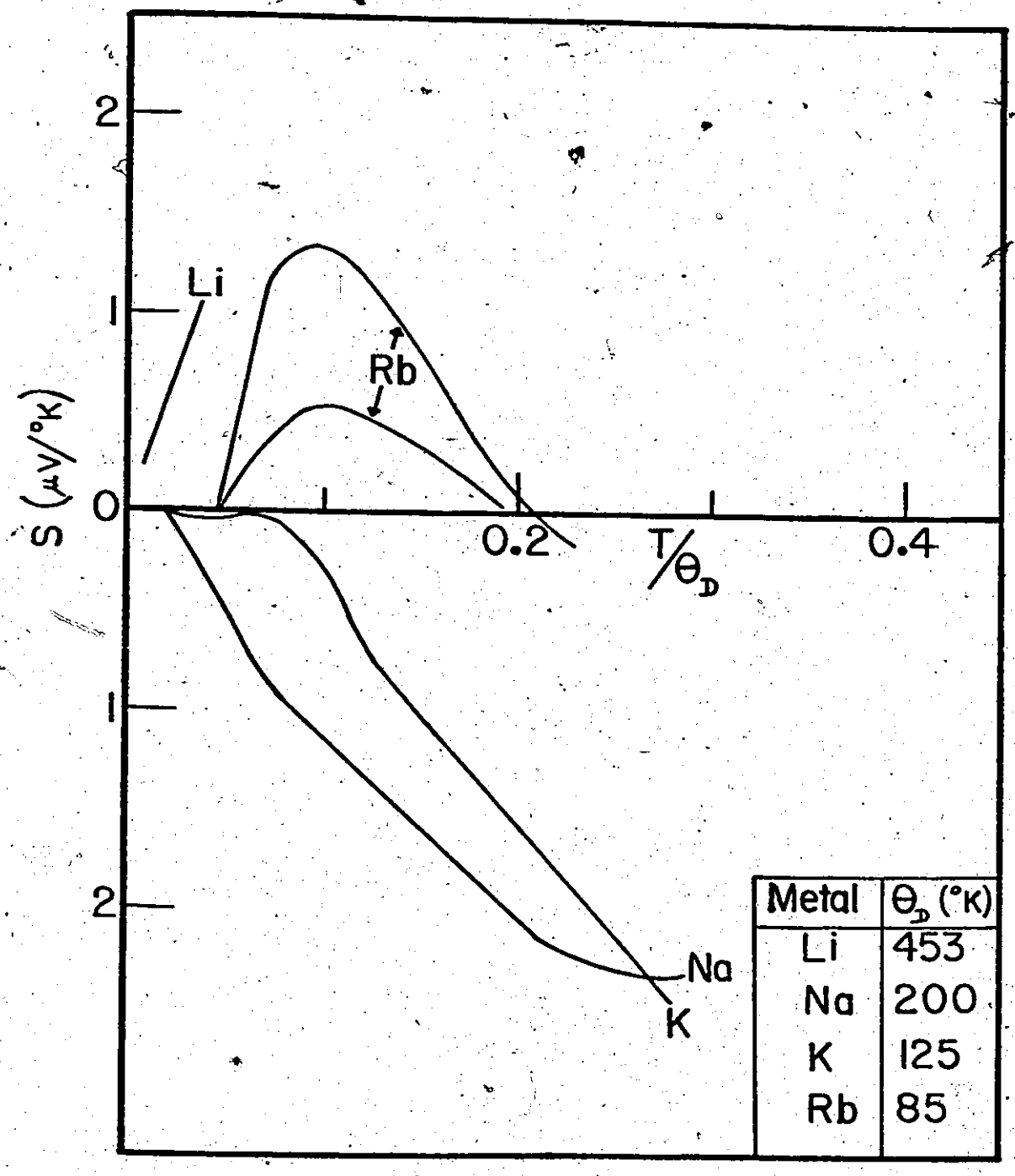

Metal	θ_D (°K)
Li	453
Na	200
K	125
Rb	85

Umklapps" discussed by Ziman (1960), Collins and Ziman (1961), Bailyn (1960). Thus in the $\alpha^2_{IL}F(\omega)$ distribution the lowest region is always positive and S is thus negative. However, as the exponentials in the expression for P_{IL} (2.5.9) begin to sample higher regions in ω the negative contributions come into play and, depending on how strong they are, affect the shape of the S(T) curves. In Li, which has the most negative $\alpha^2_{IL}F(\omega)$, the negative regions dominate and S goes through zero and continues increasingly positive. In Rb, S goes through zero, becomes positive, but then as the negative regions of $\alpha^2_{IL}F(\omega)$ are not as strong as in Li, comes back down through another zero and continues negative. In Na and K S(T) is always negative.

This behaviour in our calculated curves is in remarkable qualitative agreement with experiment. Essentially these features are displayed by the experimental curves of MacDonald, Pearson, and Templeton (1958). These are shown in Figure (2.5.6). One notes here that there are no adjustable parameters in our calculations. The values of R_c in the Ashcroft potential used have been fixed since the original calculations of the resistivity in section 2.3. The quantitative difference which exists between the two sets of curves is due to the fact that we have not included a phonon-phonon scattering time which appears as an additional contribution to the $P_{LL}(T)$ integral. Collins and Ziman (1961) indicate how this time might be estimated but, as there appears to be some considerable uncertainty in obtaining a reliable value for it, we have decided to exclude this effect. Collins and Ziman (1961), however, do show that the inclusion of this time does reduce the magnitude of S(T) while not significantly affecting the

shape of the curves.

We have indicated above that this effect is very sensitive to the shape of the pseudo-potential employed and although this is to some extent brought out in the different behaviours of the four metals we would like to emphasize this further by considering four different pseudo-potentials in K. The potentials considered are (a) Ashcroft with our "best" R_c of ~ 1.04Å, (b) Ashcroft with our "rejected" R_c of ~ 1.27Å, (c) the Bardeen pseudo-potential (Bardeen 1937) and (d) the lower Lee-Falicov (LLF) potential (Lee and Falicov 1968). This last potential has been obtained from a fit to Fermi surface data. Plots of the four potentials are shown in Figure (2.5.7). In Figure (2.5.8) we show the $\alpha^2_{IL}F(\omega)$ function over the whole frequency range for the other three potentials used and though some differences appear, we would like to emphasize these by showing in Figure (2.5.9) the low frequency part of the $\alpha^2_{IL}F(\omega)$ distributions for each of the four potentials. As is obvious from the plots the behaviour depends very much in detail on the form factors employed. In particular the shape and size of the negative region varies considerably with potential. This is, of course, due to the delicate balance which exists between amounts of Umklapp processes with $q_{red}\cdot q$ negative compared with $q_{red}\cdot q$ positive and Normal processes. This, in turn, depends on the shape of the pseudo-potential and in particular W(q) at $q \sim 2k_f$.

The different shapes of the $\alpha^2_{IL}F(\omega)$ function affect the S(T) vs. T curves which are shown in Figure (2.5.10) and one observes the very different behaviour which results with each potential.

Fig. 2.5.7 Plots of the various pseudo-potential form factors in K. o - o Ashcroft $R_c \sim 1.27\text{Å}$; —— Ashcroft $R_c \sim 1.04\text{Å}$; x - Lower Lee-Falicov; --- Bardeen.

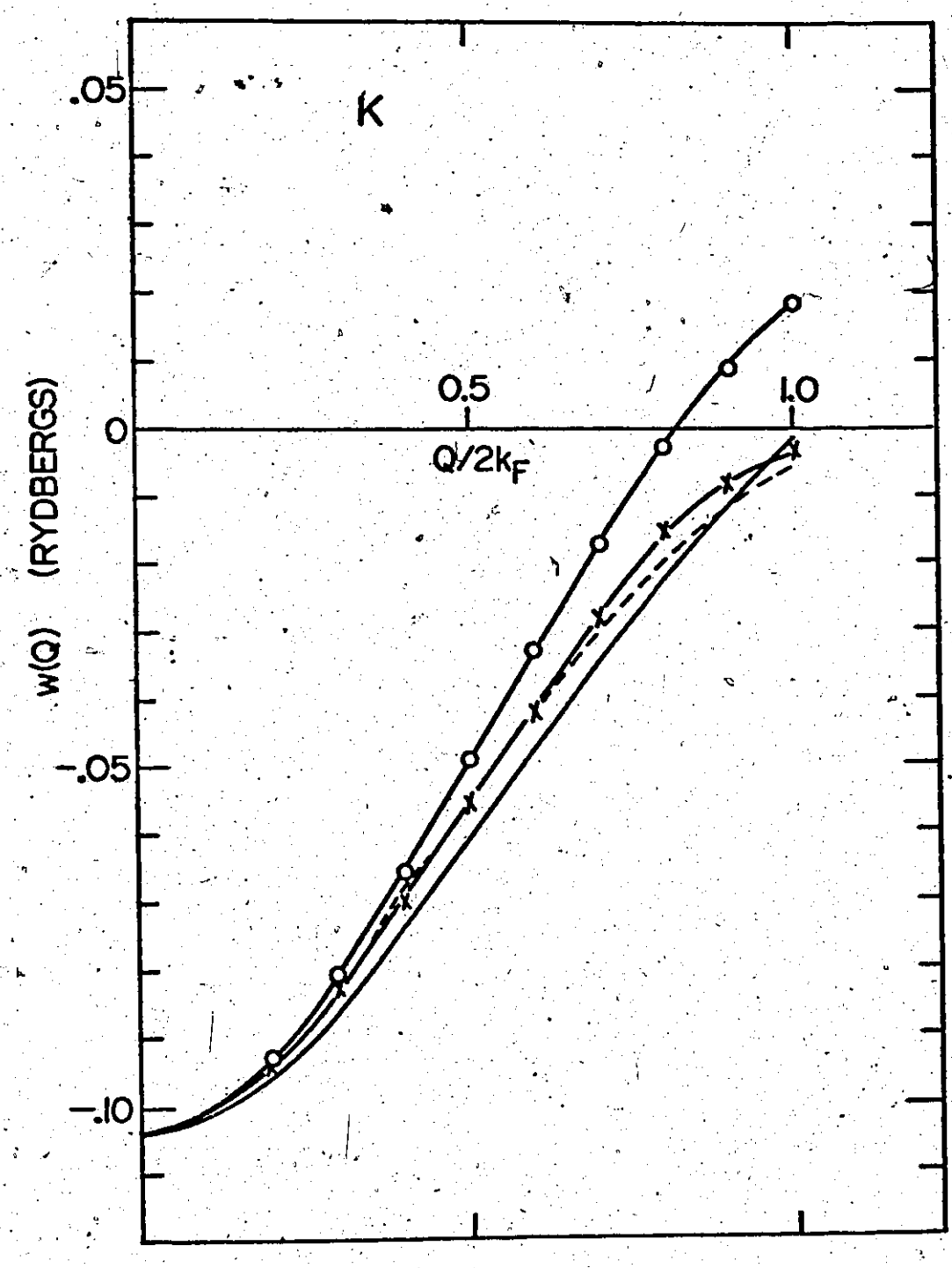
K
.05
0
-.05
-.10
0.5
1.0
Q/2k_F
w(Q) (RYDBERGS)

Fig. 2.5.8 The $\alpha^2_{IL}F(\omega)$ functions over the whole frequency range in K using the Ashcroft ($R_c \sim 1.27\text{Å}$), the Bardeen, and the lower Lee-Falicov potentials.

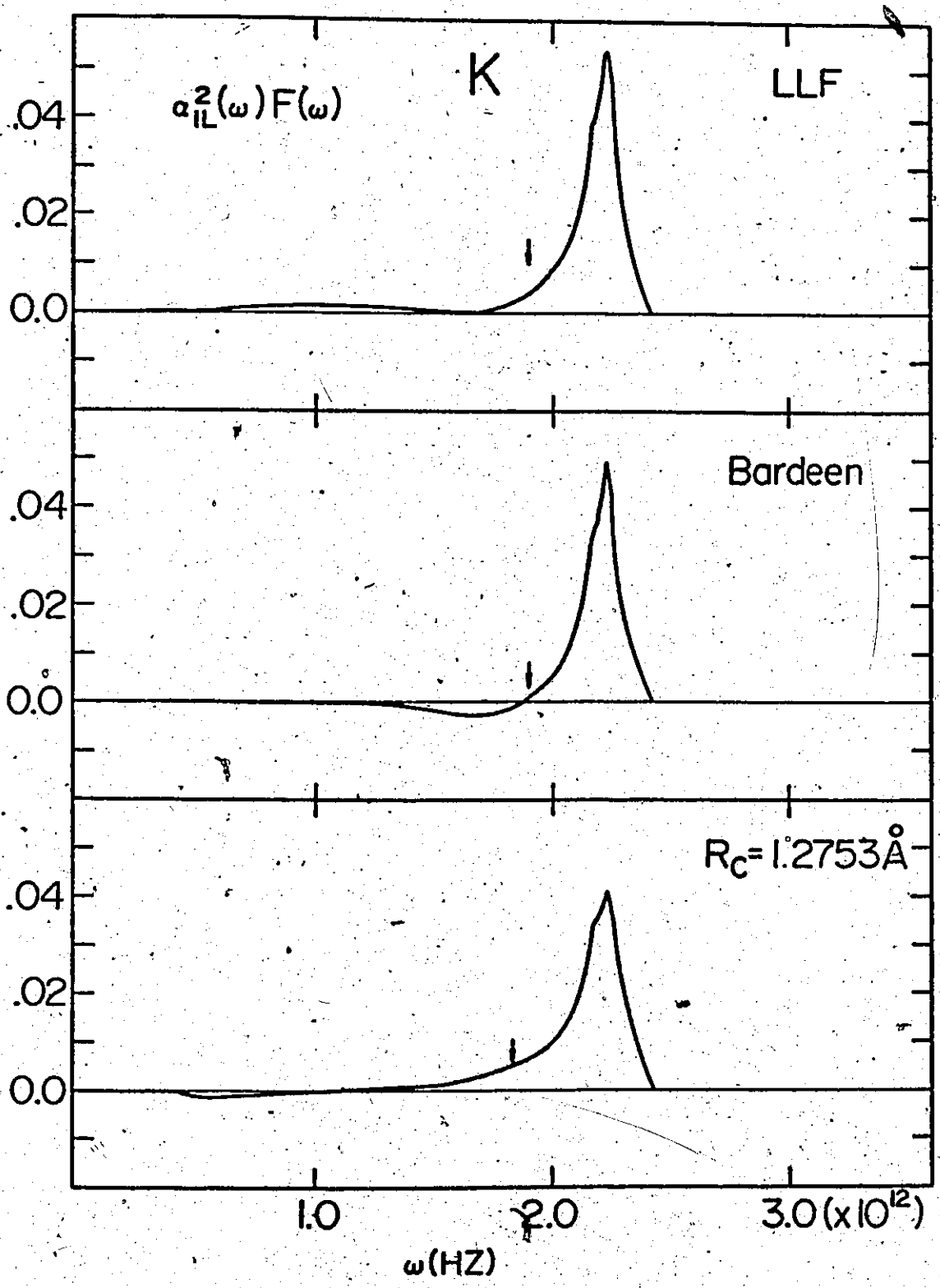
K
LLF
$\alpha^2_{IL}(\omega)F(\omega)$
.04
.02
0.0
Bardeen
R_c= 1.2753Å
1.0
2.0
3.0 (x10^{12})
ω(HZ)

Fig. 2.5.9 The low frequency parts of the $\alpha^2_{IL}F(\omega)$ functions in K using the four potentials of Fig. 2.5.7.

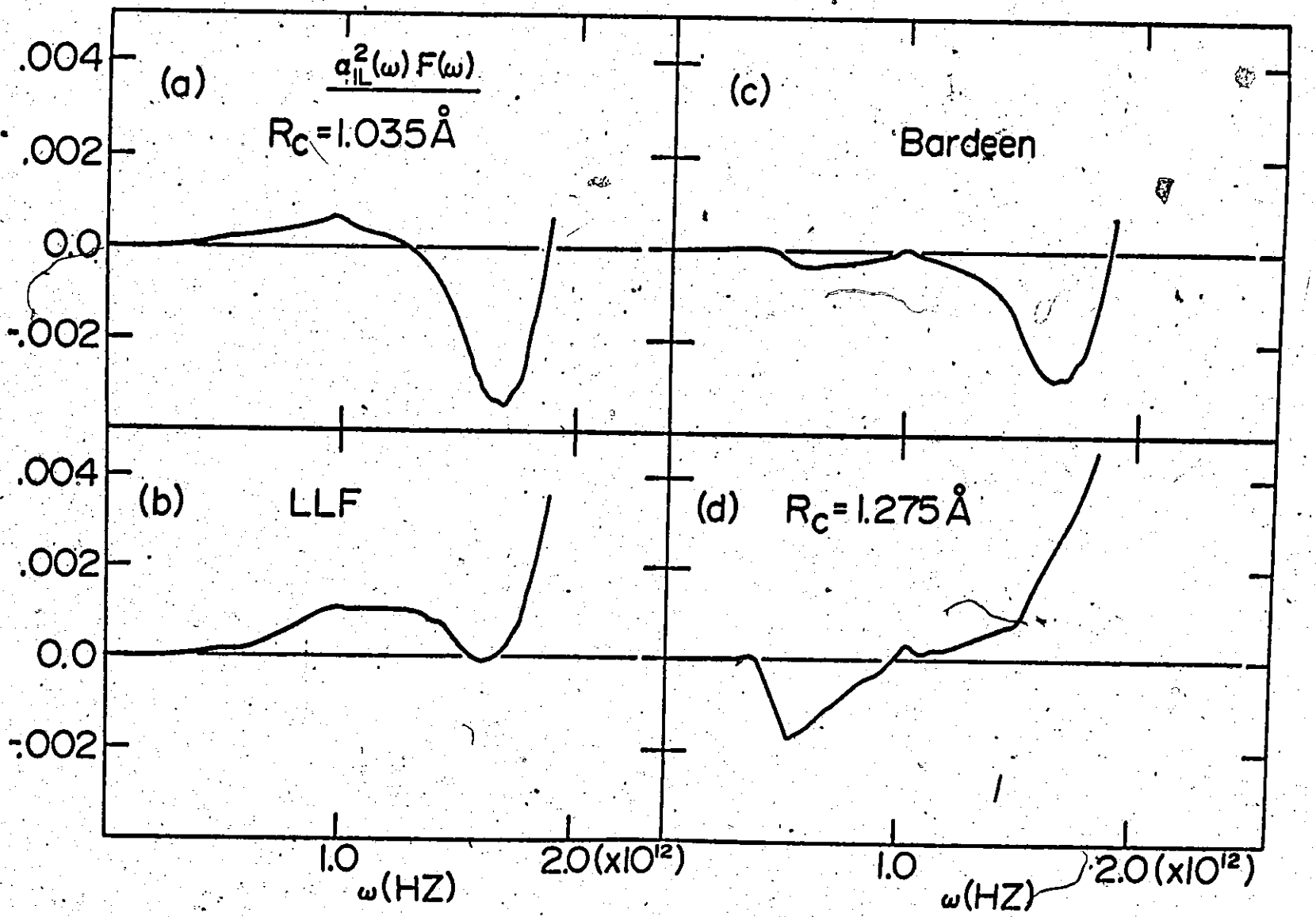
.004
.002
0.0
-.002
(a)
$\alpha^2_{IL}(\omega)\,F(\omega)$
R_c = 1.035 Å
(c)
Bardeen
(b)
LLF
(d)
R_c = 1.275 Å
1.0
2.0 (x10¹²)
ω(HZ)

Fig. 2.5.10 The phonon drag component of the thermopower as a function of temperature in K for the four potentials of Fig. 2.5.7.

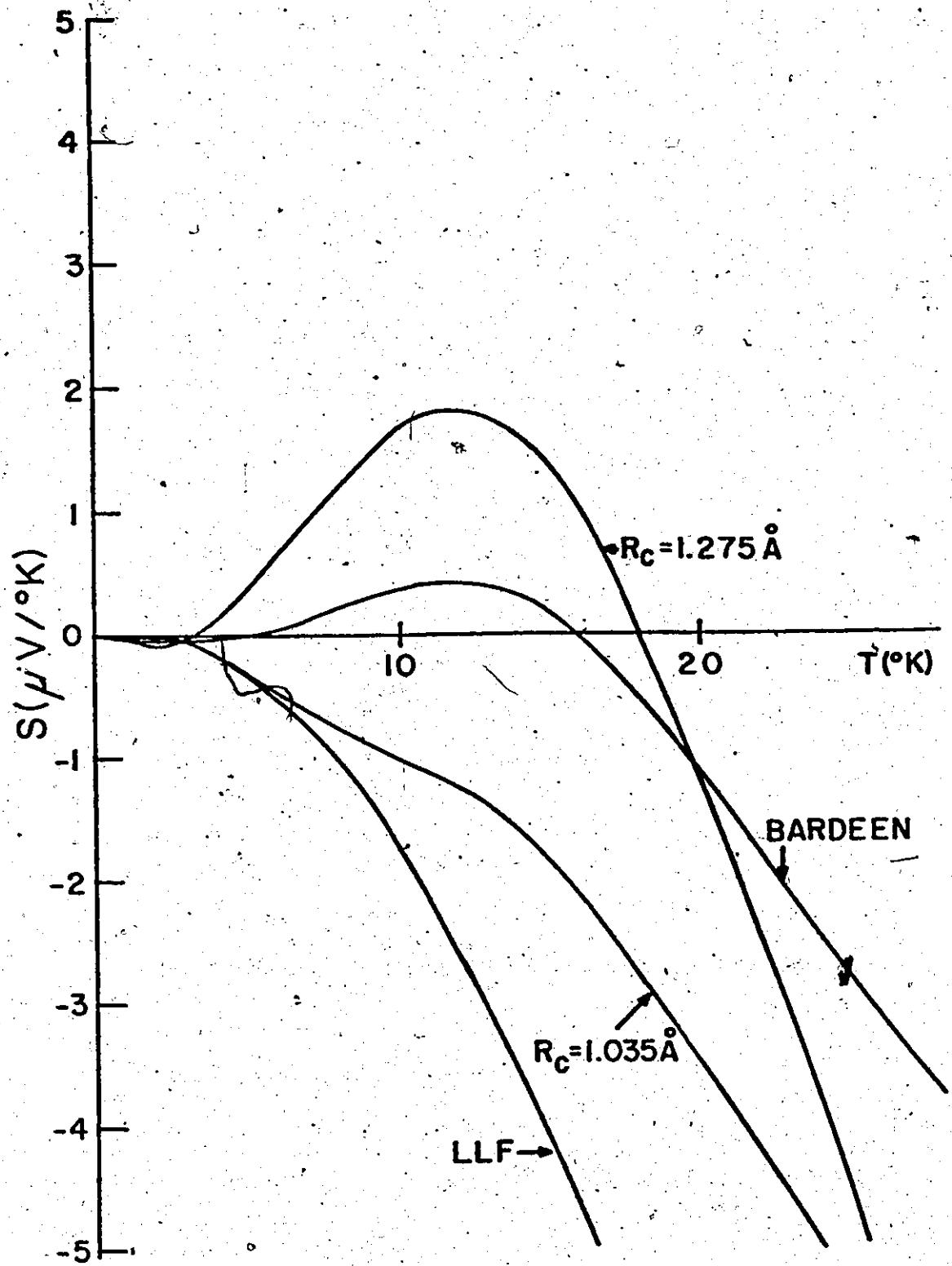
5
4
3
2
1
0
-1
-2
-3
-4
-5
S(μV/°K)
10
20
T(°K)
R_c=1.275 Å
BARDEEN
R_c=1.035Å
LLF

Having hopefully demonstrated that this effect is particularly sensitive to the form of pseudo-potential employed, we feel quite gratified that our original potentials have been able (with no further adjustment) to account for the observed experimental behaviour.

The phonon drag effect also has quite a major effect on the very low temperature electrical resistivity as can be seen from (2.5.7). We will consider this in some detail in the concluding section of this chapter (section 2.6) where we will briefly discuss the very low T behaviour of the electrical and thermal resistivities in the context of the most elementary variational solutions to the Boltzmann equation, and in particular will look at the supposed T^5 and T^2 behaviours of $\rho(T)$ and $W_{th}(T)$ which are expected in the Bloch model.

2.6 The Very Low Temperature Behaviour Of The Electrical And Thermal Resistivities. The Bloch T^5 And T^2 Laws. The Effect Of Phonon Drag On The Low Temperature Electrical Resistivity

The standard assumption in the Bloch-Grüneisen theory is that for $T \ll \theta_D$ (the Debye temperature) $\rho(T)$ will go as T^5, and $W_{th}(T)$ will go as T^2. These behaviours are predicated on the following assumptions (Ziman 1960):

(a) Neglect of Umklapp processes.

(b) A Debye spectrum for the phonons.

(c) A constant electron-ion scattering amplitude (no q dependence of $W(q)$).

In the alkalis considered here the Fermi surface does not touch the zone boundaries. Therefore, for very small phonon frequencies only

Fig. 2.6.1 A plot of $\rho(T)/T^5$ and $\omega(T)/T^2$ vs T in K showing the Normal plus Umklapp (N+U) and Normal only (N) contributions.

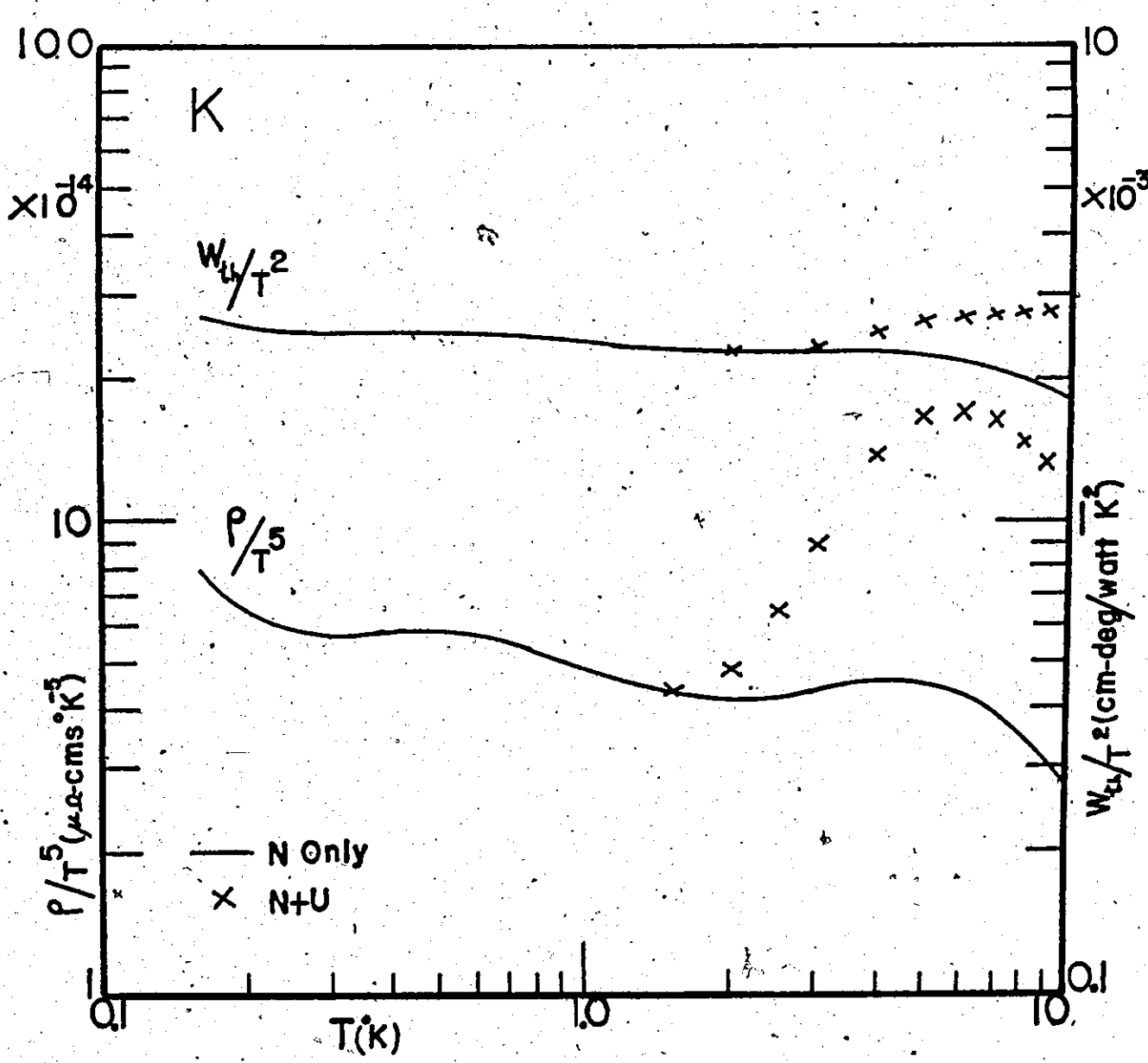
K
100
10
0.1
1.0
10
$\times 10^{-4}$
$\times 10^{-3}$
W_{LL}/T^2
ρ/T^5
ρ/T^5 ($\mu\Omega$-cms°K^{-3})
W_{LL}/T^2 (cm-deg/watt K^2)
T(K)
N Only
N+U

Normal processes are possible and the low ω ends of $\alpha^2_{tr}F(\omega)$ and $\alpha^2F(\omega)$ will be completely determined by Normal processes only. Thus for very low T, (a) is reasonably tenable. Assumption (b) is also reasonable since for very low ω the dispersion curves are essentially linear. However, assumption (c) is untenable. Even for very small q there is still some q dependence of $W(q)$.

In order to see to what extent the T^5 and T^2 are valid (at least theoretically) we have calculated especially accurately (particularly near the origin) $\alpha^2_{tr}F(\omega)$ and $\alpha^2F(\omega)$ in K and in Figure (2.6.1) we show plots of $\rho(T)/T^5$ and $W_{th}(T)/T^2$ in K. The crossed curves are when both Normal and Umklapp processes are present and the solid curves when only Normal processes are allowed. It is clear that the onset of Umklapp processes occurs at $T \sim 1.5°K$ in $\rho(T)$ and for $T \sim 2.5°K$ in $W_{th}(T)$. Below those temperatures one would expect the T^5 and T^2 behaviours to manifest themselves. However, as is clear from the general downward trend of the two curves, the q dependence of the pseudo-potential, however small for low q, is still sufficient to alter the behaviour to T dependences which are slower than T^5 and T^2. We consider these calculations to be as accurate numerically as is presently possible and thus feel safe in concluding that the T^5 and T^2 laws do not hold even in the simplest model.

In the above considerations we have neglected the effect of phonon drag on the electrical resistivity and that this effect is quite significant is demonstrated below.

In section 2.5, we indicated that when the effects of phonon drag are considered (Ziman 1960) the resistivity is given by

$$\rho(T) = \rho_i(T)\left[1 - \frac{P_{IL}^2(T)}{P_{II}(T)P_{LL}(T)}\right] \qquad (2.6.1)$$

where $\rho_i(T)$ is the resistivity without phonon drag corrections and $P_{IL}(T)$, $P_{II}(T)$, and $P_{LL}(T)$ are given by equations (2.5.9). The P_{IL}, P_{II}, and P_{LL} integrals are in turn determined by the $\alpha^2_{IL}F(\omega)$, $\alpha^2_{II}F(\omega)$, and $\alpha^2_{LL}F(\omega)$ distributions as given by (2.5.10).

One notes first of all that for the very lowest frequencies only Normal processes are possible and that, therefore, the three distributions will be identical for very low ω. This is, of course, due to the fact that $\mathbf{q} \cdot \mathbf{q} = \mathbf{q}_{red} \cdot \mathbf{q} = \mathbf{q}_{red} \cdot \mathbf{q}_{red}$ for Normal processes. Thus the factor in brackets in (2.6.1) will go exponentially to zero for very low T, (the exponential behaviour arising from the thermal factors which appear in each of the integrals (2.5.9)), and thus the resistivity can be expected to have an exponential dependence on T as opposed to power laws as mentioned above. This has been noted recently in a calculation by Kaveh and Wiser (1972b) and also in an experimental measurement of the very low T($\lesssim$ 4.0°K) resistivity in potassium done by Gugan (1971).

In addition, the shape of the $\alpha^2_{IL}F(\omega)$ functions have interesting effects on the correction term which appears in (2.6.1). In Tables (2.6.1) and (2.6.2) we have shown the size of the correction term in the four metals as a function of T for various select temperatures. One notes that in K the effect is negligible above 10°K, and in Rb

TABLE 2.6.1

THE RATIO OF THE RESISTIVITY WITH ($\rho(T)$) AND WITHOUT ($\rho_i(T)$) PHONON DRAG CORRECTIONS AS A FUNCTION OF TEMPERATURE IN K AND Rb

K		Rb	
T(°K)	$\rho(T)/\rho_L(T)$	T(°K)	$\rho(T)/\rho_L(T)$
1.0	.00061	1.0	.35855
1.2	.00332	1.1	.54380
1.4	.01359	1.2	.70733
1.6	.04192	1.3	.8277
1.8	.09978	1.4	.9059
2.0	.19052	1.5	.95238
2.6	.53674	1.6	.97811
3.0	.70831	1.7	.99134
3.6	.84929	1.8	.99745
4.0	.89731	1.9	.99970
5.0	.95198	2.0	.99993
6.0	.97242		
7.0	.98216		
10.0	.99333		

TABLE 2.6.2

THE RATIO OF THE RESISTIVITY WITH ($\rho(T)$) AND WITHOUT ($\rho_i(T)$) PHONON DRAG CONTRIBUTIONS AS A FUNCTION OF TEMPERATURE IN Na AND Li

Na		Li	
T(°K)	$\rho(T)/\rho_L(T)$	T(°K)	$\rho(T)/\rho_L(T)$
2.0	.00129	2.0	.00011
2.2	.00352	2.4	.00102
2.4	.00856	3.0	.00946
2.6	.01859	3.4	.03008
2.8	.03629	3.6	.05110
3.0	.06425	4.0	.13366
3.4	.15601	4.6	.39834
3.6	.21815	5.0	.62525
4.0	.35959	5.6	.88045
4.6	.56162	6.0	.96328
5.0	.66643	7.0	.99608
5.6	.77624	8.0	.96849
6.0	.82506	9.0	.94911
6.6	.87428	10.0	.93969
7.0	.89644	12.0	.93432
8.0	.93077	14.0	.93485
9.0	.94919	20.0	.94101
10.0	.96019	30.0	.94879

Fig. 2.6.2 A plot of the ratio of the resistivity with phonon drag contributions $\rho(T)$, to the resistivity without phonon drag $\rho_i(T)$, as a function of temperature, in Li.

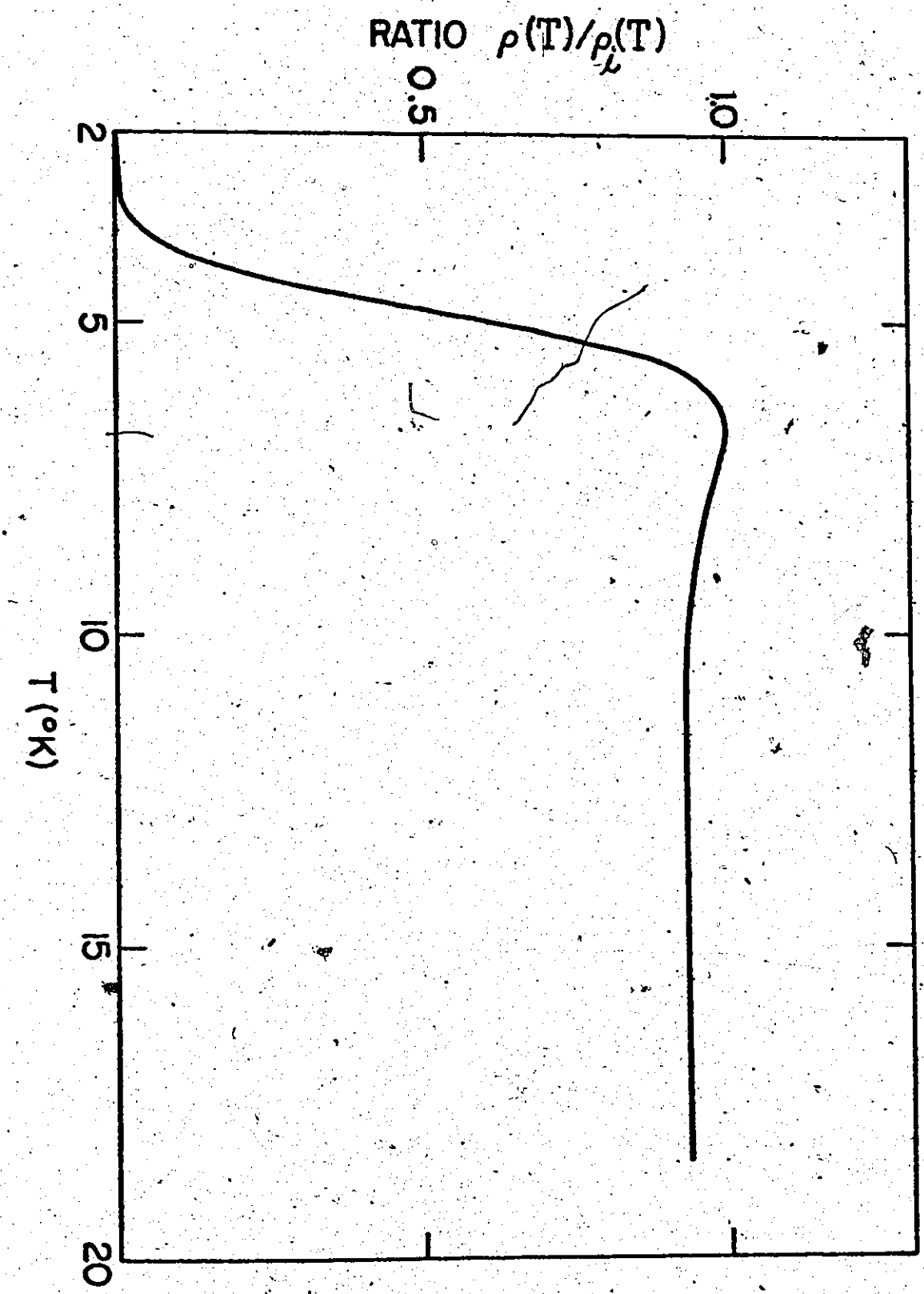
RATIO $\rho(T)/\rho_{\mu}(T)$
0.5
1.0
2
5
10
15
20
T (°K)

above ~ 1.7°K. However, in Na at 10°K it still accounts for a 4% correction. In lithium the correction term oscillates, reaching about 1% at ~ 7°K and dropping off on either side of that temperature. This is, of course, due to the initially positive and then extensively negative behaviour of the $\alpha^2_{IL}F(\omega)$ function for this metal. This is shown somewhat more graphically in Figure (2.6.2), where we have plotted this term as a function of temperature. One also notes that in Li, even at high T (≈ 30°K), the effect is still of the order of 6%.

It is clear, then, that the effects of phonon drag on the resistivity are quite significant and should not be ignored in any calculation of the very low T behaviour of the electrical resistivity.

CHAPTER III

THE EFFECTS OF ANISOTROPY IN THE ELECTRON-PHONON INTERACTION ON SOME TRANSPORT PROPERTIES

3.1 The Scattering Time Solution To The Boltzmann Equation

The main effort in this Chapter is to specifically consider the directional dependence of the electron-phonon interaction, as it appears in calculations of the electrical resistivity and related effects. This will be done by considering an alternative solution to the Boltzmann equation (2.1.10) which determines the transport properties.

Robinson and Dow (1968) (RD) have pointed out that, given the fact of the strong elastic anisotropy of the alkali metals, one would expect a substantial anisotropy in the electronic free path when it is limited by electron-phonon scattering. Deutsch, Paul, and Brooks (1961), suggest angular variations in the conductivity relaxation time in the alkalis by as much as a factor of three. Their conclusions are based on an experimental study of the low field Hall coefficients. The necessity of considering the specific anisotropy of an electron-phonon mean free path has also been pointed out in an excensive calculation of transport properties in the alkalis, carried out by Collins and Ziman (1961).

In their treatment of the problem, RD observe that in the presence of highly anisotropic scattering the standard variational solutions to the Boltzmann equation are clearly inadequate, and

further note that to attempt to incorporate anisotropy into the trial functions used in the variational procedure is a somewhat ambiguous and also very cumbersome procedure. RD, therefore, suggest avoiding the variational procedure entirely and instead, present an approximate solution to the Boltzmann equation working within the context of an anisotropic scattering time. The advantage of this formulation lies in the fact that the anisotropy appears in a very natural and physical way. Our approach to the problem is essentially that used by RD except that we will not confine our calculations to high temperatures as was done in their case.

Let us start by recalling the Boltzmann equation in the presence of an external electric field of strength $\underline{E}$. The equation (2.1.10) is

$$e\underline{v}_{\underline{k}} \cdot \underline{E} \frac{\partial f^{\circ}_{\underline{k}}}{\partial \epsilon_{\underline{k}}} = \beta \sum_{\underline{k}'} (\Phi_{\underline{k}'} - \Phi_{\underline{k}}) P^{\underline{k}'}_{\underline{k}} \qquad (3.1.1)$$

Here, $f^{\circ}_{\underline{k}}$ is the equilibrium electron distribution, $\Phi_{\underline{k}}$ its deviation from equilibrium related to $f^{\circ}_{\underline{k}}$ through

$$f_{\underline{k}} = f^{\circ}_{\underline{k}} - \Phi_{\underline{k}} \frac{\partial f^{\circ}_{\underline{k}}}{\partial \epsilon_{\underline{k}}} \qquad (3.1.2)$$

$P^{\underline{k}'}_{\underline{k}}$ is the scattering-rate from states $\underline{k}$ to $\underline{k}'$, $\beta = (k_B T)^{-1}$, $\epsilon_{\underline{k}}$ the energy of the $\underline{k}^{th}$ electron state, and $\underline{v}_{\underline{k}}$ the velocity of the $\underline{k}^{th}$ state.

Implicit in (3.1.1) is the assumption that the phonon distribution is in equilibrium. We will, of course, only be considering electron-phonon scattering. Since the exact solution $\Phi_{\underline{k}}$ for (3.1.1) is unavailable, the variational procedure is to obtain an expression for the resistivity ρ_T (2.1.13) in terms of possible trial functions $\Phi_{\underline{k}}$ and to minimize ρ_T with respect to coefficients that might appear in the

Φ's used. Of course, in the simplest variational solution $\Phi_{\underline{k}} \alpha \underline{k} \cdot \underline{u}$ the minimization procedure is not used at all.

In the alternative procedure being considered here, we write $\Phi'_{\underline{k}}$ as

$$\Phi_{\underline{k}} = e \underline{\Lambda}_{\underline{k}} \cdot \underline{u} \qquad (3.1.3)$$

and proceed directly to attempt to approximately solve the Boltzmann equation by substituting (3.1.3) in (3.1.1). $\underline{\Lambda}_{\underline{k}}$ is now the mean free path for the state $\underline{k}$. If (3.1.3) is substituted in (3.1.1), one obtains

$$\underline{v}_{\underline{k}} \cdot \underline{u} \frac{\partial f^{\circ}_{\underline{k}}}{\partial \varepsilon_{\underline{k}}} = \beta \sum_{\underline{k}'} \left(\underline{\Lambda}_{\underline{k}'} - \underline{\Lambda}_{\underline{k}}\right) \cdot \underline{u} \, P^{\underline{k}'}_{\underline{k}} \qquad (3.1.4)$$

We digress for a moment to take note that in what follows $P^{\underline{k}'}_{\underline{k}}$ is written as

$$P^{\underline{k}'}_{\underline{k}} = \frac{2\pi}{\hbar} \sum_{\lambda} |g_{\underline{k}\underline{k}'\lambda}|^2 n^{\circ}_{\underline{q}\lambda} f^{\circ}_{\underline{k}} (1 - f^{\circ}_{\underline{k}'}) \left\{ \delta(\varepsilon_{\underline{k}'} - \hbar\omega_{\underline{q}\lambda} - \varepsilon_{\underline{k}}) + e^{\beta\hbar\omega_{\underline{q}\lambda}} \delta(\varepsilon_{\underline{k}'} + \hbar\omega_{\underline{q}\lambda} - \varepsilon_{\underline{k}}) \right\} \qquad (3.1.5)$$

where, $g_{\underline{k}\underline{k}'\lambda}$, the usual electron-phonon coupling parameter is given by

$$g_{\underline{k}\underline{k}'\lambda} = -i \left(\frac{\hbar}{2MN\omega_{\underline{q}\lambda}}\right)^{\frac{1}{2}} W(\underline{q}) \, \underline{q} \cdot \varepsilon_{\underline{q}\lambda} \qquad (3.1.6)$$

Here, $n^{\circ}_{\underline{q}\lambda}$ is the Bose distribution for phonons, M is the ionic mass, N is the number of ions per unit volume, $\varepsilon_{\underline{q}\lambda}$ the phonon polarization vector for the mode $\underline{q}\lambda$, and $W(\underline{q})$ is the pseudo-potential form factor for scattering from $\underline{k}$ to $\underline{k}'$. The assumptions made in writing down (3.1.5) and (3.1.6) are exactly the same as used in our treatment of the electron-phonon interaction in Chapter II and essentially consist

in treating the interaction in the "one-phonon" approximation with a rigid-ion potential. The scattering is, of course, treated in the Born approximation with electrons in single OPW states scattering off a weak ionic pseudo-potential. For a detailed treatment which derives (3.1.6) and (3.1.5) the reader is referred to the work of Dynes and Carbotte (1968).

Substituting (3.1.5) into (3.1.4) and integrating both sides of (3.1.4) over energy, one obtains (Greene and Kohn 1965)

$$\int_0^\infty \underline{v}_{\underline{k}} \cdot \underline{u} \frac{df^\circ_{\underline{k}}}{d\varepsilon_{\underline{k}}} d\varepsilon_{\underline{k}} = \frac{\beta V}{8\pi^3} \int \frac{d\Omega_{\underline{k}'} d\varepsilon_{\underline{k}'}}{\hbar |v_{\underline{k}'}|} \int d\varepsilon_{\underline{k}} (\underline{\Lambda}_{\underline{k}'} - \underline{\Lambda}_{\underline{k}}) \cdot \underline{u} \times$$

$$\frac{2\pi}{\hbar} \sum_\lambda \left| g_{\underline{k}\underline{k}'\lambda} \right|^2 f^\circ_{\underline{k}} (1 - f^\circ_{\underline{k}'}) n^\circ_{\underline{q}\lambda} \left\{ \delta(\varepsilon_{\underline{k}'} - \varepsilon_{\underline{k}} - \hbar\omega_{\underline{q}\lambda}) + e^{\beta\hbar\omega_{\underline{q}\lambda}} \delta(\varepsilon_{\underline{k}'} - \varepsilon_{\underline{k}} + \hbar\omega_{\underline{q}\lambda}) \right\} \qquad (3.1.7)$$

In (3.1.7) we have used $\sum_{\underline{k}'} \to \frac{V}{8\pi^3} \int d^3\underline{k}' \to \frac{V}{8\pi^3} \int \frac{d\Omega_{\underline{k}'} d\varepsilon_{\underline{k}'}}{\hbar |v_{\underline{k}'}|}$ where $d\Omega_{\underline{k}'}$ is a surface element.

Making use of the quasi δ-function $\frac{\partial f_{\underline{k}}}{\partial \varepsilon_{\underline{k}}}$ on the left hand side and using the real δ-functions on the right hand side of (3.1.7), one obtains

$$v_{\underline{k}} \cdot \underline{u} = \frac{4\pi\beta}{\hbar} N(o) \int_{F.S.} \frac{d\Omega_{\underline{k}'}}{4\pi} (\underline{\Lambda}_{\underline{k}'} - \underline{\Lambda}_{\underline{k}}) \cdot \underline{u} \sum_\lambda g_{\underline{k}'\underline{k}'} \frac{\hbar\omega_{\underline{q}\lambda}}{(e^{\beta\hbar\omega_{\underline{q}\lambda}} - 1)(1 - e^{-\beta\omega_{\underline{q}\lambda}})} \qquad (3.1.8)$$

where one notes that N(o) is the density of electronic states at the Fermi surface and is given by (Kittel 1966)

$$N(o) = \frac{V m_e k_F}{2\pi^2 \hbar^2}$$

and, in addition, all velocities etc. are now evaluated at the FS. Introducing an integration over ω, (3.1.8) can be rewritten as,

$$\underline{v}_{\underline{k}} = \frac{4\pi\beta}{\hbar}\int d\omega\, R(\omega) N(o) \int_{F.S.} \frac{d\Omega_{\underline{k}'}}{4\pi} \sum_{\lambda} \left| g_{\underline{k}\underline{k}'\lambda} \right|^2 (\Lambda_{\underline{k}} - \Lambda_{\underline{k}'}) \delta(\omega - \omega_{\underline{q}\lambda}) \quad (3.1.9)$$

where $R(\omega) = \dfrac{\hbar\omega}{(e^{\beta\hbar\omega} - 1)(1 - e^{-\beta\hbar\omega})}$

Now, for $\Lambda_{\underline{k}}$ the mean free path, we write

$$\Lambda_{\underline{k}} = \tau_{\underline{k}}\, v_{\underline{k}} \quad (3.1.10)$$

where $\tau_{\underline{k}}$ is now the relevant scattering time ($\tau_{\underline{k}}$ is implicitly temperature dependent) and with $\hbar\underline{k} = m\underline{v}_{\underline{k}}$, for a spherical FS, one obtains

$$\underline{k} = \frac{4\pi\beta}{\hbar}\int d\omega\, R(\omega) N(o) \int_{F.S.} \frac{d\Omega_{\underline{k}'}}{4\pi} \sum_{\lambda} \left| g_{\underline{k}\underline{k}'\lambda} \right|^2 (\tau_{\underline{k}}\underline{k} - \tau_{\underline{k}'}\underline{k}') \delta(\omega - \omega_{\underline{q}\lambda}) \quad (3.1.11)$$

If $\tau_{\underline{k}}\underline{k}'$ is added and subtracted on the right hand side of (3.1.11) and, in addition, we take the dot product with $\underline{k}$ on both sides of (3.1.11), one obtains (noting that $\underline{k}\cdot\underline{k}$ on the FS is k_f^2)

$$\frac{1}{\tau_{\underline{k}}} = \frac{4\pi\beta}{\hbar}\int d\omega\, R(\omega) N(o) \int_{F.S.} \frac{d\Omega_{\underline{k}'}}{4\pi} \sum_{\lambda} \left| g_{\underline{k}\underline{k}'\lambda} \right|^2 \times \left[(1 - \cos(\underline{k}\underline{k}')) + \left(1 - \frac{\tau_{\underline{k}'}}{\tau_{\underline{k}}}\right) \cos(\underline{k}\underline{k}') \right] \delta(\omega - \omega_{\underline{q}\lambda}) \quad (3.1.12)$$

At this point we take note of the fact that in the [ ] bracket the first term is always positive, whereas the second term will pass through zero 48 times (in a cubic system) when the $\underline{k}'$ integral is done

for an arbitrary $\underline{k}$ (Robinson and Dow 1968; Truant 1972). The contribution from this term can then be neglected and one obtains for $\tau_{\underline{k}}$ the formula

$$\frac{1}{\tau(\underline{k},T)} = 4\pi\beta\int d\omega R(\omega)\alpha^2_{tr}F_{\underline{k}}(\omega) \qquad (3.1.13)$$

where $\alpha^2_{tr}F_{\underline{k}}(\omega)$ is defined as

$$\alpha^2_{tr}F_{\underline{k}}(\omega) = N(o)\int_{F.S.}\frac{d\Omega_{\underline{k}'}}{4\pi}\sum_{\lambda}|g_{\underline{k}\underline{k}'\lambda}|^2(1-\cos(\underline{k}\underline{k}'))\delta(\omega-\omega_{\underline{q}\lambda})$$

.....(3.1.14)

We would like to point out here that in addition to the treatment of Robinson and Dow, whom we have followed rather closely, this scattering time solution to the Boltzmann equation has been discussed extensively before (Mott and Jones 1936; Deutsch, Paul, and Brooks 1961). However, we believe that this is the first time it has been formulated in terms of the $\alpha^2_{tr}F_{\underline{k}}(\omega)$ function, which, of course, allows temperature effects to be treated very simply and economically.

It is clear, then, that once the $\alpha^2_{tr}F_{\underline{k}}$ function is obtained for an arbitrary point $\underline{k}$ on the FS, and insomuch that the function does not change significantly with volume the scattering time $\tau(\underline{k},T)$ can be obtained for all temperatures T.

To obtain the resistivity $\rho(T)$ in this formulation, one quite simply writes down

$$\rho(T) = \frac{m}{n e^2 \tau_{av}(T)} \qquad (3.1.15)$$

where τ_{av} is now the FS average of the $\tau(\underline{k},T)$ given by (3.1.13), n is

the number of electrons per unit volume, m is the electron mass.

$$\tau_{av}(T) = \langle \tau(\underline{k},T) \rangle_{F.S.} \qquad (3.1.16)$$

To obtain the $\alpha^2_{tr}F_{\underline{k}}$ functions, what is necessary is a description of the phonons and the electron-ion scattering. As before we will take the phonons from Born-von Kármán force constant fits to the dispersion curves and, to describe the electron-ion scattering cross sections, will use the Ashcroft potentials developed in connection with our calculations of the variational resistivities.

To calculate the $\alpha^2_{tr}F_{\underline{k}}$ functions, we have made use of a computer programme, developed by Leavens (1970), which calculates the $\alpha^2F_{\underline{k}}(\omega)$ functions which are involved in a discussion of anisotropy in the superconducting gap and in the electron-phonon mass enhancement.

The method consists essentially of the following steps:

(a) an initial point $\underline{k}$ is chosen on the FS by specifying θ and Φ the polar angles,

(b) all final states $\underline{k}'$ on the FS are determined by choosing random points within elements of a surface mesh determined through suitable values of $\Delta\theta$ and $\Delta\Phi$,

(c) a contribution proportional to

$$\frac{\Delta\Omega_{\underline{k}'}}{4\pi} \sum_{\lambda} \left| g_{\underline{k}\underline{k}'\lambda} \right|^2 \left(1 - \cos(\underline{k}\underline{k}')\right)$$

is placed in the relevant frequency bin defined through the value of ω ($\Delta\Omega_{\underline{k}'}$ is the area of the element from which $\underline{k}'$ is chosen) and finally,

(d) the distribution is normalized so that

$$\int F_{\underline{k}}(\omega)\, d\omega = 3$$

where $F_{\underline{k}}(\omega)$, a directional phonon density of states is defined as

$$F_{\underline{k}}(\omega) = \sum_{\lambda} \int_{FS.} \frac{d\Omega_{\underline{k}'}}{4\pi} \delta(\omega - \omega_{\underline{q}\lambda}) \qquad (3.1.17)$$

The reader is referred to Leavens (1970), Leavens and Carbotte (1972) for further details.

The expression for $\alpha^2 F_{\underline{k}}(\omega)$ is given below

$$\alpha^2 F_{\underline{k}}(\omega) = N(o) \int_{F.S.} \frac{d\Omega_{\underline{k}'}}{4\pi} \sum_{\lambda} |g_{\underline{k}\underline{k}'\lambda}|^2 \delta(\omega - \omega_{\underline{q}\lambda}) \qquad (3.1.18)$$

and it is clear that the only modification necessary is to incorporate the $1 - \cos(\underline{k}\underline{k}')$ term into the integration over $\underline{k}'$.

In the next section we turn to a discussion of the anisotropy in the scattering times which will, in turn, lead to interesting effects in the resistivity and the low field Hall coefficients.

3.2 The Anisotropy In The Scattering Times

We have computed the $\alpha^2_{tr} F_{\underline{k}}(\omega)$ functions for 21 points on the irreducible $1/48^{th}$ of the FS in the alkali metals Na, K, Rb, and Li, using our Ashcroft potentials developed in Chapter II. The phonons are again taken from Born-von Kármán force constant fits to the dispersion curves. In Figure (3.2.1) we show a plot of the irreducible $1/48^{th}$ of the FS and the points for which the distributions have been calculated. θ and ϕ are the usual polar angles. In Figures (3.2.2), (3.2.3), (3.2.4), and (3.2.5) we show plots of the $\alpha^2_{tr} F_{\underline{k}}(\omega)$ functions, for $\underline{k}$ in the 3 high symmetry directions, in each of the metals. In the cases of Li and Rb we also include plots of the functions obtained if Umklapp

Fig. 3.2.1 The irreducible $1/48^{th}$ of the Fermi surface in the alkali metals. The points marked with a ● indicate the values of $\underline{k}$ at which the $\alpha^2_{tr}F_{\underline{k}}(\omega)$ functions were calculated. θ and Φ are the usual polar angles.

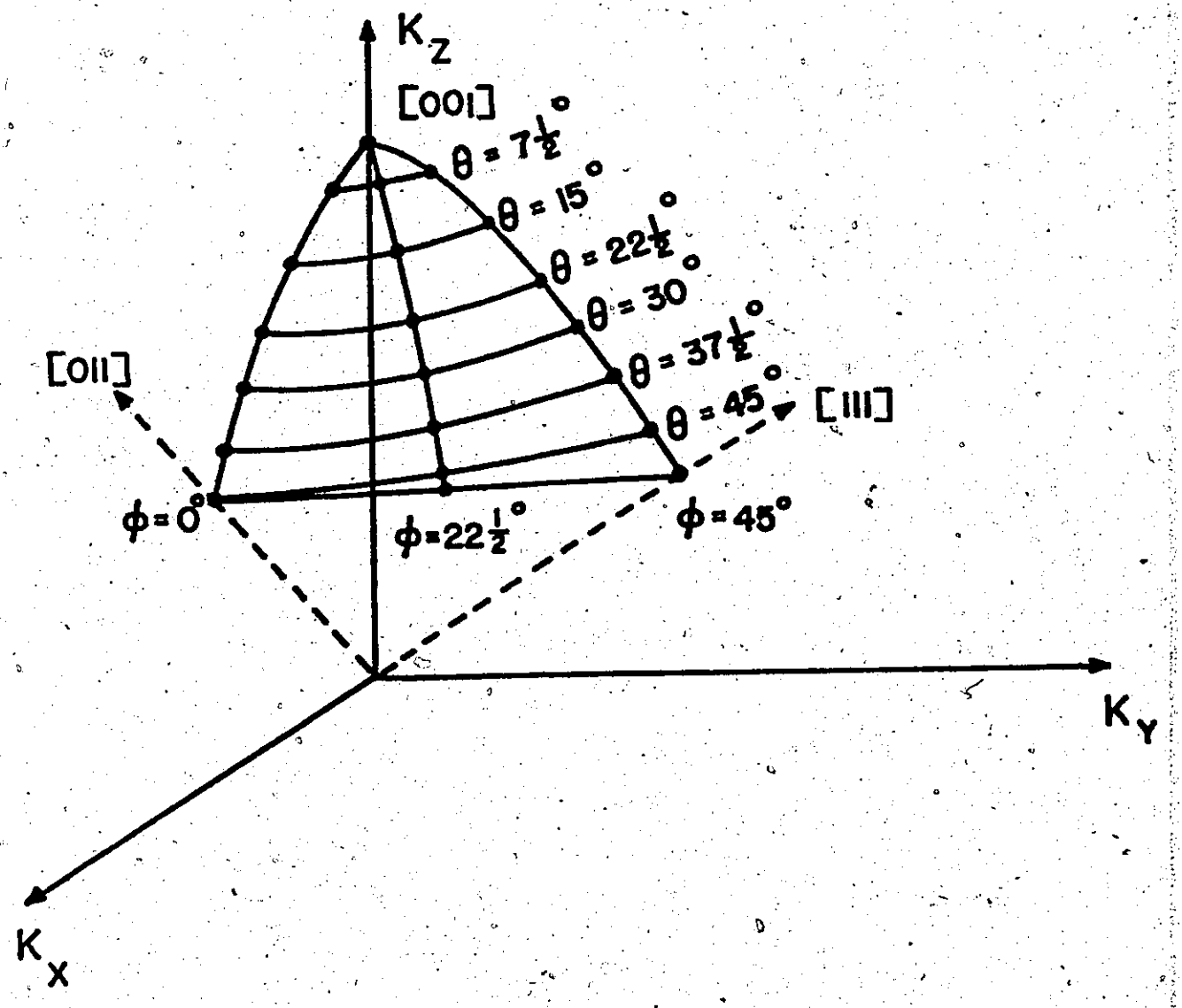
K_Z
[001]
$\theta = 7\frac{1}{2}°$
$\theta = 15°$
$\theta = 22\frac{1}{2}°$
$\theta = 30°$
$\theta = 37\frac{1}{2}°$
$\theta = 45°$
[011]
[111]
$\phi = 0°$
$\phi = 22\frac{1}{2}°$
$\phi = 45°$
K_Y
K_X

Fig. 3.2.2 The $\alpha^2_{tr}F_{\underline{k}}(\omega)$ functions for $\underline{k}$ in the three high symmetry directions in K. The function $\alpha^2_{tr}F_{\underline{k}}(\omega)$ is dimensionless and the frequency ω is in the units of 10^{12} cps.

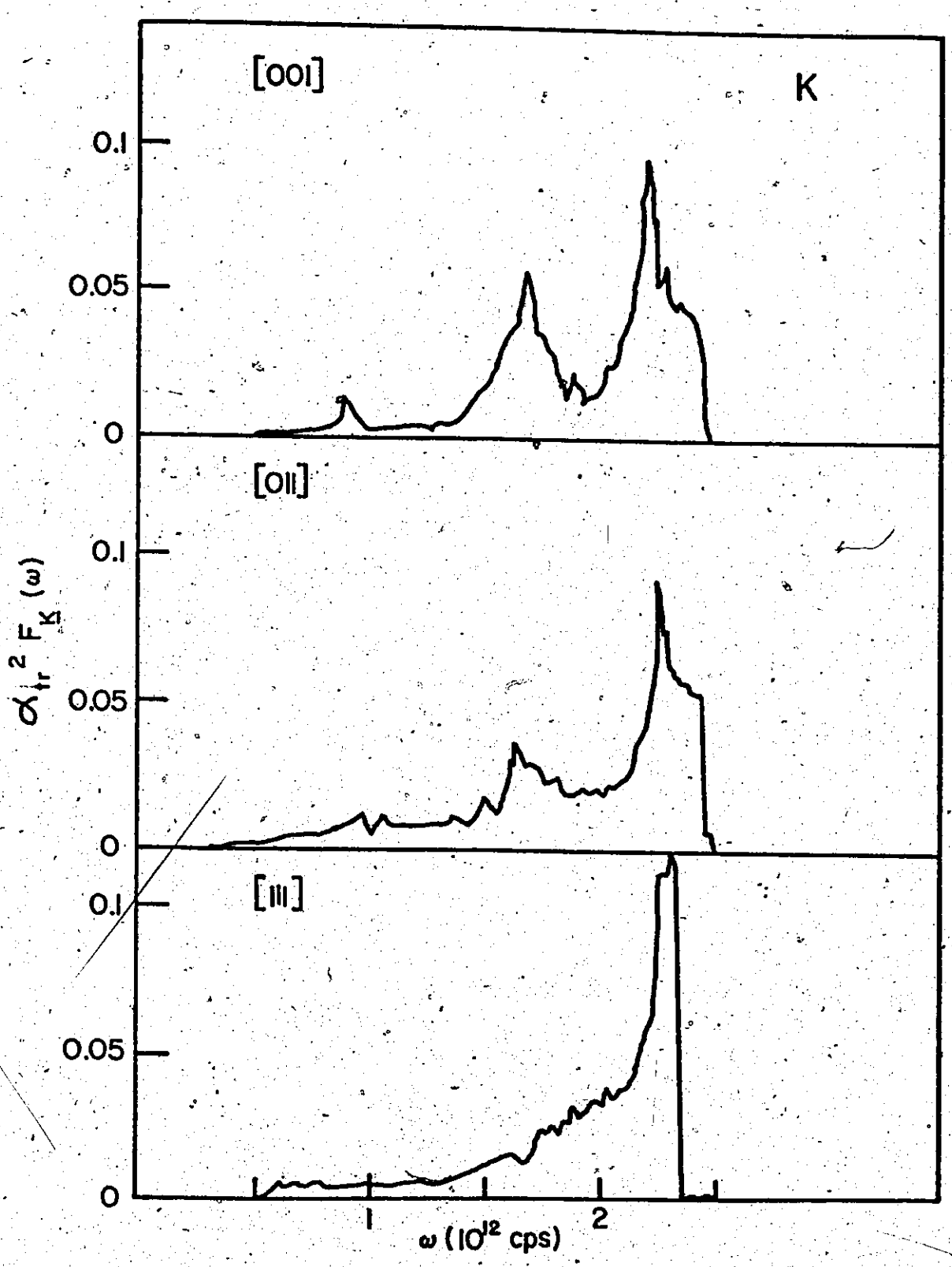
[001]
K
0.1
0.05
0
[011]
0.1
0.05
0
[111]
0.1
0.05
0
$\alpha^2_{tr} F_{K1}(\omega)$
1
2
ω (10^{12} cps)

Fig. 3.2.3 The $\alpha^2_{tr}F_{\underline{k}}(\omega)$ functions for $\underline{k}$ in the three high symmetry directions in Na.

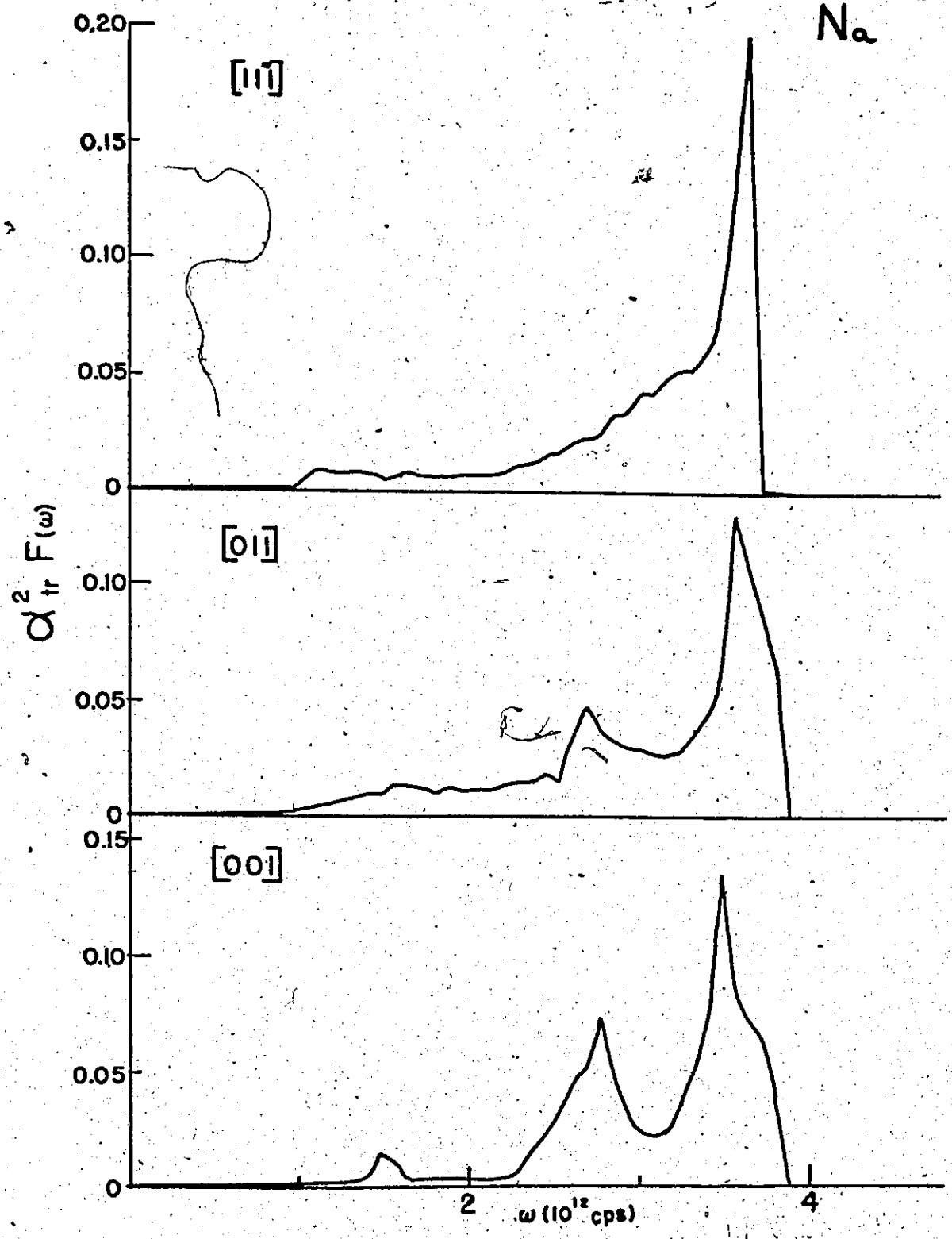
Na
[111]
[011]
[001]
0.20
0.15
0.10
0.05
0
$\alpha^2_{tr} F(\omega)$
2
4
ω (10^{12} cps)

Fig. 3.2.4 The $\alpha^2_{tr} F_{\underline{k}}(\omega)$ functions for $\underline{k}$ in the three high symmetry directions in Rb. The dotted curves are the same functions calculated on the basis of Normal processes only.

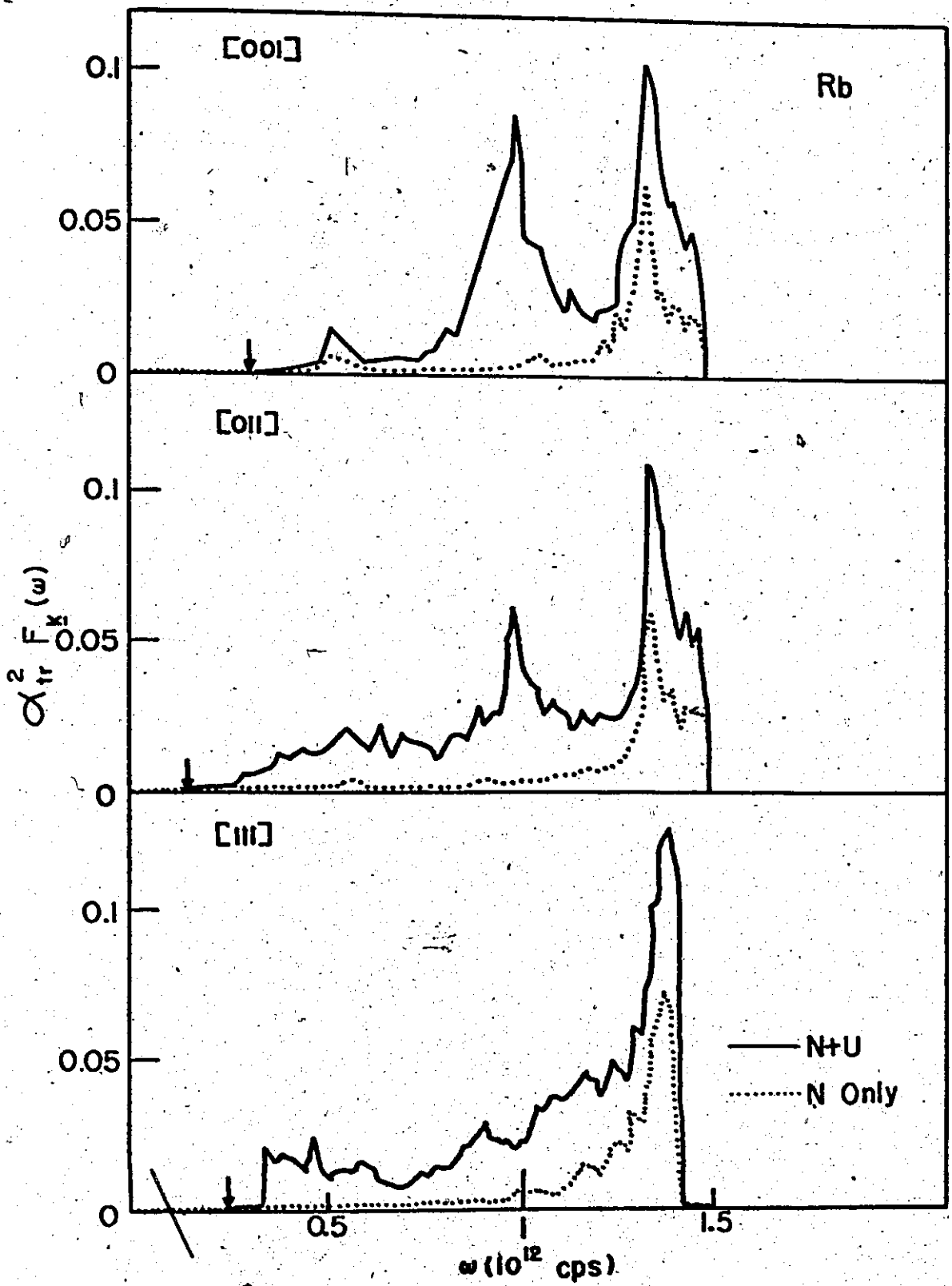
[001]
Rb
0.1
0.05
0
[011]
0.1
0.05
0
[111]
0.1
0.05
0
N+U
N Only
0.5
1
1.5
ω (10^12 cps)
α²tr Fk(ω)

Fig. 3.2.5 The $\alpha^2_{tr}F_{\underline{k}}(\omega)$ functions for $\underline{k}$ in the three high symmetry directions in Li. The dotted curves are the same functions calculated on the basis of Normal processes only.

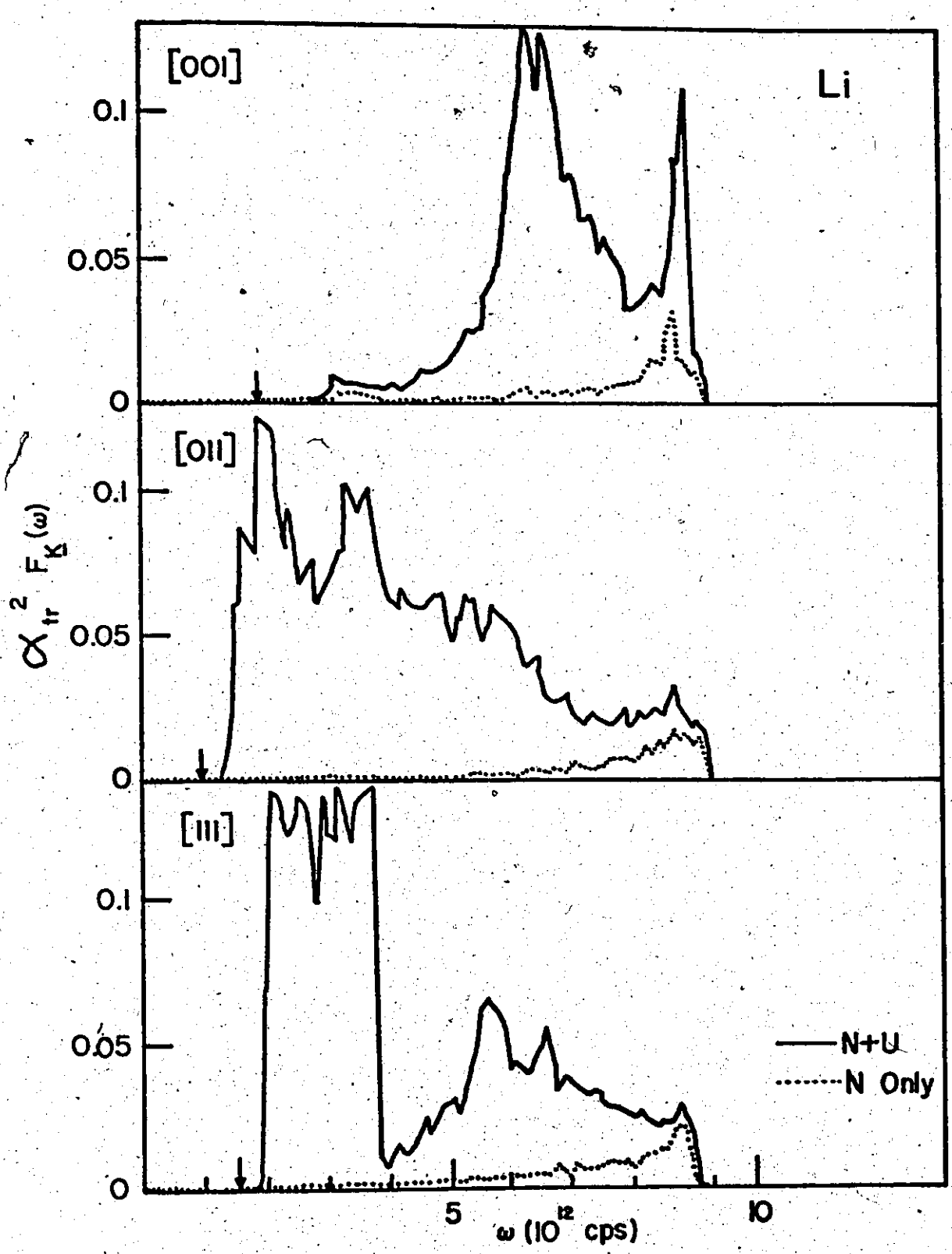
[001]
Li
0.1
0.05
0
[011]
0.1
0.05
0
[111]
0.1
0.05
0
$\alpha^2_{tr} F_K(\omega)$
N+U
N Only
5
10
ω (10^12 cps)

processes are arbitrarily excluded from the integrations.

That the distributions are quite different in different directions is rather obvious, and Li stands out as the metal in which these differences are the most pronounced. The anisotropy in the distributions is what will lead to anisotropy in the scattering times and since this will be of central importance in discussions of the Hall effect and the resistivity, we should consider the reasons for the anisotropy in some detail.

Since we are using a spherical FS we are obviously ignoring any anisotropy from that source but for the alkalis that should be a quite reasonable assumption. The three basic reasons for the anisotropy in our situation, then, are

(a) the inherent anisotropy of the dispersion curves in the metals,

(b) the geometry of the Brillouin zone, and

(c) the role of Umklapp processes.

(a) is self-explanatory and needs no further amplification except to point out that (Dugdale and Phillips, 1965) the velocities of shear waves in the (100) and (110) directions can differ by a factor of approximately 3 in the alkali metals, so that the anisotropy in the dispersion curves is quite appreciable. However, as we will see, this cause is only of minor importance in comparison with the other two.

In considering how the geometry of the zone affects the anisotropy in the distributions, we note the important fact that in the alkalis, since the FS does not touch zone boundaries at all, one can

never have an Umklapp process in which the reduced wave vector (q_{red} = $q - G$; G is a reciprocal lattice vector, $q = k' - k$) is zero. As such, processes involving the very lowest phonon frequencies and hence appearing as contributions to the low ω end of the $\alpha^2_{tr}F_k(\omega)$ distributions will be exclusively Normal processes. This is, of course, the oft quoted "freezing out" of Umklapps (Ziman 1960; Bailyn 1960). The minimum value of q_{red} that can be obtained given a fixed initial state $|k\rangle$ is clearly a function of the geometry of the zone, and hence the exact value of frequency, below which the Umklapp cut-off occurs, will vary with $|k\rangle$ and thus be different in each distribution. This is demonstrated in Figures (3.2.4) and (3.2.5). On each distribution the arrow marks this cut-off frequency. It is quite clearly different in different directions. Since the main source of the anisotropy is from the Umklapp processes, at the very lowest temperatures when the low ω ends of the distributions dominate, we would expect the anisotropy to vanish and this is indeed what is observed. This point will be discussed further. We turn now to effect (c) which is the role of the Umklapp processes.

As can be seen from Figures (3.2.4) and (3.2.5), by far the major contribution to the $\alpha^2_{tr}F_k(\omega)$ functions is from Umklapp processes. Also, it is clear that the differences between distributions arise mainly from this Umklapp contribution. Normal processes alone give rise to distributions that are essentially the same in different directions. This effect is most pronounced in the case of Li where, since the pseudo-potential is large at $q \sim 2k_f$, the Umklapp contribution

is very striking. The effect can be understood quite simply. Together with the strong orientational dependence of the Umklapp processes, which arises essentially from the fact that the particular reciprocal lattice vector $\underline{G}$ which is involved in the relation $\underline{q}_{red.} = \underline{q} - \underline{G}$ is a function of the position of the initial state $|\underline{k}>$, is the consideration that all processes are weighted by the factor $(1 - \cos(\underline{k}\underline{k}'))$, which is simply $q^2/2k_f^2$ for a spherical FS.

In addition, one obtains a further q^2 contribution from the $|\underline{q} \cdot \underline{\epsilon}_{\underline{q}\lambda}|^2$ term which appears in $g_{\underline{k}\underline{k}'\lambda}$. Thus, one has an effective q^4 weighting attached to each process. Umklapp processes are, by definition, processes with large $\underline{q}$ and, therefore, this q^4 factor will greatly emphasize the role that they play and indeed leads to their complete dominance in determining the anisotropy.

We would like to note here that the formulation of the transport properties in terms of weighted frequency distributions allows a much clearer description of the relative role of Umklapp and Normal processes, as opposed to the traditional formulation in terms of structure factors etc. This is made abundantly clear in what we are discussing now. The traditional formulation could not present anywhere as transparent a picture of the anisotropy as is available by looking at pictures of the $\alpha_{tr}^2 F$ distributions presented here.

To summarize, then, the main sources of the anisotropy in decreasing order of importance are, the role of the Umklapp processes (which is intimately related to the shape of the pseudo-potential form factors), the geometry of the Brillouin zone, and the inherent aniso-

tropy of the phonon spectrum. The distinctions between the first two effects (U-processes and zone geometry) are perhaps less clear than indicated here since the geometry of the zone is clearly involved in determining the anisotropy due to the Umklapp processes.

To illustrate how the anisotropy in the scattering times varies with temperature, we have plotted the ratio of $\tau_{\underline{k}}$ to τ_{001}, for the 21 points used in the calculation, at 4 different temperatures in each metal. These plots are shown in Figures (3.2.6), (3.2.7), (3.2.8), and (3.2.9).

One notes first of all that the anisotropy is clearly a function of temperature. At the highest and lowest temperatures considered, the anisotropy is less than for the two intermediate temperatures. This is understood as follows. At the highest temperature, the thermal factors which appear in the expression for $\frac{1}{\tau(\underline{k},T)}$ namely (3.1.13), sample the entire range of the frequency distributions, and as such differences tend to be averaged out. As the temperature is lowered the thermal factors will sample less of the distributions and consequently differences will now be emphasized, getting greater with decreasing temperature and leading to anisotropy which increases with lowered T. However, when the temperature is lowered sufficiently such that the very lowest ends of the distributions are being sampled, which we will recall are exclusively due to Normal processes only, the anisotropy will begin to disappear. Thus, with decreasing temperature the anisotropy will first increase, pass through a maximum, and finally decrease again.

To emphasize the point that the anisotropy in the τ's is due essentially to the Umklapp component of the interaction, in Figure

Fig. 3.2.6 Scattering times $\tau(\underline{k},T)$ for four different temperatures in Na as a function of position on the irreducible $1/48^{th}$ of the Fermi surface. For $\underline{k} \equiv (\theta, \Phi, k_f)$, the results for the three arcs $\Phi = 0°$, $22\frac{1}{2}°$, and $45°$ are to be distinguished as follows: ● , $\Phi = 0°$, x, $\Phi = 22\frac{1}{2}$; 0, $\Phi = 45°$. For each temperature $\tau(o,o)$ is entered on the graph.

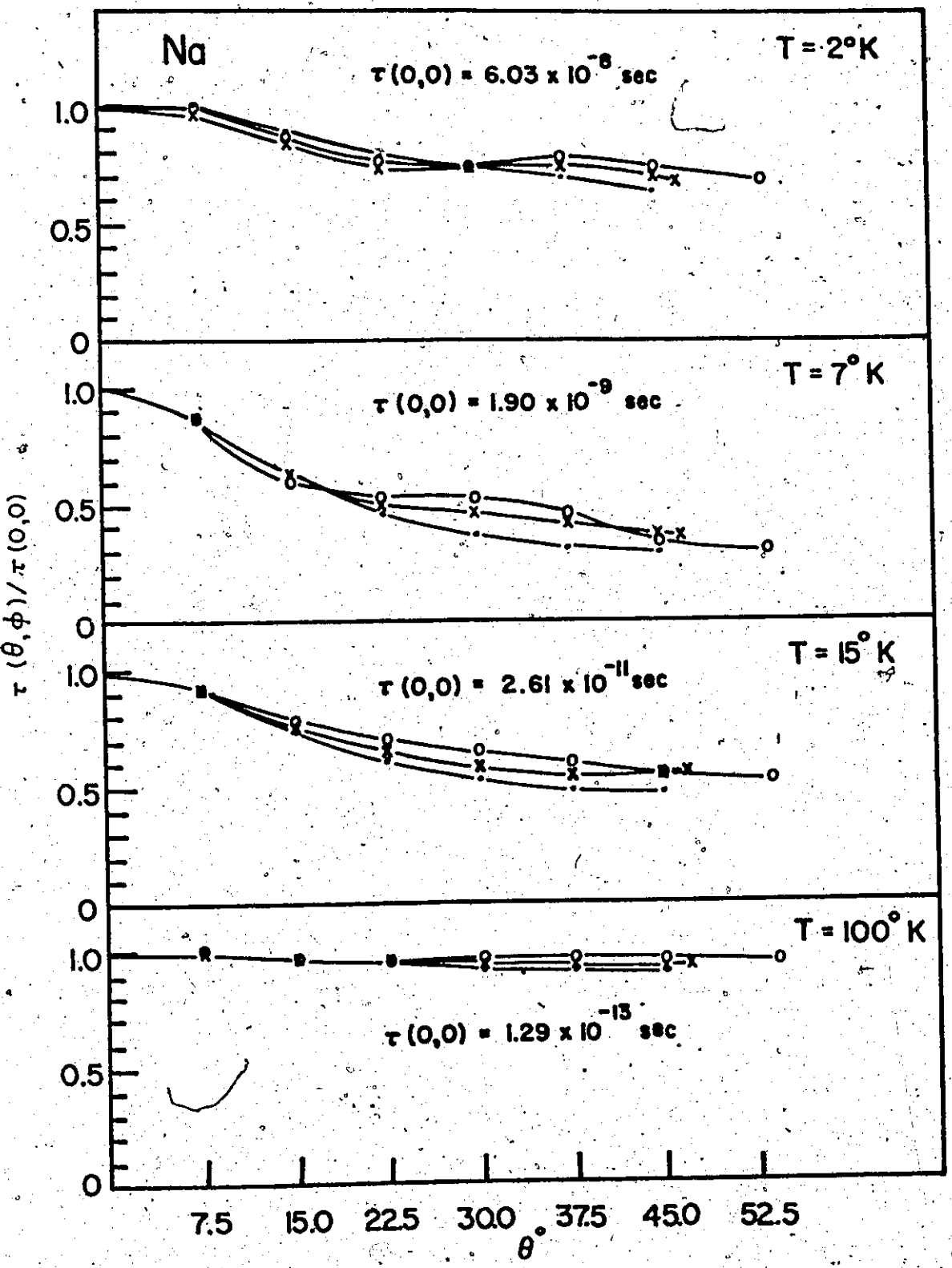
Na
T = 2°K
τ(0,0) = 6.03 x 10⁻⁸ sec
T = 7° K
τ(0,0) = 1.90 x 10⁻⁹ sec
T = 15° K
τ(0,0) = 2.61 x 10⁻¹¹ sec
T = 100° K
τ(0,0) = 1.29 x 10⁻¹³ sec
τ(θ,φ)/τ(0,0)
1.0
0.5
0
7.5
15.0
22.5
30.0
37.5
45.0
52.5
θ°

Fig. 3.2.7 Scattering times $\tau(\underline{k},T)$ for four different temperatures in K. The notation is the same as Fig. 3.2.6.

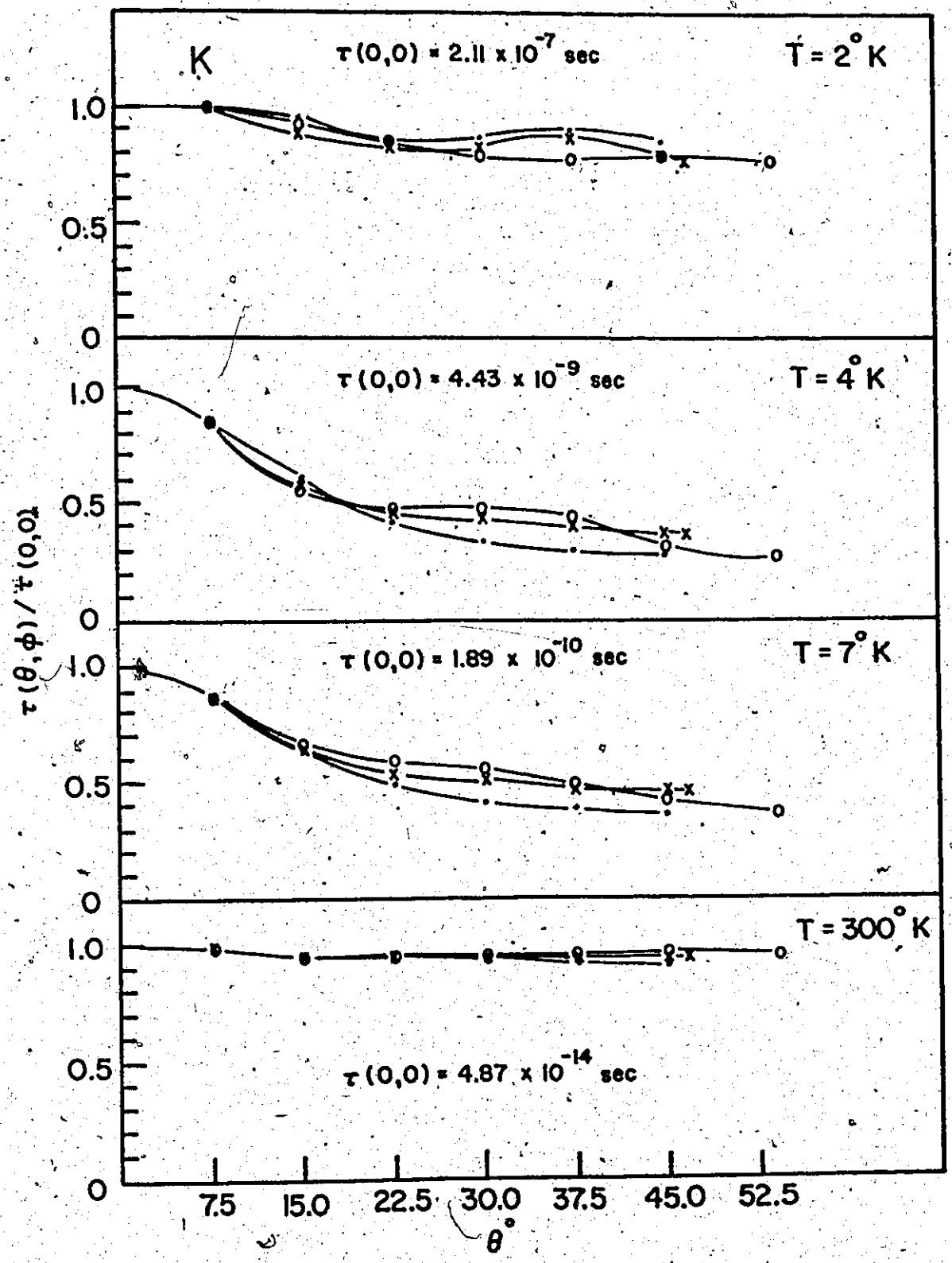
K
τ(0,0) = 2.11 x 10^-7 sec
T = 2° K
τ(0,0) = 4.43 x 10^-9 sec
T = 4° K
τ(0,0) = 1.89 x 10^-10 sec
T = 7° K
T = 300° K
τ(0,0) = 4.87 x 10^-14 sec
1.0
0.5
0
7.5
15.0
22.5
30.0
37.5
45.0
52.5
θ°
τ(0,0) ÷ / (φ, θ) τ

Fig. 3.2.8 Scattering times $\tau(\underline{k},T)$ for four different temperatures in Rb. The notation is the same as Fig. 3.2.6.

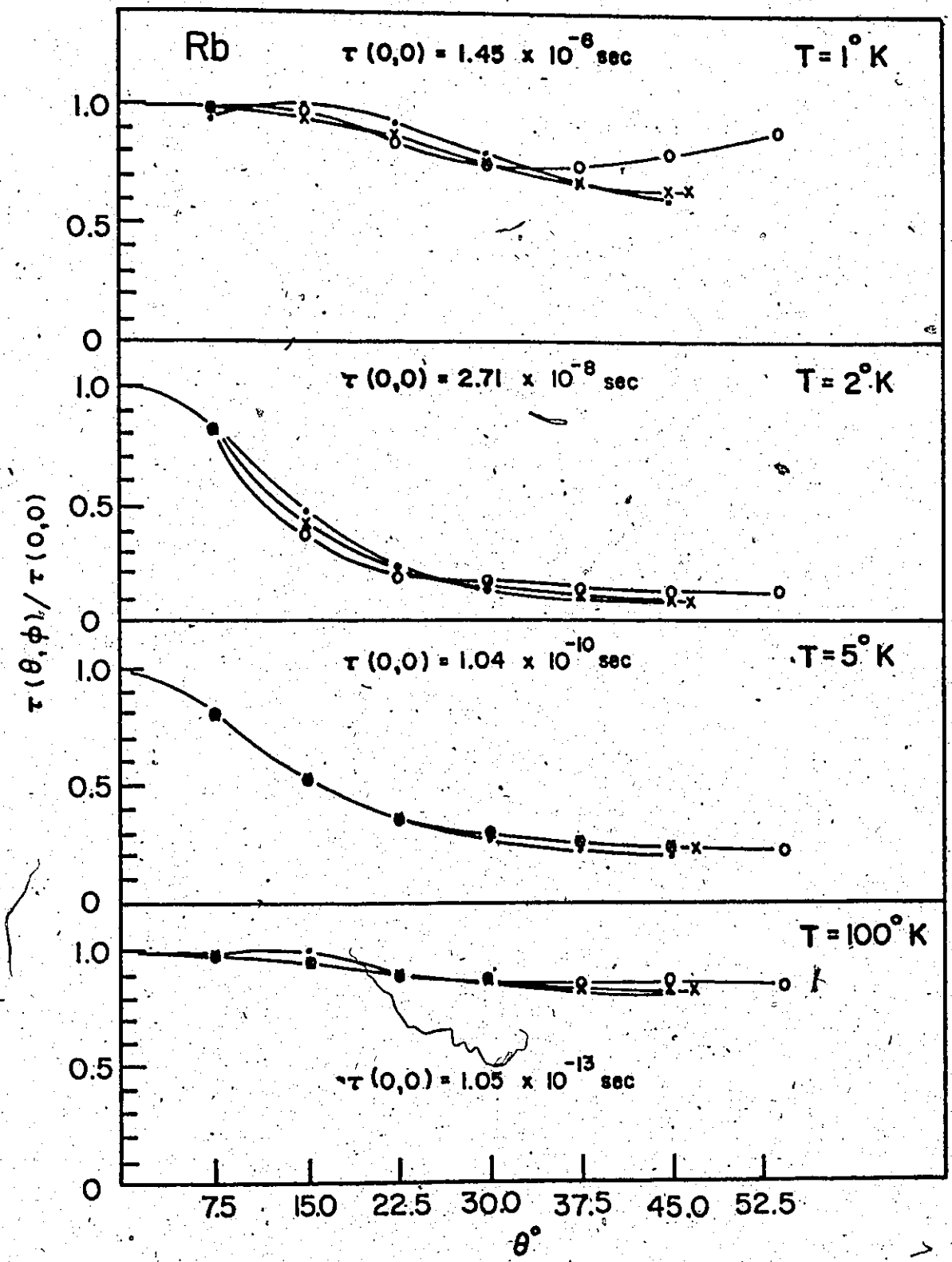
Rb
τ (0,0) = 1.45 x 10^-6 sec
T = 1° K
τ (0,0) = 2.71 x 10^-8 sec
T = 2° K
τ (0,0) = 1.04 x 10^-10 sec
T = 5° K
T = 100° K
τ (0,0) = 1.05 x 10^-13 sec
τ (θ, φ) / τ (0,0)
1.0
0.5
0
7.5
15.0
22.5
30.0
37.5
45.0
52.5
θ°

Fig. 3.2.9 Scattering times $\tau(\underline{k},T)$ for four different temperatures in Li. The notation is the same as Fig. 3.2.6.

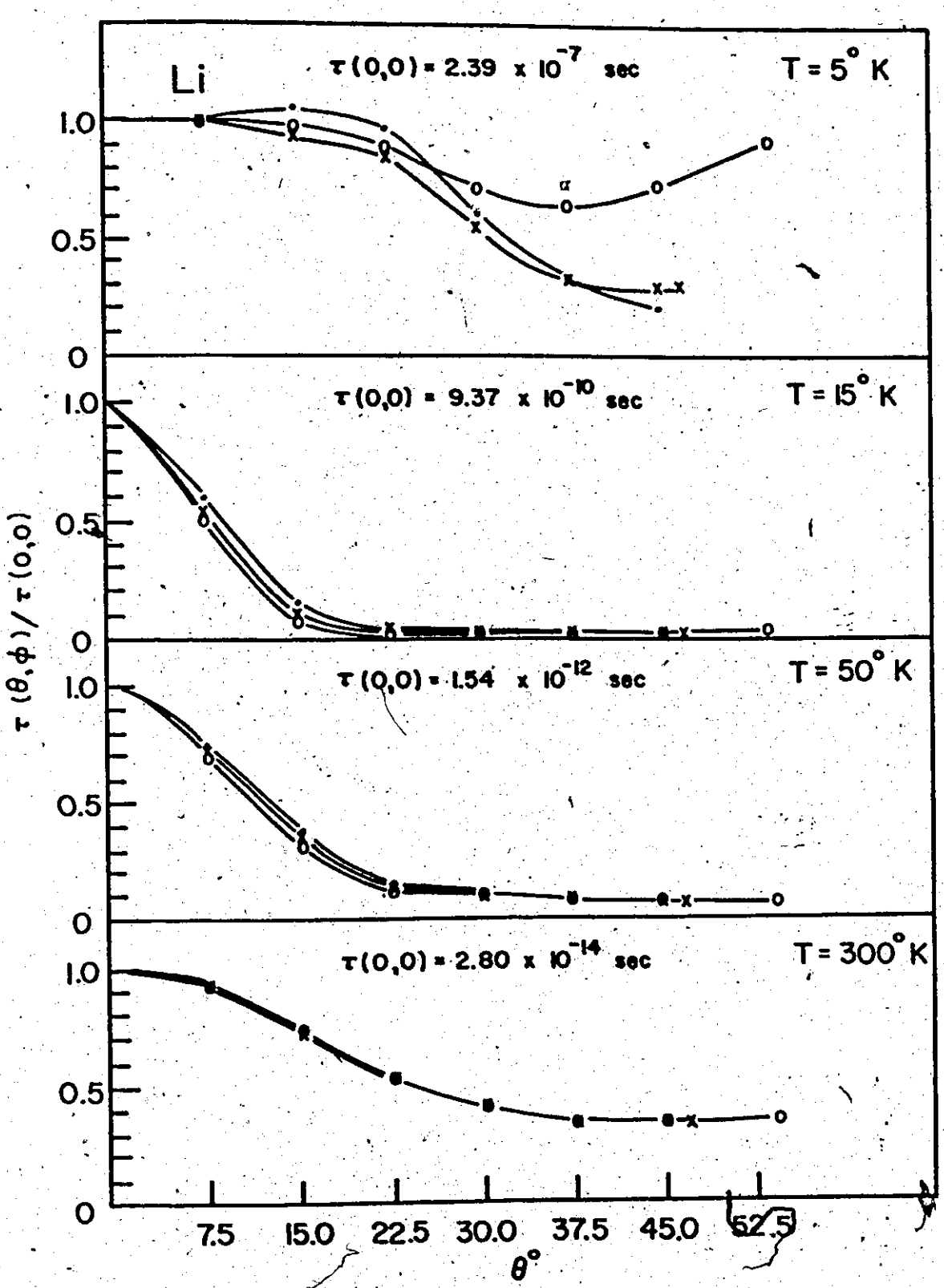
Li
τ(0,0) = 2.39 x 10⁻⁷ sec
T = 5° K
τ(0,0) = 9.37 x 10⁻¹⁰ sec
T = 15° K
τ(0,0) = 1.54 x 10⁻¹² sec
T = 50° K
τ(0,0) = 2.80 x 10⁻¹⁴ sec
T = 300° K
τ (θ, φ) / τ (0,0)
1.0
0.5
0
7.5
15.0
22.5
30.0
37.5
45.0
62.5
θ°

Fig. 3.2.10 Scattering times $\tau(\underline{k},T)$ in Li, at three different temperatures, due to Normal processes only. The notation is the same as Fig. 3.2.6.

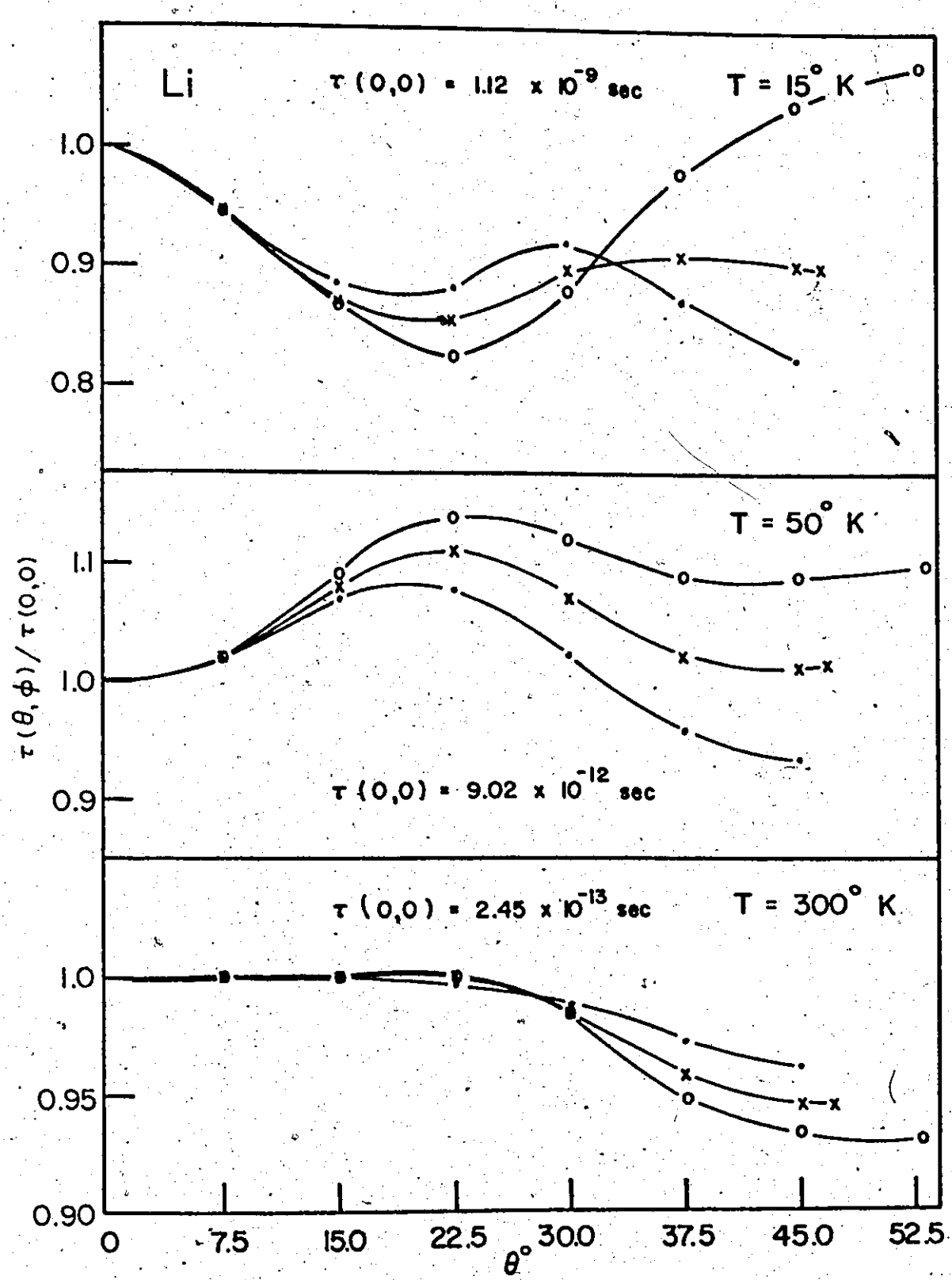
Li
τ (0,0) = 1.12 x 10⁻⁹ sec
T = 15° K
T = 50° K
τ (0,0) = 9.02 x 10⁻¹² sec
τ (0,0) = 2.45 x 10⁻¹³ sec
T = 300° K
τ(θ, φ) / τ(0,0)
θ°
1.0
0.9
0.8
1.1
0.95
0.90
0
7.5
15.0
22.5
30.0
37.5
45.0
52.5

(3.2.10) we have plotted the variation of the τ's in Li at 3 different temperatures. However, here the τ's are determined only by Normal processes. It is quite clear that, though anisotropy is still quite evident, it is orders of magnitude less than the anisotropy displayed in Figure (3.2.9) where the τ's include Umklapp processes as well.

We turn now to the actual quantitative variation of the τ's in the four metals and observe that the anisotropy is most severe, at all temperatures, in Li. The maximum variation ($\tau_{max.}/\tau_{min.}$) is ~ 3 at 300°K, ~ 10 at 50°K, ~ 100 at 15°K, and ~ 5 at 5°K. In Rb this ratio is ~ 1.25 at 100°K, ~ 5 at 5°K, ~ 10 at 2°K, and ~ 1.6 at 1°K. In K the ratio is ~ 1.1 at 300°K, ~ 3 at 7°K, ~ 4 at 4°K, and ~ 1.2 at 2°K. In Na the ratio is ~ 1.1 at 100°K, ~ 2 at 15°K, ~ 3 at 7°K, and ~ 1.6 at 2°K. It is clear then that there indeed is a significant variation in the scattering times across the FS and that the variation is very sensitive to temperature.

To indicate how the pseudo-potential form factors affect the anisotropy, all else being constant, we have plotted the τ's in K at 4°K for the four different pseudo-potentials mentioned in the treatment of the phonon-drag effect in Chapter II (see Figure (2.5.7)). The τ's are shown in Figure (3.2.11) and as one can readily observe the anisotropy is a function of the potential. This is, of course, due to the different amounts of Umklapps that each potential introduces. The Ashcroft potential with $R_c \sim 1.275$ is largest at $q \sim 2k_f$ and hence has the greatest anisotropy. The low q portions of each pseudo-potential are essentially the same and hence Normal processes will contribute

Fig. 3.2.11 Scattering times $\tau(\underline{k},T)$ in K at 4°K for four different choices of pseudo-potential. The notation is the same as Fig. 3.2.6.

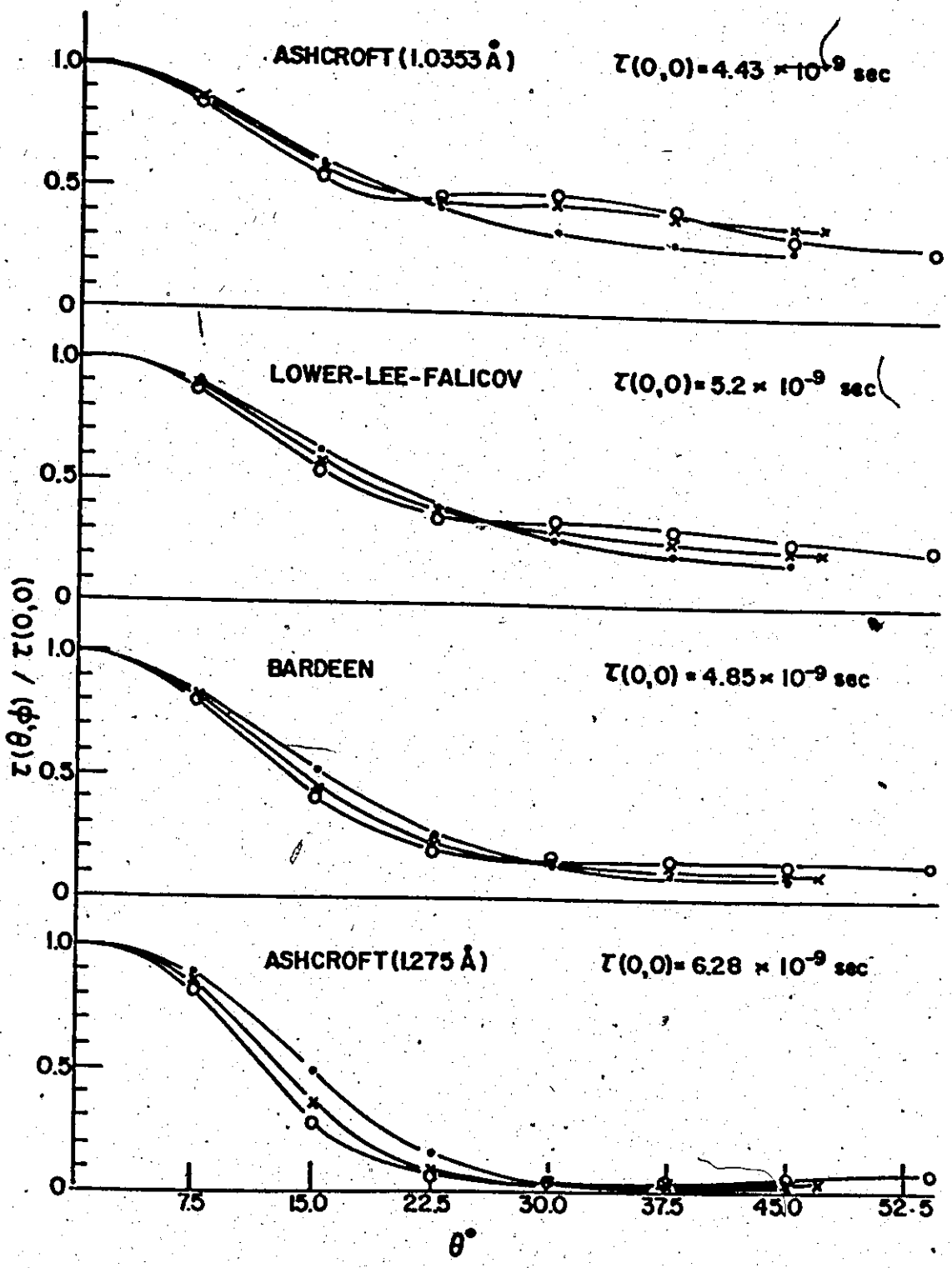
ASHCROFT (1.0353 Å)
τ(0,0) = 4.43 × 10⁻⁹ sec
LOWER-LEE-FALICOV
τ(0,0) = 5.2 × 10⁻⁹ sec
BARDEEN
τ(0,0) = 4.85 × 10⁻⁹ sec
ASHCROFT (1.275 Å)
τ(0,0) = 6.28 × 10⁻⁹ sec
τ(θ,φ) / τ(0,0)
1.0
0.5
0
7.5
15.0
22.5
30.0
37.5
45.0
52.5
θ°

Fig. 3.2.12 $\alpha^2_{tr}F_{\underline{k}}(\omega)$'s for $\underline{k}$ in the [001] direction for four different pseudo-potentials in K.

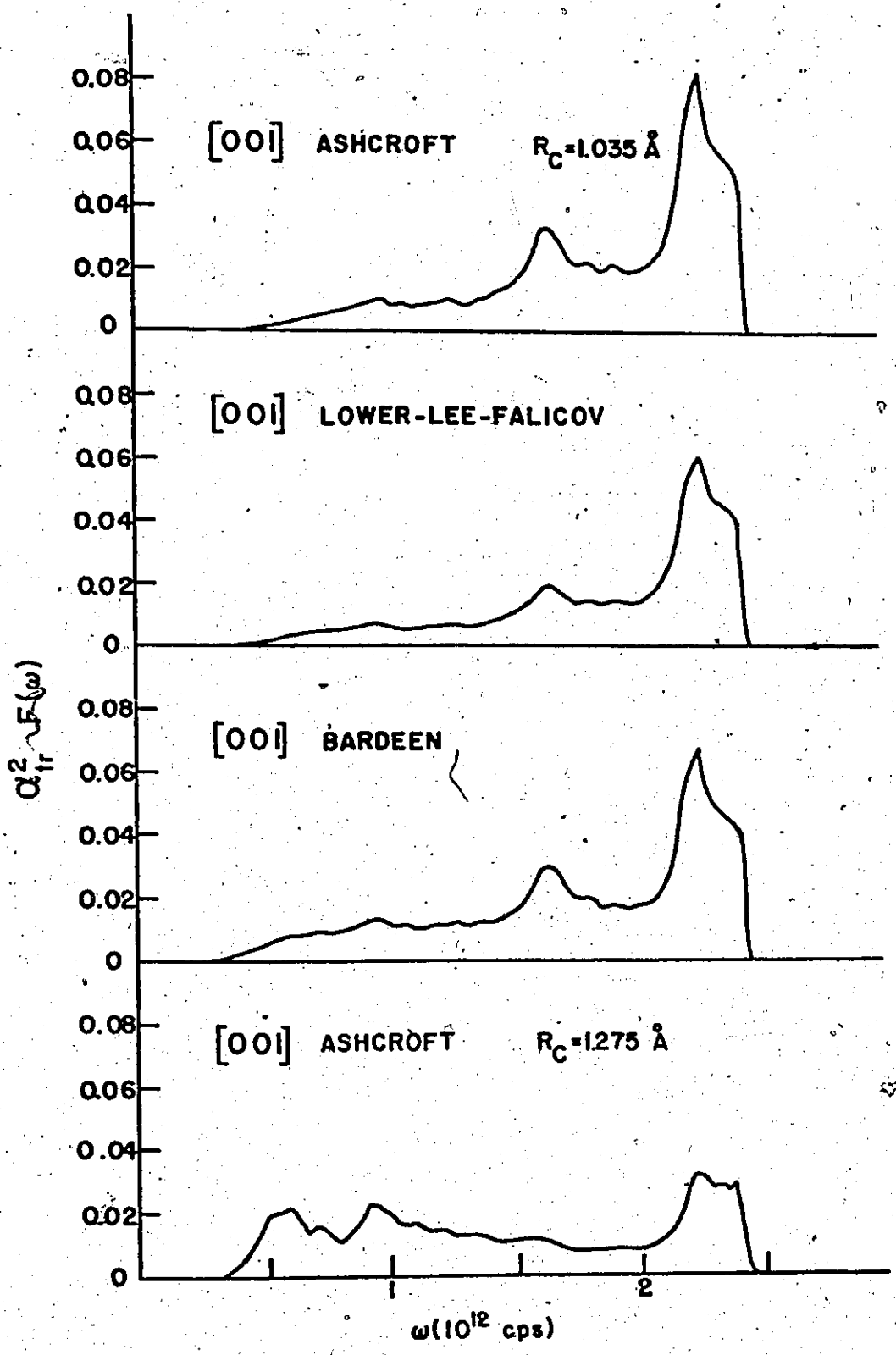
[001] ASHCROFT R_c=1.035 Å
[001] LOWER-LEE-FALICOV
[001] BARDEEN
[001] ASHCROFT R_c=1.275 Å
0.08
0.06
0.04
0.02
0
$\alpha^2_{tr}F(\omega)$
1
2
$\omega(10^{12}$ cps)

in essentially the same way in each potential. However, the differences at $q \sim 2k_f$ lead to different Umklapp contributions, which we have seen are dominant in determining the final anisotropy.

In Figure (3.2.12) we show the $\alpha^2_{tr}F_{\underline{k}}(\omega)$ function for $|\underline{k}>$ in the [001] direction for the four different potentials. The differences between the various functions are reasonably obvious, in particular one should look at the shapes in the low frequency region as this part dominates in determining the low temperature behaviour of the $\tau(\underline{k},T)$. $\alpha^2_{tr}F_{\underline{k}}(\omega)$ for the Ashcroft potential with $R_c \sim 1.28\text{Å}$ is clearly the most different of the set, for the reasons mentioned above.

Having discussed the anisotropy in the scattering times, in the next two sections of this Chapter we will look at some interesting consequences of this anisotropy.

3.3 The Low Field Hall Constant In The Alkali Metals

In this section we will consider one of the more interesting consequences of the anisotropy of the electron-phonon interaction in the alkalis as it appears in a consideration of the absolute magnitude and temperature variation of the low field Hall constant in these metals.

The familiar Hall constant R can be written in terms of the effective density of charge carriers n*, as

$$R = -\frac{1}{n^*|e|c}$$

where e is the electron charge and c is the velocity of light. Tsuji (1958) has shown that in the low field limit, which is defined through

$$\omega_c \tau \ll 1 \qquad (3.3.1)$$

where ω_c is the usual cyclotron frequency of the representative state in momentum space in a magnetic field $\underline{H}$ and τ is the average relaxation time for an electron in that orbit, n^* is related to n, number of free electrons per unit volume, through the relation

$$\frac{n^*}{n}(T) = \frac{\langle \tau(k,T) \rangle^2}{\langle \tau^2(k,T) \rangle} \qquad (3.3.2)$$

where $\tau(\underline{k},T)$ is the scattering time for an electron in state $|\underline{k}\rangle$ at temperature T. The averages indicated in (3.3.2) are over the FS. If the scattering times are completely isotropic the ratio n^*/n is equal to one — any anisotropy lowers the value below one.

It should be clear that since we have available the $\tau(\underline{k},T)$ necessary to compute (3.3.2), it is a simple matter to obtain the variation of n^*/n with T. Accordingly, then, (Hayman and Carbotte 1972a) we have computed the value of n^*/n as a function of T in Na, K, Rb, and Li and our results are presented in Figures (3.3.1) and (3.3.2). In Figure (3.3.2) we have also shown the results obtained with some other pseudo-potentials in the case of K. The potentials used are the same as those considered in the treatment of the low temperature phonon drag thermopower in K. The reader is referred to Figure (2.5.7) for a plot of the different pseudo-potentials.

We take note of the general behaviour and observe that in each case n^*/n is close to 1 at high T, drops as T is lowered, passes through a well-defined minimum, and finally rises back to approach unity. This behaviour is clearly understood on the basis of the temperature dependence of the anisotropy in the scattering times which has been discussed at some length in the previous section. To reiterate briefly, the aniso-

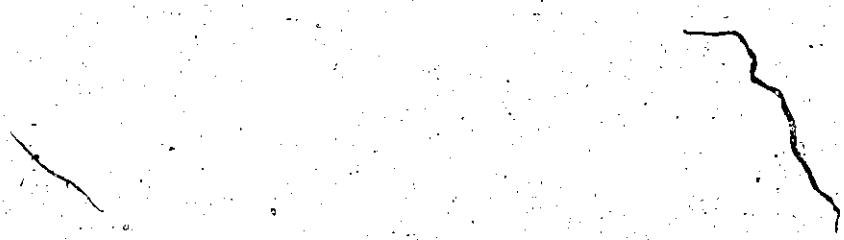

Fig. 3.3.1 Effective number of carriers n*/n as a function of temperature for Na, Rb, and Li. In each case the "best" Ashcroft pseudo-potentials from Chapter II have been used.

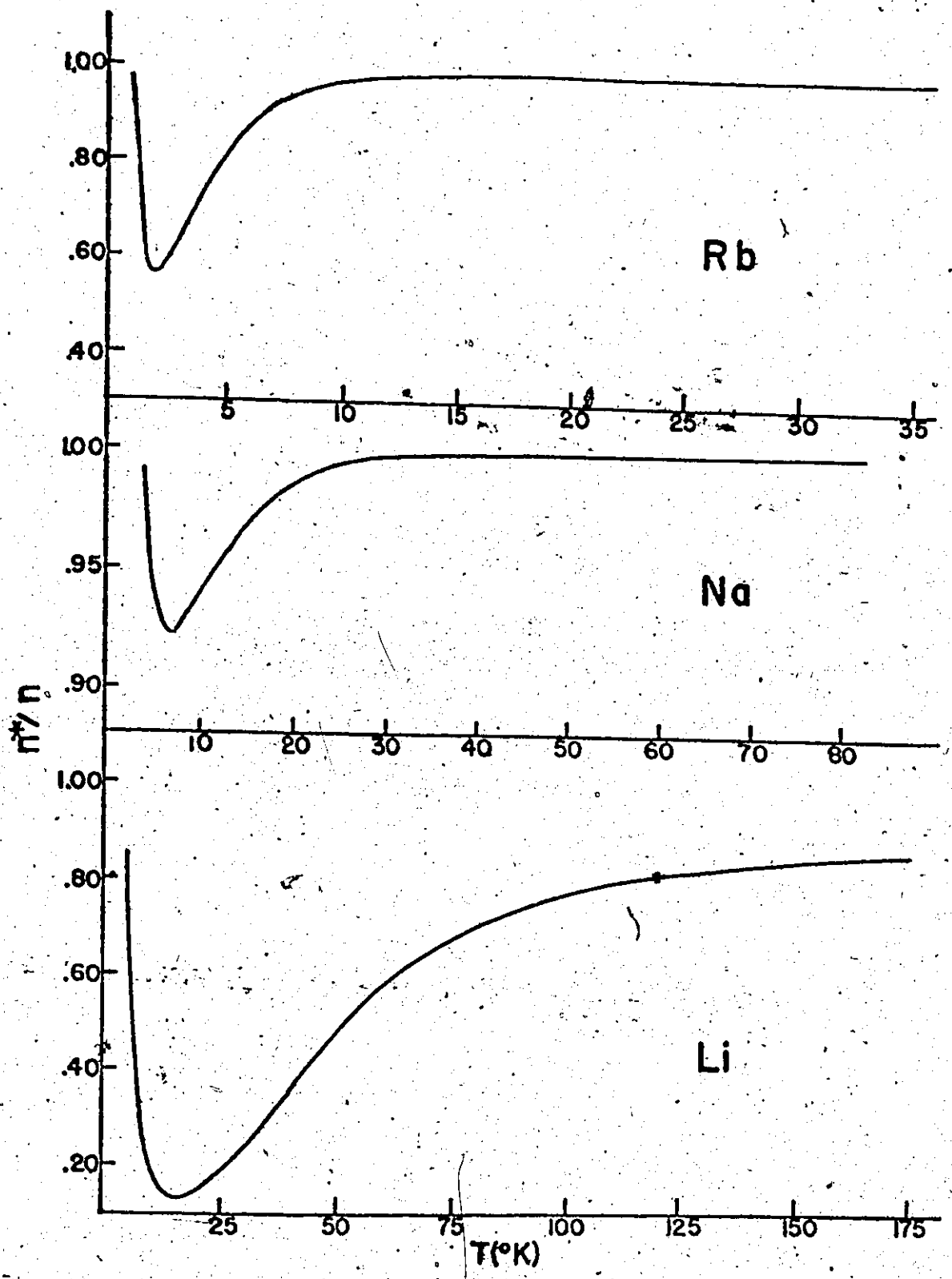
1.00
.80
.60
.40
Rb
5
10
15
20
25
30
35
1.00
.95
.90
Na
10
20
30
40
50
60
70
80
n*/ n
1.00
.80
.60
.40
.20
Li
25
50
75
100
125
150
175
T(°K)

Fig. 3.3.2 Effective number of carriers n^*/n as a function of temperature in K. 1 - Ashcroft with $R_c \sim 1.04\text{Å}$; 2 - Lower Lee-Falicov; 3 - Bardeen; 4 - Ashcroft with $R_c \sim 1.28\text{Å}$.

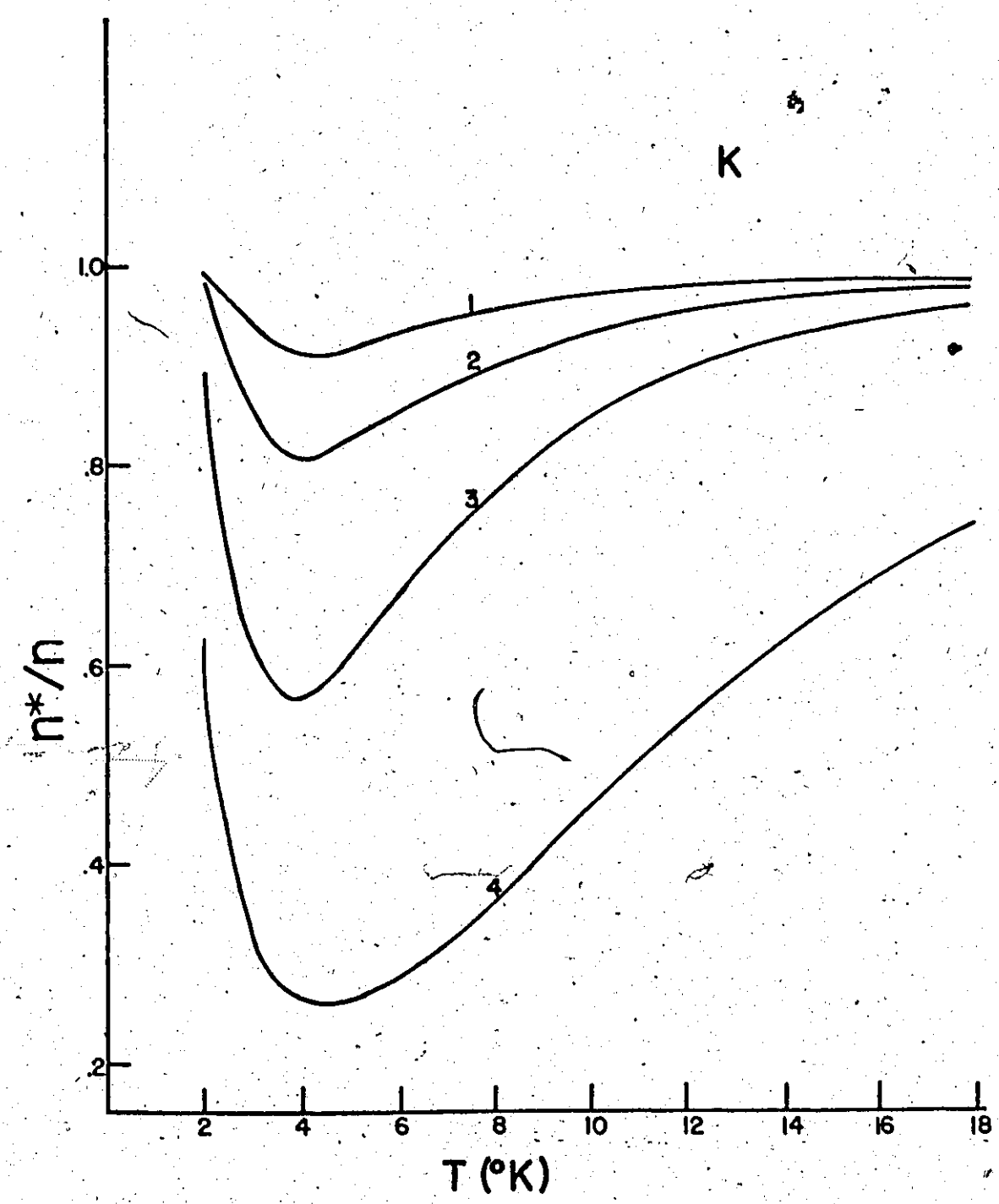
K
1.0
.8
.6
.4
.2
n*/n
1
2
3
4
2
4
6
8
10
12
14
16
18
T (°K)

tropy increases with decreasing temperature, and then passes through a maximum and decreases as the lowest ends of the $\alpha^2_{tr}F_{\underline{k}}(\omega)$ functions (which we recall are determined solely by Normal processes) begin to dominate in the frequency integrations which determine the $\tau(\underline{k},T)$.

We believe these calculations to be the first to demonstrate the variation of n^*/n with T.

Recently, Alderson and Farrell (1969) have measured n^*/n in Li, Na, and K in the temperature range from 6 - 300°K. It is observed that n^*/n decreases slowly with T in qualitative agreement with our calculations. Na and K show the least variation while the behaviour in Li is more severe, again in general agreement with our calculations. They also observe a minimum in n^*/n as a function of T. However, their experimental minimum occurs at temperatures somewhat higher than our calculated minimum (~ 20°K in potassium as opposed to ~ 4°K). The discrepancy can, perhaps, be attributed to a combination of factors. (a) Our calculations are for the case of the ideally pure metal, and as recent calculations by Kus and Carbotte (1973) have indicated, the effects of even the smallest amounts of impurity are crucial in washing out the anisotropy (impurity scattering is essentially elastic and isotropic) in the scattering times; (b) As Hurd (1972) points out, the experimental measurements of Alderson and Farrell are not strictly in the low field limit due to the presence of impurities and the magnitudes of the magnetic fields employed, and finally (c) Alderson and Farrell speculate that either phonon drag effects or impurity scattering could give rise to the minimum observed.

Our theoretical minimum is clearly due to the onset of Umklapp processes and we would expect this effect to still be present in any further calculation which might try to incorporate some of the effects mentioned above, in particular, a solution of the transport problem in the intermediate field region ($\omega_c \tau \sim 1$).

However, we have clearly demonstrated the qualitative behaviour of n^*/n with T and in terms of a quantitative comparison with experiment we note that Robinson and Dow (1968) quote room temperature experimental results for n^*/n of 0.87 (0.79) in Li, 0.95 (1.17) in Na, 0.95 (1.11) in K, and 0.94 in Rb. The numbers in parentheses are other experimental numbers which are included to indicate the uncertainty which exists at the present time. For Li we obtain 0.87 and in the other metals we obtain numbers slightly less than one. We consider this agreement satisfactory.

We refer, once again, to Figure (3.3.2) where plots of n^*/n vs T for different pseudo-potentials in K are shown. One notes that the general behaviour of the different curves is similar but there are significant quantitative differences. The differences arise solely due to the different amounts of Umklapp scattering introduced by each potential — the more the Umklapp contribution (determined essentially by how large the potential is at $q \sim 2k_f$) the greater the anisotropy and the deeper the minimum in the n^*/n vs T curve. It is clear, then, that the variation of n^* with T is quite sensitive to the choice of pseudo-potential.

We would like to conclude this section by demonstrating conclusively the role of the Umklapp processes in determining the anisotropy

Fig. 3.3.3 Effective number of carriers n*/n as a function of temperature, calculated on the basis of Normal processes only.

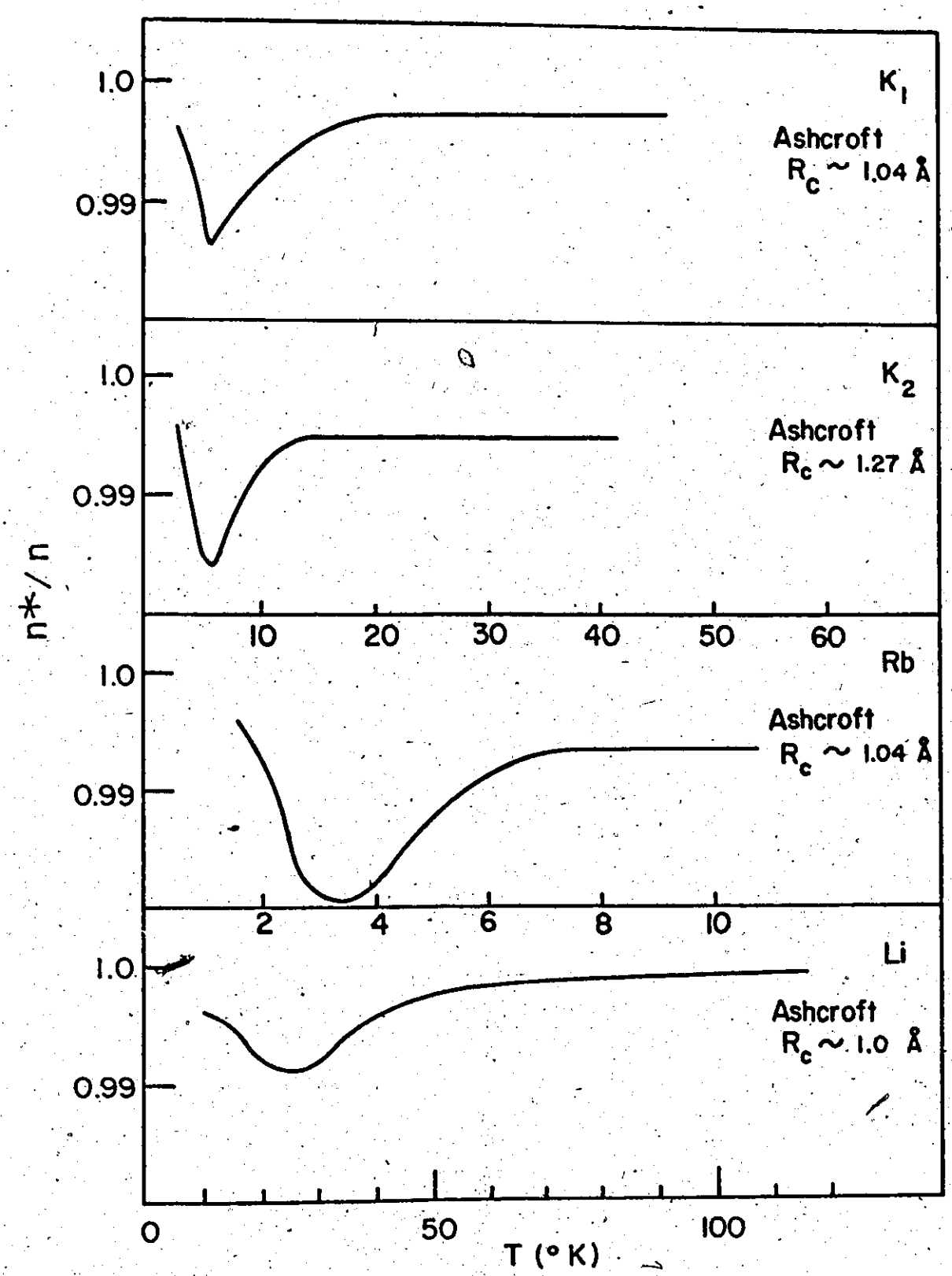
1.0
0.99
K1
Ashcroft
Rc ~ 1.04 Å
K2
Ashcroft
Rc ~ 1.27 Å
n*/n
10
20
30
40
50
60
Rb
Ashcroft
Rc ~ 1.04 Å
2
4
6
8
10
Li
Ashcroft
Rc ~ 1.0 Å
0
50
100
T (°K)

by showing plots of n^*/n vs T in K, Rb, and Li except that here, the $\tau(\underline{k},T)$ have been calculated solely on the basis of Normal processes only. These are shown in Figure (3.3.3).

One first notes that the variation in n^*/n with T is qualitatively similar to that previously shown, except that quantitatively is orders of magnitude less. This clearly demonstrates the dominant role of the Umklapp component of the interaction in determining the overall behaviour. The presence of a minimum here is interesting as our previous explanation (the onset of Umklapp processes) is obviously not valid. Perhaps the explanation lies in the following argument. At high temperatures, once again, the entire phonon spectrum is sampled and the anisotropy washes out. As T is lowered, however, anisotropy, which we believe comes from the difference in energy of the various branches for a given $\underline{q}$, coupled with the fact that $\underline{q} \cdot \underline{\varepsilon}_{\underline{q}\lambda}$ is zero for purely transverse modes, will begin to play a role and finally, at the lowest T's, where the energy differences between the branches are now minimized, the anisotropy washes out again. However, we emphasize that these considerations are essentially negligible since, in determining the overall anisotropy, the role of the Umklapp processes are predominant.

In the final section of this Chapter, we would like to consider the effect of the anisotropy in the scattering times, on the electrical resistivity.

3.4 The Effect Of Anisotropy In The Scattering Times On The Electrical Resistivity

In this, the final section of this Chapter, we would like to

consider the effect that a consideration of the anisotropy in the scattering times has in calculation of the ideal electrical resistivity (Hayman and Carbotte 1972b).

As pointed out in Section 3.1, the resistivity as obtained in the scattering time solution to the Boltzmann equation is given by

$$\rho_{ST}(T) = \frac{m}{ne^2 \tau_{av}(T)} \tag{3.4.1}$$

where m is the electron mass, n the number of electrons per unit volume, e the electronic charge and $\tau_{av}(T)$ is given by

$$\tau_{av}(T) = \langle \tau(\underline{k},T) \rangle_{F.S.} = \int_{F.S.} \frac{d\Omega_{\underline{k}}}{4\pi} \tau(\underline{k},T) \tag{3.4.2}$$

Robinson and Dow (1968) point out that the standard variational solution to the Boltzmann equation, which we employed in Chapter II, is equivalent to the following expression for a resistivity in terms of scattering times

$$\rho_{v}(T) = \frac{m}{ne^2} \left\langle \frac{1}{\tau(\underline{k},T)} \right\rangle_{F.S.} \tag{3.4.3}$$

This follows quite simply from the fact that the $\alpha^2_{tr}F(\omega)$ function used to determine the resistivities in the variational solution is merely the Fermi surface average of the $\alpha^2_{tr}F_{\underline{k}}(\omega)$ functions used to determine the scattering times

$$\alpha^2_{tr}F(\omega) = \int_{F.S.} \frac{d\Omega_{\underline{k}}}{4\pi} \alpha^2_{tr}F_{\underline{k}}(\omega) \tag{3.4.4}$$

In the limit of completely isotropic scattering, it is clear that the expressions (3.4.1) and (3.4.3) will yield identical resistivities. However, in the presence of anisotropic scattering, as RD

point out, (3.4.3) is equivalent to adding the resistivities of a parallel circuit, whereas we should be adding the conductivities. This is indeed what is done when the resistivity is obtained by (3.4.1). This again points out an advantage of the scattering time solution; it offers one a much more physically transparent approach to the problem.

It is clear, then, that an unambiguous comparison is possible between the resistivities obtained from the two different solutions — one merely computes the two different averages implied in (3.4.1) and (3.4.3). Accordingly, then, in Tables (3.4.1), (3.4.2), (3.4.3) and (3.4.4) we show the resistivities obtained, as a function of temperature, in the four metals. In each case the Ashcroft potentials developed in Chapter II have been used exclusively.

One first of all notes that the general behaviour of the anisotropy in the $\tau(\underline{k},T)$ (discussed in Section 3.2) manifests itself once again. The differences between the two resistivities are minimum at the very highest and lowest temperatures (least anisotropy) and are maximum at some intermediate temperatures. In all cases ρ_{ST} is less than ρ_V. This is an important point as it indicates that the scattering time solution to the Boltzmann equation is definitely a superior solution, relative to the standard variational solution. This is so of course because, as Ziman (1960) points out, the lowest order variational trial function yields an upper bound to the resistivity — better solutions to the Boltzmann equation will lower the resistivity towards the "true" resistivity, which would be obtainable if one had the exact solution to the Boltzmann equation.

TABLE 3.4.1

RESISTIVITIES AS A FUNCTION OF TEMPERATURE IN Na, ρ_{ST} AND ρ_V RESPECTIVELY REFER TO RESISTIVITIES OBTAINED FROM THE SCATTERING TIME AND THE FIRST ORDER VARIATIONAL SOLUTIONS TO THE BOLTZMANN EQUATION

Na (Ashcroft R_c = 0.8282Å)			
T(°K)	ρ_{ST}(Ω-cm)	ρ_V(Ω-cm)	ρ_{ST}/ρ_V
3	5.06×10^{-13}	5.10×10^{-13}	0.992
4	2.93×10^{-12}	2.96×10^{-12}	0.991
5	1.42×10^{-11}	1.48×10^{-11}	0.959
6	5.26×10^{-11}	5.61×10^{-11}	0.938
7	1.50×10^{-10}	1.61×10^{-10}	0.934
8	3.50×10^{-10}	3.74×10^{-10}	0.937
9	7.00×10^{-10}	7.43×10^{-10}	0.942
12	3.12×10^{-9}	3.25×10^{-9}	0.959
20	2.62×10^{-8}	2.66×10^{-8}	0.986
30	1.02×10^{-7}	1.02×10^{-7}	0.996
40	2.21×10^{-7}	2.21×10^{-7}	0.998
60	5.11×10^{-7}	5.11×10^{-7}	0.999

TABLE 3.4.2

RESISTIVITIES AS A FUNCTION OF TEMPERATURE IN K. THE NOTATION IS THE SAME AS IN TABLE (3.4.1)

K (Ashcroft R_c = 1.0353Å)			
T(°K)	ρ_{ST} (Ω-cm)	ρ_V (Ω-cm)	ρ_{ST}/ρ_V
2	1.41×10^{-12}	1.42×10^{-12}	0.995
3	1.98×10^{-11}	2.09×10^{-11}	0.949
4	1.30×10^{-10}	1.40×10^{-10}	0.930
5	4.81×10^{-10}	5.14×10^{-10}	0.935
6	1.25×10^{-9}	1.32×10^{-9}	0.946
7	2.61×10^{-9}	2.73×10^{-9}	0.955
8	4.68×10^{-9}	4.85×10^{-9}	0.964
9	7.60×10^{-9}	7.83×10^{-9}	0.971
10	1.15×10^{-8}	1.18×10^{-8}	0.977
12	2.26×10^{-8}	2.29×10^{-8}	0.986
14	3.84×10^{-8}	3.87×10^{-8}	0.991
16	5.91×10^{-8}	5.95×10^{-8}	0.994
18	8.46×10^{-8}	8.49×10^{-8}	0.996
20	1.14×10^{-7}	1.14×10^{-7}	0.997

TABLE 3.4.3

RESISTIVITIES AS A FUNCTION OF TEMPERATURE IN Rb. THE NOTATION IS THE SAME AS IN TABLE (3.4.1)

Rb (Ashcroft R_c = 1.0422Å)			
T(°K)	ρ_{ST} (Ω-cm)	ρ_V (Ω-cm)	ρ_{ST}/ρ_V
1.0	2.74×10^{-13}	2.80×10^{-13}	0.979
1.4	3.47×10^{-12}	4.46×10^{-12}	0.777
1.8	2.53×10^{-11}	3.65×10^{-11}	0.692
2.0	5.57×10^{-11}	8.07×10^{-11}	0.690
2.4	2.00×10^{-10}	2.80×10^{-10}	0.716
3.0	7.89×10^{-10}	1.03×10^{-9}	0.766
5.0	9.11×10^{-9}	1.04×10^{-8}	0.876
7.0	3.16×10^{-8}	3.38×10^{-8}	0.934
10.0	9.50×10^{-8}	9.76×10^{-8}	0.973
20.0	4.57×10^{-7}	4.60×10^{-7}	0.994
30.0	8.65×10^{-7}	8.68×10^{-7}	0.996
50.0	1.65×10^{-6}	1.65×10^{-6}	0.997

TABLE 3.4.4

RESISTIVITIES AS A FUNCTION OF TEMPERATURE IN Li. THE NOTATION IS THE SAME AS IN TABLE (3.4.1)

Li (Ashcroft R_c = 1.0005Å)			
T(°K)	ρ_{ST}(Ω-cm)	ρ_V(Ω-cm)	ρ_{ST}/ρ_V
5	4.92×10^{-13}	6.17×10^{-13}	0.798
7	6.61×10^{-12}	2.11×10^{-11}	0.314
11	1.79×10^{-10}	1.06×10^{-9}	0.169
15	1.43×10^{-9}	7.33×10^{-9}	0.195
20	7.81×10^{-9}	2.90×10^{-8}	0.269
30	5.27×10^{-8}	1.28×10^{-7}	0.419
50	3.03×10^{-7}	4.73×10^{-7}	0.640
100	1.39×10^{-6}	1.68×10^{-6}	0.830
150	2.58×10^{-6}	2.95×10^{-6}	0.874
250	4.84×10^{-6}	5.40×10^{-6}	0.897
300	5.94×10^{-6}	6.59×10^{-6}	0.901

In the cases of Na, K, and Rb, one notes that at high temperatures, the two resistivities are essentially identical and that differences arise in a relatively small temperature range around a few °K. In Na the maximum difference is ~ 6%, in K ~ 7%, and in Rb ~ 30%. However, in the case of Li the differences are quite significant over the entire temperature range being ~ 10% at 300°K and rising to a maximum of ~.83% at 11°K. This, of course, is in keeping with the fact that Li has the severest anisotropy. From these behaviours one can conclude

(a) in Na, K, and Rb, anisotropy in the electron-phonon interaction (as it appears in the electrical resistivity) can safely be neglected at high temperatures (T > 30°K); however,

(b) any low temperature calculations in these metals must be done in a formulation which properly includes anisotropy and,

(c) in the case of Li, anisotropy is important over the entire temperature range and ignoring it can lead to quite significant effects.

At this stage we remind the reader that all the above comments are for the pure metals only. The presence of impurities drastically reduces the anisotropy (impurity scattering is essentially elastic and isotropic) and consequently affects the degree to which the above conclusions will apply. The reader is referred to the work of Kus and Carbotte (1973) for further details in this regard.

To illustrate the effect of using different pseudo-potentials in a given metal, we have calculated the resistivities obtained, in the two different solutions in K for a number of different pseudo-potentials. The potentials considered are the same as those considered in our treatment of the phonon drag effect and later in the behaviour of the Hall

TABLE 3.4.5

RESISTIVITIES AS A FUNCTION OF TEMPERATURE FOR FOUR DIFFERENT CHOICES OF PSEUDO-POTENTIAL IN K.

THE NOTATION IS THE SAME AS IN TABLE (3.4.1)

	Bardeen		Lower Lee-Falicov		Ashcroft ($R_c \sim 1.04$Å)		Ashcroft ($R_c \sim 1.28$Å)	
T(°K)	ρ_{ST}/ρ_V	ρ_V(Ω-cm)	ρ_{ST}/ρ_V	ρ_V(Ω-cm)	ρ_{ST}/ρ_V	ρ_V(Ω-cm)	ρ_{ST}/ρ_V	ρ_V(Ω-cm)
2	0.891	2.28×10^{-12}	0.984	1.52×10^{-12}	0.995	1.42×10^{-12}	0.529	5.82×10^{-12}
3	0.688	5.32×10^{-11}	0.882	2.50×10^{-11}	0.949	2.09×10^{-11}	0.309	1.69×10^{-10}
4	0.687	3.49×10^{-10}	0.860	1.58×10^{-10}	0.930	1.40×10^{-10}	0.302	1.03×10^{-9}
5	0.730	1.18×10^{-9}	0.873	5.43×10^{-10}	0.935	5.14×10^{-10}	0.339	3.20×10^{-9}
6	0.772	2.77×10^{-9}	0.891	1.32×10^{-9}	0.946	1.32×10^{-9}	0.387	6.96×10^{-9}
7	0.809	5.28×10^{-9}	0.908	2.57×10^{-9}	0.955	2.73×10^{-9}	0.438	1.24×10^{-8}
8	0.840	8.81×10^{-9}	0.923	4.38×10^{-9}	0.964	4.85×10^{-9}	0.488	1.94×10^{-8}
9	0.866	1.34×10^{-8}	0.936	6.82×10^{-9}	0.971	7.83×10^{-9}	0.536	2.80×10^{-8}
10	0.888	1.91×10^{-8}	0.948	9.96×10^{-9}	0.977	1.18×10^{-8}	0.581	3.76×10^{-8}
12	0.923	3.41×10^{-8}	0.965	1.84×10^{-8}	0.986	2.29×10^{-8}	0.660	6.05×10^{-8}
14	0.946	5.38×10^{-8}	0.977	3.02×10^{-8}	0.991	3.87×10^{-8}	0.712	8.73×10^{-8}
16	0.961	7.81×10^{-8}	0.984	4.54×10^{-8}	0.994	5.95×10^{-8}	0.770	1.17×10^{-7}
18	0.971	1.07×10^{-7}	0.988	6.37×10^{-8}	0.996	8.49×10^{-8}	0.805	1.51×10^{-7}
20	0.977	1.39×10^{-7}	0.991	8.49×10^{-8}	0.997	1.14×10^{-7}	0.832	1.85×10^{-7}

Fig. 3.4.1 Plots of ρ/T^5 in the temperature range 2 - 20°K in potassium for four different choices of pseudo-potential. ρ_{N+U}/T^5 corresponds to resistivities calculated with Normal and Umklapp processes. ρ_N/T^5 corresponds to resistivities calculated with Normal processes only. In each case the lower curve corresponds to ρ_{ST}/T^5 and the upper curve ρ_V/T^5.

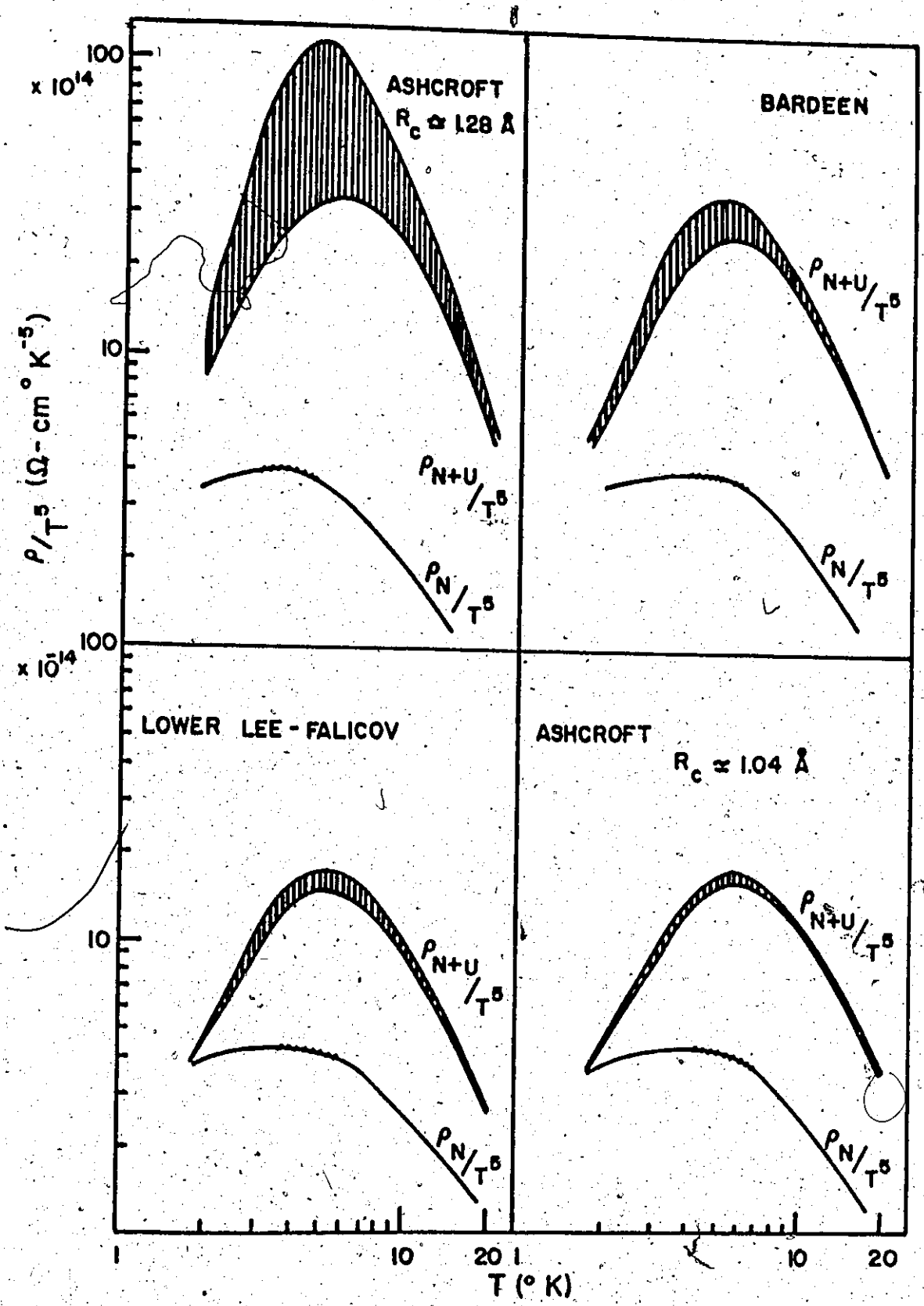
ASHCROFT
$R_c \simeq 1.28$ Å
BARDEEN
ρ_{N+U}/T^5
ρ_N/T^5
LOWER LEE - FALICOV
ASHCROFT
$R_c \simeq 1.04$ Å
ρ/T^5 (Ω-cm °K^{-5})
x 10^{14}
100
10
1
20
T (° K)

coefficient. The results obtained are shown in Table (3.4.5). In Figure (3.4.1) we show plots of ρ/T^5 both for the total resistivities and for resistivities obtained if Umklapp processes are arbitrarily excluded from the integrations.

One notes that the differences between ρ_{ST} and ρ_V are very much a function of the pseudo-potential used. In particular, the more heavily weighted the Umklapps (the size of the potential at $q \sim 2k_f$) the more the anisotropy and consequently the greater the difference between ρ_{ST} and ρ_V. The differences are most pronounced in the case of the Ashcroft potential with $R_c \sim 1.28\text{Å}$, and least for the Ashcroft with $R_c \sim 1.04\text{Å}$. The Bardeen and Lee-Falicov potentials provide intermediate cases.

It is interesting to observe that the differences between the resistivities obtained with the different pseudo-potentials are very much less in the case of ρ_{ST} than for ρ_V. This, of course, is due to the fact that a greater Umklapp contribution leads to more anisotropy which in turn leads to a greater lowering of the resistivity when the more physical averaging of the $\tau(\underline{k},T)$, as given by (3.4.1) and (3.4.2), is carried out. One also observes that the Normal contributions to the resistivity are essentially the same in each potential and there is essentially no difference between ρ_{ST} and ρ_V in this case.

Recently, Ekin and Bringer (1973) have approached the problem of including anisotropy in the electron-phonon interaction into calculations of the electrical resistivity from the viewpoint of the variational solution to the Boltzmann equation. They include higher order-

terms in the trial functions used in the variational expression for the resistivity. These extra terms specifically include an orientational dependence into the electron-phonon interaction. Their final results are qualitatively similar to ours—including anisotropy reduces the resistivity relative to the first order variational resistivity — however, the magnitudes of the reductions obtained are somewhat less for the same pseudo-potential than what we observe. Also, as mentioned previously, their variational procedure suffers from the defect of not being as physically transparent as the scattering time approach we employ.

In conclusion, then, one observes that anisotropy in the electron-phonon interaction can have quite significant effects on calculations of the electrical resistivity, the effect being most pronounced at the lowest temperatures.

CHAPTER IV

THE FAILURE OF THE ONE OPW APPROXIMATION IN POLYVALENT METALS AND A DISCUSSION OF A SIMPLE DEVICE TO TREAT IT

4.1 The Bross and Bohn Correction To The Bardeen Pseudo-Potential

It is a well-known fact (Sham and Ziman 1963) that when one is considering the electron-phonon interaction in systems where the Fermi surface intersects zone boundaries (either in polyvalent metals or monovalent metals with severely distorted Fermi surfaces), the one OPW electron-phonon coupling constant $g_{\underline{k}\underline{k}'\lambda}$, given by

$$g_{\underline{k}\underline{k}'\lambda} = -i\left(\frac{\hbar}{2MN\omega_{\underline{q}\lambda}}\right)^{\frac{1}{2}} W(\underline{q})\, \underline{q}\cdot\underline{\varepsilon}_{\underline{q}\lambda} \qquad (4.1.1)$$

becomes infinite whenever the momentum transfer $\underline{q}$ ($= \underline{k}' - \underline{k}$) becomes exactly equal to a reciprocal lattice vector $\underline{G}$. This divergence occurs because of the frequency factor $\omega_{\underline{q}\lambda}$ which appears in the denominator of (4.1.1). When $\underline{q} = \underline{G}$, $\omega_{\underline{q}\lambda}$ (which is determined through $\underline{q}_{red} = \underline{q} - \underline{G}$) becomes equal to zero.

The standard procedure to eliminate this difficulty is to expand the electron states $|\underline{k}\rangle$ and $|\underline{k}'\rangle$ in terms of multiple OPW's, the number of terms in the expansion being determined by the symmetry requirements of the particular state. When this is done $g_{\underline{k}\underline{k}'\lambda}$, in the limit of small q_{red}, becomes proportional to $q_{red}/\omega_{\underline{q}\lambda}$ instead of $q/\omega_{\underline{q}\lambda}$ and the divergence is removed. The reader is referred to Sham and Ziman (1963) for a detailed treatment of the problem. It is quite

obvious, however, that the numerical difficulties and computational time involved become rather prohibitive once one is dealing with a multiple, as opposed to a single, OPW system.

Bross and Bohn (1967) (BB) have proposed a simple device which enables one to eliminate the divergence while at the same time retaining the economies of a one OPW system and a spherical FS. Their method consists of merely replacing the Wigner-Seitz sphere which occurs in the familiar Bardeen (Bardeen 1937) pseudo-potential with the true Wigner-Seitz atomic polyhedron. When this is done, the spherically symmetric "shape factor" $G(|\underline{q}|)$ which appears in the standard Bardeen pseudo-potential is replaced by a new function $G'(\underline{q})$ which has the interesting property of being equal to zero whenever $\underline{q} = \underline{G}$. This, of course, eliminates the divergence in $g_{\underline{k}\underline{k}'\lambda}$.

Let us momentarily recall some of the features of the standard Bardeen pseudo-potential. The bare potential seen by the conduction electrons consists of two terms:

(a) An effective potential which represents the core. This is taken to be a square well, of radius r_s (the radius of the Wigner-Seitz sphere), and strength U_o. Sham and Ziman point out that this term should be derived from the Hartree-Fock potential of the neutral atom.

(b) The Coulomb potential of the charge of the valence electrons Ze, removed from the neutral atom to make it an ion. This is taken to be the electrostatic field of a charge $Z|e|$ spread uniformly throughout the Wigner-Seitz sphere (volume : Ω_o).

The bare potential leads to form factors given by (Ziman 1960)

$$W_o(\underline{q}) = \left[-\frac{4\pi Z e^2 N}{q^2} + U_o \right] G(|\underline{q}|) \qquad (4.1.2)$$

where $G(|\underline{q}|)$ is the "shape factor" mentioned above, and is essentially (Ziman 1960) the overlap of the electron states $|\underline{k}\rangle$ and $|\underline{k}+\underline{q}\rangle$ over the Wigner-Seitz sphere.

$$G(|\underline{q}|) = \frac{1}{\Omega_o} \int_{\text{Wigner-Seitz sphere}} e^{-i\underline{q}\cdot\underline{r}}\, d^3r \qquad (4.1.3)$$

Introducing the screening due to the electron gas, one obtains for the screened form factors

$$W(\underline{q}) = \frac{W_o(\underline{q})}{\epsilon(\underline{q})} \qquad (4.1.4)$$

where $\epsilon(q)$ is a suitable dielectric constant.

BB retain all the essentials of the original Bardeen pseudopotential except that wherever the Wigner-Seitz sphere enters into the picture (in the definition of the potential, in the integrations, etc.) it is replaced by the Wigner-Seitz polyhedron. They obtain identical expressions for $W(q)$ except that $G(|\underline{q}|)$ is replaced by $G'(q)$ given by

$$G'(\underline{q}) = \frac{1}{\Omega_o} \int_{\text{Wigner-Seitz atomic polyhedron}} e^{-i\,\underline{q}\cdot\underline{r}}\, d^3r \qquad (4.1.5)$$

$G'(q)$ is now obviously the overlap of $|\underline{k}\rangle$ and $|\underline{k}+\underline{q}\rangle$ over the atomic polyhedron.

For a fcc structure (we will be considering the case of Al in some detail) (4.1.5) can be rewritten as

$$G'(\underline{q}) = \frac{-2}{u^2+v^2+w^2}\left\{\frac{u+v}{(u-v)^2-w^2}\times\right.$$

$$\times\left[\sin v + \sin u - \sin\left(\frac{u+v+w}{2}\right) - \sin\left(\frac{u+v+w}{2}\right)\right] +$$

$$+\ \frac{u-v}{(u+v)^2-w^2}\left[\sin u - \sin v - \sin\left(\frac{u-v+w}{2}\right) - \sin\left(\frac{u-v-w}{2}\right)\right] + \qquad \ldots\ldots(4.1.6)$$

+ four additional cyclicly permuted terms, where $u = \frac{q_x a}{2}$, $v = \frac{q_y a}{2}$, $w = \frac{q_z a}{2}$ (a; lattice constant).

G'(q) as given by (4.1.5) or (4.1.6) has the following behaviour which appears to be merely a geometrical feature of the Wigner-Seitz cell,

$$G(\underline{q}) = \begin{cases} 0; & \underline{q} = \underline{G} \neq 0 \\ 1; & \underline{q} = 0 \end{cases} \qquad (4.1.7)$$

BB also point out that cubic symmetry is automatically included into W(q) by virtue of the fact that all integrations are performed over the Wigner-Seitz atomic polyhedron.

The only parameter which occurs in the pseudo-potential is the quantity U_o which BB show is essentially the difference in energy between the bottom of the conduction band and the potential on the surface of the atomic polyhedron, and can be estimated from band structure calculations. BB fit the resistivity at 300°K to obtain a value for U_o; however, we will take a value directly from the band calculations of Segall (1961). For the dielectric function $\varepsilon(q)$ we will use the familiar Lindhard expression already used in our treatment of the alkalis.

To summarize, then, the BB correction to the Bardeen pseudo-potential is to replace the "shape factor" $G(|\underline{q}|)$ with a new function

$G'(\underline{q})$ which has the required property of being equal to zero whenever $\underline{q}$ is equal to a reciprocal lattice vector. This is achieved by replacing the Wigner-Seitz sphere by a Wigner-Seitz atomic polyhedron in the definition of the potential. This new $G'(\underline{q})$ enables one to avoid the divergence which occurs in the one OPW coupling parameter $\varepsilon_{\underline{k}\underline{k}'\lambda}$ by setting $W(\underline{q})$, which appears in $\varepsilon_{\underline{k}\underline{k}'\lambda}$, equal to zero whenever $\underline{q} = \underline{G}$.

4.2 An Illustration Of The Failure Of The One OPW Approximation, And Its Rectification Using The Bross And Bohn Modification Of The Bardeen Pseudo-Potential, In Al

In this section, we will illustrate the failure of the one OPW approximation and its rectification in Al, by looking at the behaviour of $\alpha^2 F_{\underline{k}}(\omega)$, and the integral which determines the scattering time $\tau(\underline{k},T)$.

To start with, in Figure (4.2.1) we show a plot of the Heine-Abarenkov (HA) (Heine and Abarenkov, 1964) pseudo-potential in Al together with the BB pseudo-potential obtained if one uses a value of 0.335 Rydbergs for the parameter U_o. We have chosen this value on the basis of the band calculations of Segall (1961). One notes first of all that the BB pseudo-potential is not spherically symmetric and the form factors depend on $\underline{q}$ not merely $|\underline{q}|$. We have shown plots of $W(\underline{q})$ for $\underline{q}$ in the three major symmetry directions. The zeros of the BB potential occur at values of $\underline{q}$ for which $\underline{q} = \underline{G}$. Also on the q axis we have indicated the regions of exclusively Normal (N), exclusively Umklapp (U), and a mixture of the two (N+U), processes. To do this one merely looks at the largest and smallest values of $|\underline{q}|$ for which the tip of $\underline{q}$ lies on a zone boundary. An interesting feature to note here is that due to

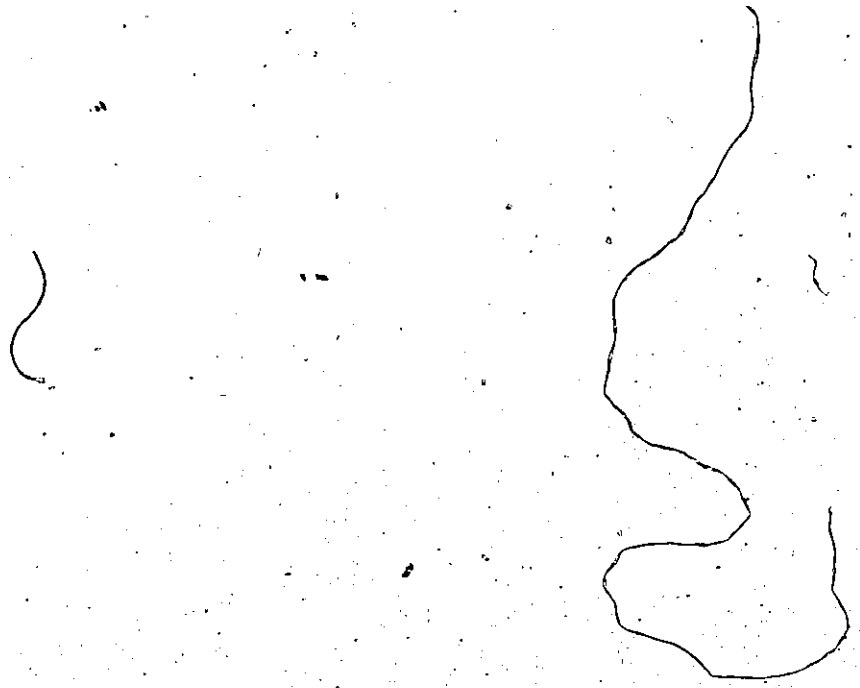

Fig. 4.2.1 A plot of the BA and BB potentials in Al. For the BB potential the three different plots are for q in the three high symmetry directions. On the q axis the three regions are: N - exclusively Normal processes, U - exclusively Umklapp processes, N + U a mixture of the two.

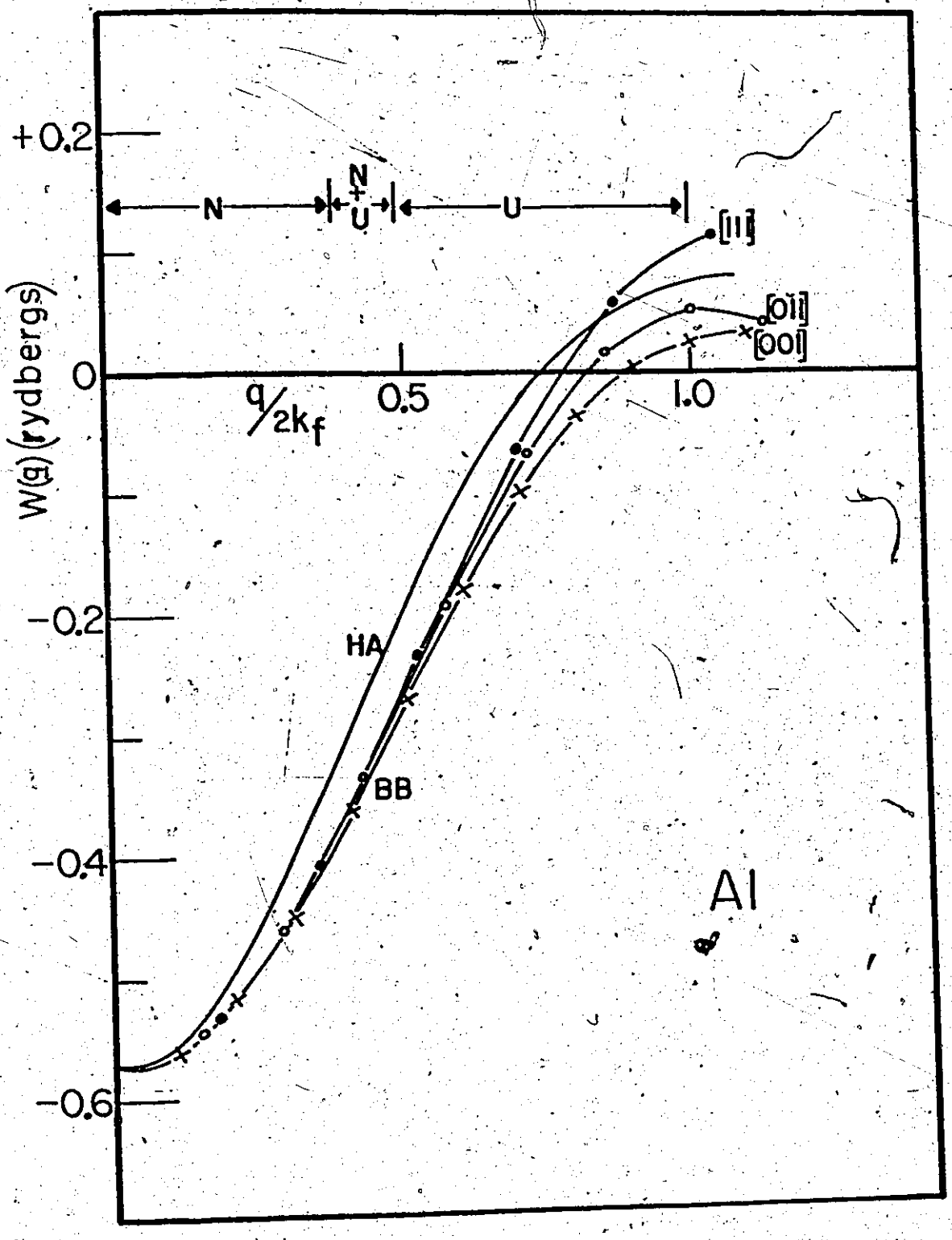
+0.2
0
−0.2
−0.4
−0.6
W(q) (rydbergs)
N
N+U
U
[111]
[011]
[001]
q/2k_f
0.5
1.0
HA
BB
Al

the polyvalent nature of Al, the Umklapp processes are going to be even more dominant here than in the case of the alkalis. One also notes that the BB potential is not too severely different from the HA potential.

Using the BB and HA pseudo-potentials mentioned above (with a spherical FS and in the one OPW approximation) and the Born-von Kármán force constants as measured by Gilat and Nicklow (1966) we have computed the directional $\alpha^2_{\underline{k}}F(\omega)$ and $\alpha^2_{tr}F_{\underline{k}}(\omega)$ functions, discussed in Chapter III, at 33 points on the irreducible $1/48^{th}$ of the FS of Al. These are the same points as used by Leavens and Carbotte (1972) in a discussion of the anisotropy in the electron-phonon contribution to the electron effective mass. The technique is exactly the same as that used in the calculations performed in the alkali metals and has been discussed in Chapter II.

For those values of $\underline{k}$ which lie close to the points of intersection of the free electron Fermi sphere and the FBZ, one can expect the divergence of the one OPW $g_{\underline{k}\underline{k}'\lambda}$ to be most obvious; as for these $\underline{k}$'s there will be many values of $\underline{q}$ for which $\underline{q} \approx \underline{G}$. Accordingly, then, we illustrate the divergence by showing plots of $\alpha^2_{\underline{k}}(\omega)$ (obtained by dividing $\alpha^2F_{\underline{k}}(\omega)$ by the directional frequency distribution $F_{\underline{k}}(\omega)$ (see 3.1.17)) vs frequency ω, for initial points $\underline{k} \equiv (k_f, \theta = 27°, \Phi = 0°)$, and $\underline{k} \equiv (k_f, \theta = 30°, \Phi = 0°)$. These points are close to Bragg planes. This is shown in Figure (4.2.2). On each plot the solid line represents $\alpha^2_{\underline{k}}(\omega)$ obtained using the BB potential, and the dotted line $\alpha^2_{\underline{k}}(\omega)$ obtained by using the HA potential.

The difference in the two behaviours is obvious and it is clear

Fig. 4.2.2 Plots of $\alpha^2_{\underline{k}}(\omega)$ $(\equiv \frac{\alpha^2 F_{\underline{k}}(\omega)}{F_{\underline{k}}(\omega)})$ vs ω for $\underline{k}$ at two points on the FS of Al. The solid line represents the results with the HA potential, the dotted line the results with the BB potential.

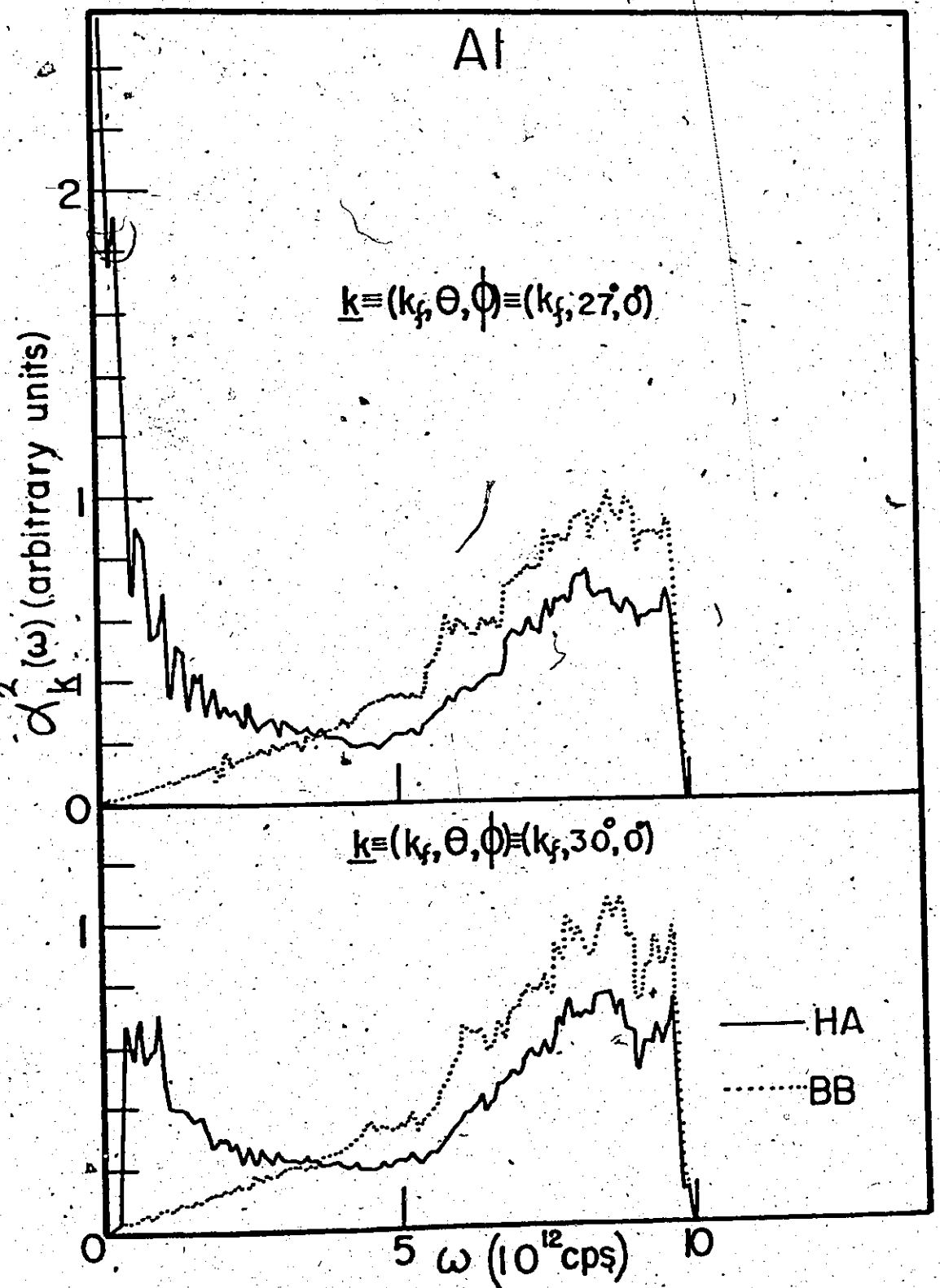
Al
k≡(k_f,θ,φ)≡(k_f,27°,0)
k≡(k_f,θ,φ)≡(k_f,30°,0)
α_k²(ω) (arbitrary units)
2
1
0
1
0
5
ω (10¹² cps)
10
HA
BB

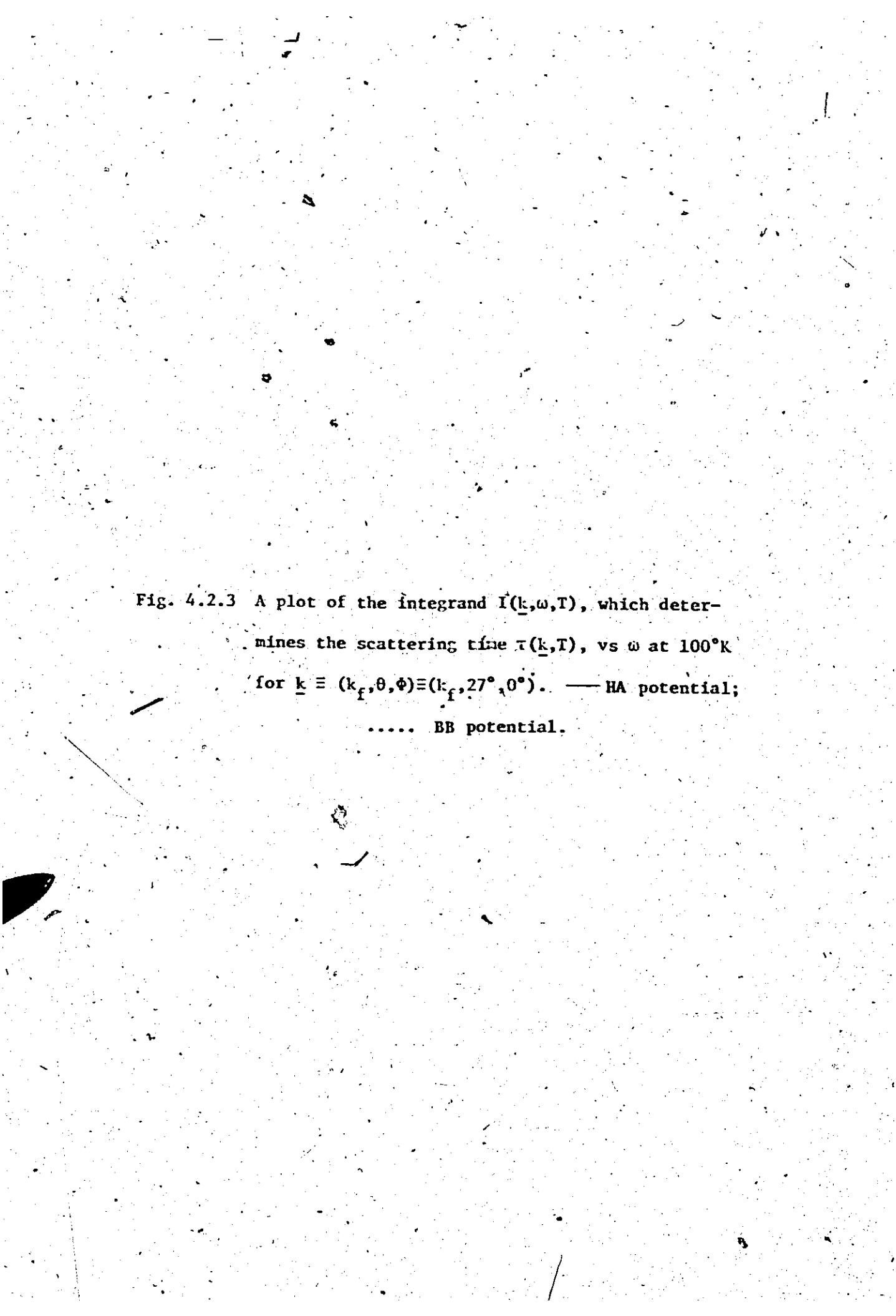

Fig. 4.2.3 A plot of the integrand $I(\underline{k},\omega,T)$, which determines the scattering time $\tau(\underline{k},T)$, vs ω at 100°K for $\underline{k} \equiv (k_f,\theta,\Phi) \equiv (k_f,27°,0°)$. —— HA potential; ..... BB potential.

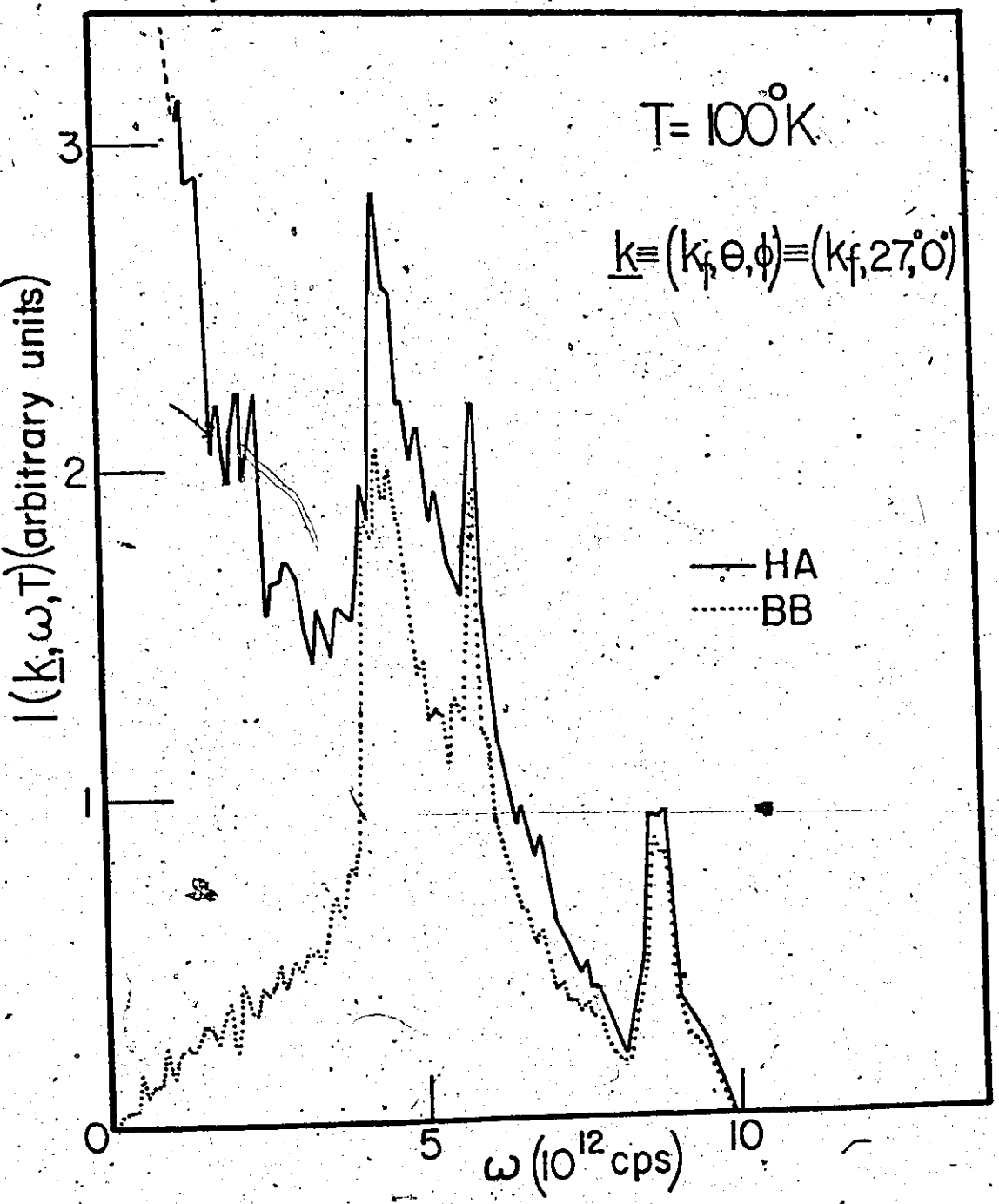
T= 100°K
k≡(kf,θ,φ)≡(kf,27°,0°)
HA
BB
I(k,ω,T)(arbitrary units)
3
2
1
0
5
10
ω (10^12 cps)

that the BB potential eliminates the divergence quite satisfactorily. The divergence also occurs in the calculation of the scattering time $\tau(\underline{k},T)$ associated with each point on the FS. This is clearly shown in Figure (4.2.3) where we have plotted the integrand $I(\underline{k},\omega,T)$ which occurs in the calculation of $\tau(\underline{k},T)$ according to (3.1.13). We have

$$\tau^{-1}(\underline{k},T) \propto \int_0^\infty I(\underline{k},\omega,T)\, d\omega \qquad (4.2.1)$$

where $I(\underline{k},\omega,T)$ is given by

$$I(\underline{k},\omega,T) = \frac{\omega \alpha^2_{tr} F_{\underline{k}}(\omega)}{(e^{\beta\omega}-1)(1-e^{-\beta\omega})} \qquad (4.2.2)$$

β is, of course, $(k_B T)^{-1}$.

At both temperatures considered, the divergence of $g_{\underline{k}\underline{k}'\lambda}$ for the HA potential shows up as an abnormally large contribution to $I(\underline{k},\omega,T)$ in the low frequency region. Also, it is clear that the BB potential adequately eliminates the divergence.

Having illustrated the failure of the conventional one OPW approximation and its rectification, in the next section we will consider some of the results obtained in Al using the BB potential.

4.3 Results Obtained In Aluminum Using The BB Pseudo-Potential

As previously mentioned, we have calculated the $\alpha^2 F_{\underline{k}}(\omega)$ and $\alpha^2_{tr} F_{\underline{k}}(\omega)$ functions in Al at 33 points on the irreducible $1/48^{th}$ of the FS using the one OPW approximation with the BB pseudo-potential.

We will use these functions to discuss the anisotropy in the scattering times, the phonon limited resistivity (both in terms of the scattering time and first order variational solutions to the Boltzmann

Fig. 4.3.1 The $\alpha^2 F_{\underline{k}}(\omega)$ functions for $\underline{k}$ in the three high symmetry directions in Al. All calculation with the BB potential.

—— Normal plus Umklapp;

..... Normal only.

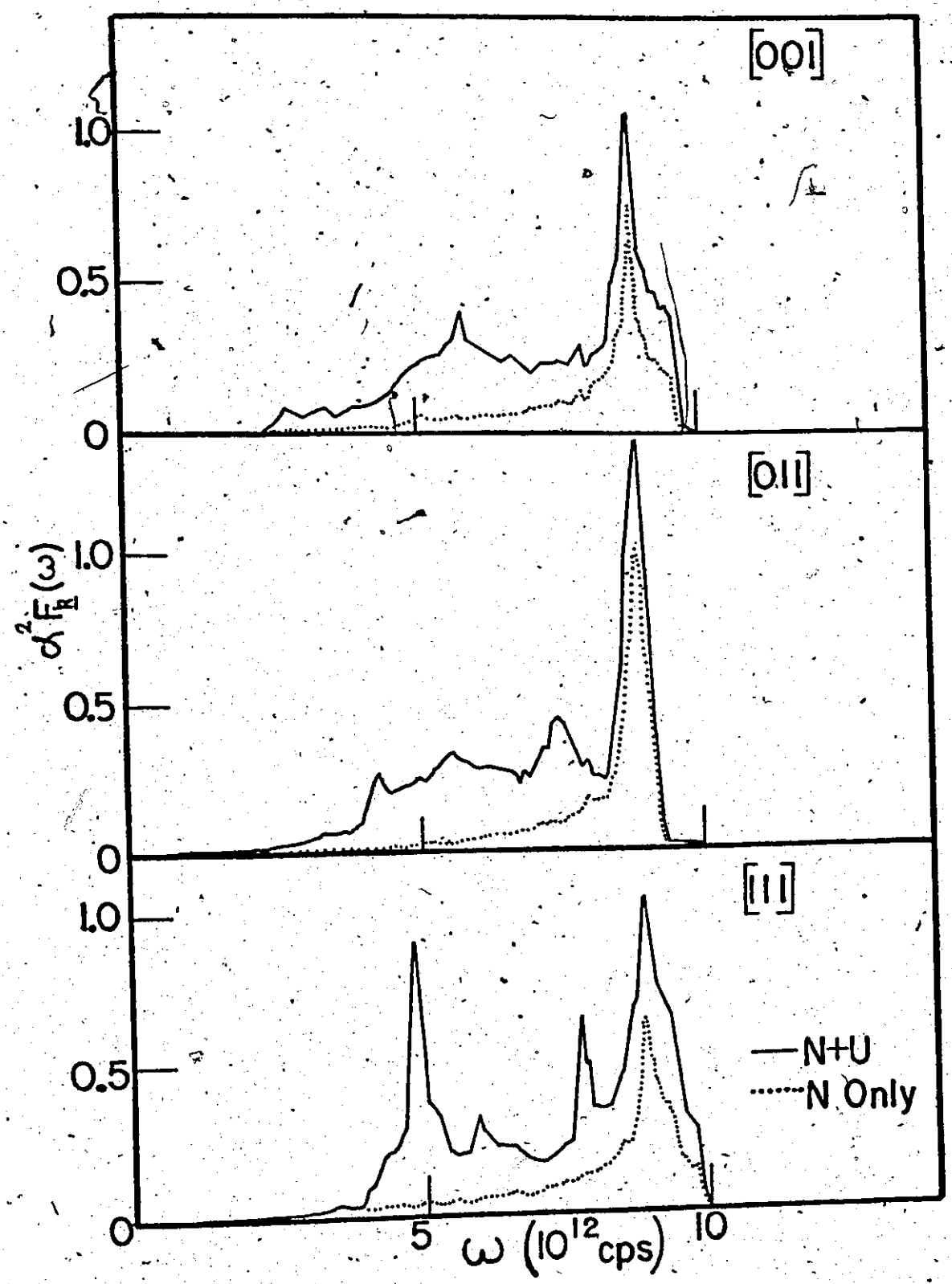
[001]
[011]
[111]
1.0
0.5
0
$\alpha^2 F_R(\omega)$
5
ω (10^{12}cps)
10
—N+U
·····N Only

Fig. 4.3.2 The $\alpha^2_{tr}F_{\underline{k}}(\omega)$ functions in Al. The notation is the same as Fig. 4.3.1.

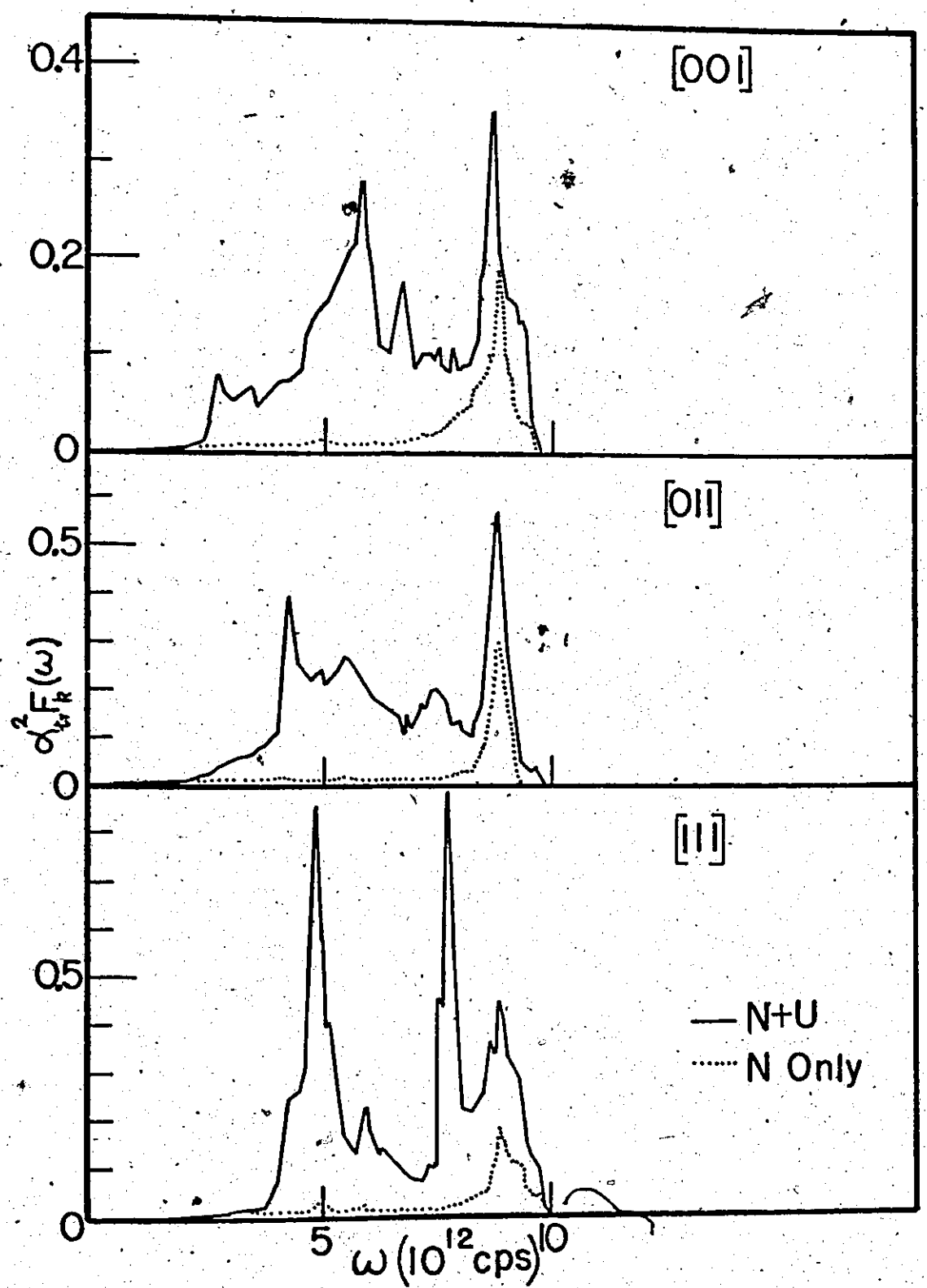
[001]
[011]
[111]
0.4
0.2
0
0.5
0
0.5
0
$\alpha^2 F_R(\omega)$
— N+U
····· N Only
5
$\omega\,(10^{12}\,cps)$
10

equation), and finally the anisotropy in the electron-phonon contribution to the electron effective mass.

In Figures (4.3.1) and (4.3.2), we show plots of the $\alpha^2 F_{\underline{k}}(\omega)$ and $\alpha^2_{tr} F_{\underline{k}}(\omega)$ functions in Al for $\underline{k}$ in the three high symmetry directions. In each plot we have included the functions obtained if Umklapp processes are arbitrarily excluded from the integrations. This is to demonstrate the crucial role played by Umklapp processes in determining the difference between the distributions and hence the anisotropy. It is interesting to note that the Umklapps are more dominant in $\alpha^2_{tr} F$ as opposed to $\alpha^2 F$. This is, of course, due to the extra q^2 term which appears in $\alpha^2_{tr} F$ as opposed to $\alpha^2 F$.

In Figure (4.3.3), we show plots of the scattering times as a function of position on the FS for three different temperatures. The same features as displayed in the alkali metals are present here. The anisotropy is minimum at high temperatures and increases as the temperature is lowered.

In Figure (4.3.4), we show plots of the resistivities obtained, in comparison with experiment. The experimental values are taken from Seth and Woods (1970).

We recall that, in terms of the $\tau(\underline{k},T)$, ρ_{ST} and ρ_V are given by

$$\rho_{ST}(T) = \frac{m}{ne^2} \cdot \frac{1}{\langle \tau(\underline{k},T) \rangle_{F.S.}} \qquad (4.3.1)$$

and

$$\rho_V(T) = \frac{m}{ne^2} \cdot \left\langle \frac{1}{\tau(\underline{k},T)} \right\rangle_{F.S.}$$

ρ_{ST} corresponds to the resistivity as obtained in the scattering time solution to the Boltzmann equation and ρ_V the resistivity as ob-

Fig. 4.3.3 The scattering times $\tau(\underline{k},T)$ as a function of position on the $1/48^{th}$ of the FS of Al.

• $\Phi = 0°$; x $\Phi = 22\frac{1}{2}°$; • $\Phi = 45°$.

All calculations are with the BB potential.

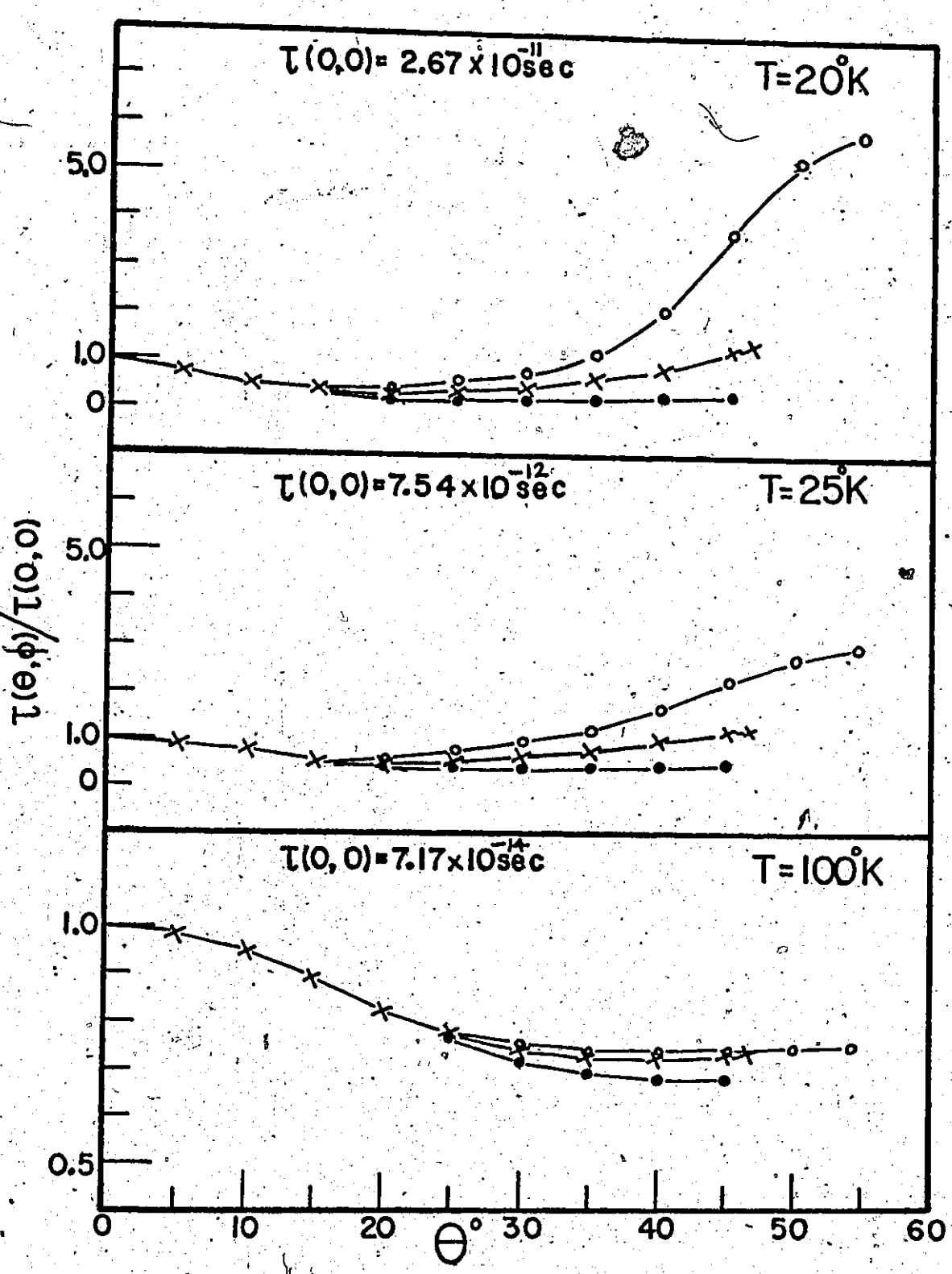
τ(0,0)= 2.67 x 10⁻¹¹ sec
T=20°K
τ(0,0)=7.54 x 10⁻¹² sec
T=25°K
τ(0,0)=7.17 x 10⁻¹⁴ sec
T=100°K
τ(θ,φ)/τ(0,0)
5.0
1.0
0
0.5
0
10
20
30
40
50
60
θ°

tained in the first order variational solution. From the figure, it is clear that the HA potential severely overestimates the resistivity at low temperatures. This is due to the divergence of the one OPW $g_{\underline{k}\underline{k}'\lambda}$ which leads to an abnormally large contribution to $\alpha^2_{tr}F_{\underline{k}}(\omega)$ at low frequency. The low frequency ends are emphasized at low temperature.

The best agreement is obtained with the BB potential and the resistivity as calculated in the scattering time approximation. It is quite clear that any attempt to reproduce the resistivity of Al over a wide temperature range must include a proper treatment of the divergence of the one OPW $g_{\underline{k}\underline{k}'\lambda}$. The discrepancies at high temperatures are attributable to our neglect of volume effects. We have in essence calculated a constant (zero volume) resistivity whereas the experimental values are for a constant (atmospheric) pressure situation.

In Figure (4.3.5), we show a plot of n*/n, the ratio of the effective carrier density to the free electron carrier density vs temperature. It is interesting to note that the behaviour is identical to that observed in the alkalis. The presence of a minimum, which indicates a maximum in the anisotropy of the scattering times, is worth discussing a little further. We momentarily recall that in terms of the $\tau(\underline{k},T)$, $\frac{n^*}{n}(T)$ is given by

$$\frac{n^*}{n}(T) = \frac{\langle \tau(\underline{k},T)\rangle^2_{F.S.}}{\langle \tau^2(\underline{k},T)\rangle_{F.S.}} \qquad (4.3.2)$$

The presence of a minimum can be understood as follows. For a majority of the points on the FS the geometry of the scattering processes will be such that the very low ω regions of the $\alpha^2_{tr}F_{\underline{k}}(\omega)$ will be determined exclusively by Normal processes, in analogy with the alkali

Fig. 4.3.4 The phonon limited resistivities $\rho(T)$ in Al.

The notation is explained in the text.

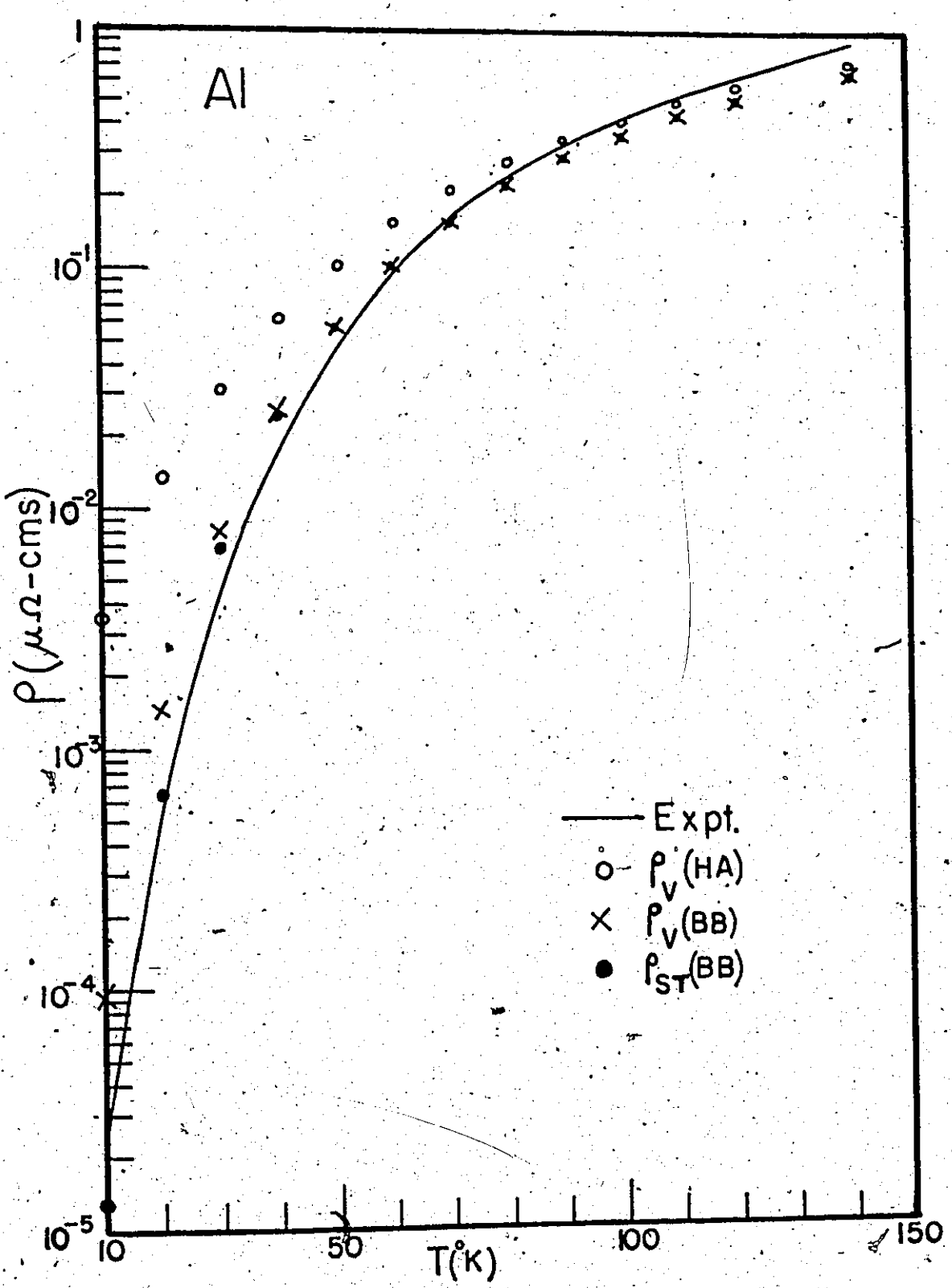
Al
1
10^{-1}
10^{-2}
10^{-3}
10^{-4}
10^{-5}
$\rho(\mu\Omega\text{-cms})$
10
50
100
150
T(°K)
Expt.
ρ_V(HA)
ρ_V(BB)
ρ_{ST}(BB)

Fig. 4.3.5 The effective number of carriers n*/n vs T in Al. All calculations with the BB potential.

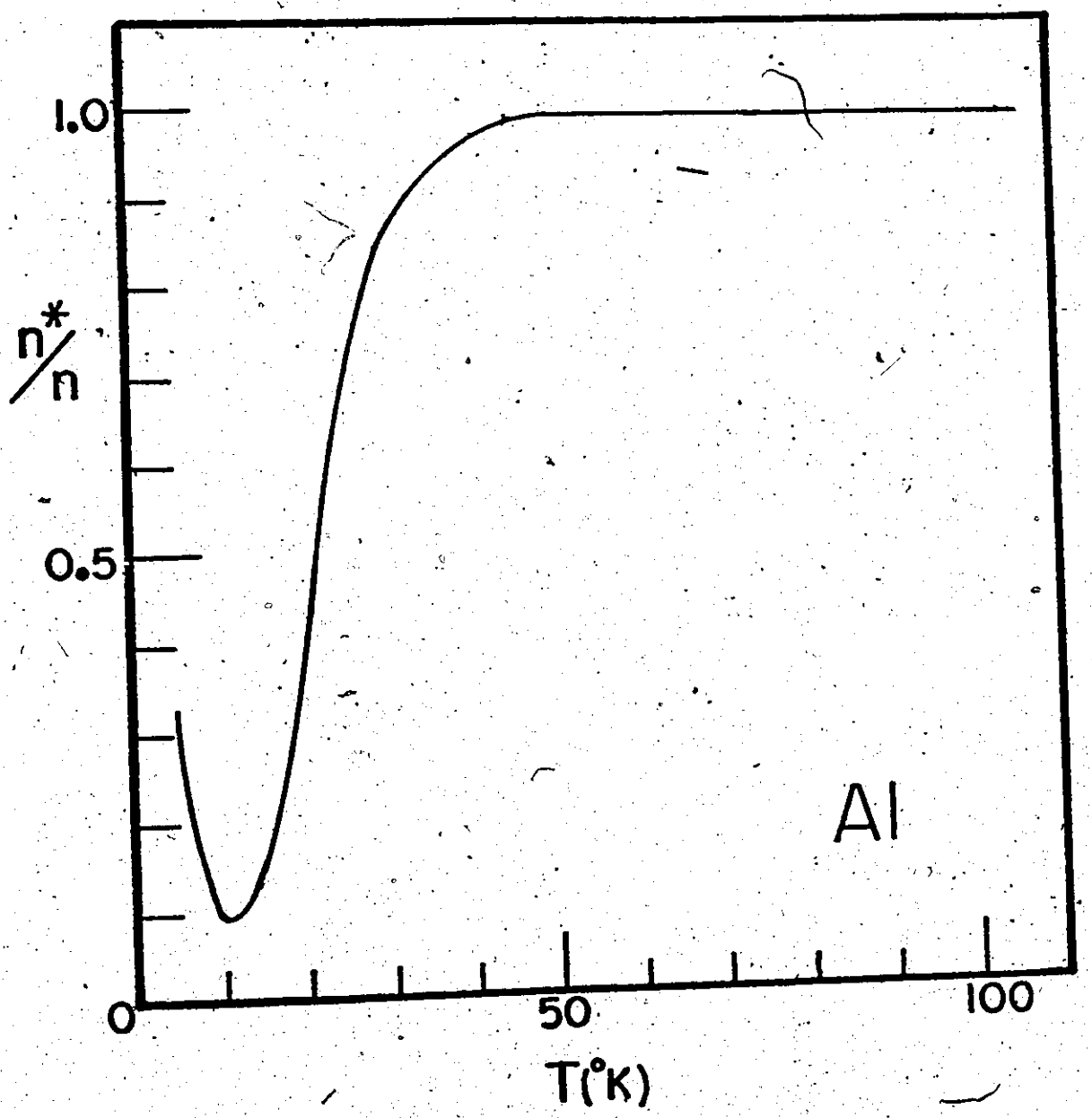
1.0
0.5
0
n*/n
50
100
T(°K)
Al

metals. For those points which lie on or near points of intersection of the FS and Bragg planes, although Umklapps can now contribute down to the very lowest frequencies, a proper treatment of the scattering ensures that these contributions will vanish as q_{red}, and consequently ω, approach zero. Thus one is assured that at the lowest temperatures, which implies the lowest frequency regions of the $\alpha^2_{tr}F_{\underline{k}}(\omega)$, the scattering is dominated by Normal processes or very weakly weighted Umklapps. Thus the anisotropy will disappear at low T. Since the above arguments are equally valid even on a distorted FS, one should expect to see essentially the same behaviour in all metals.

Finally in Figure (4.3.6), we show a plot of the variation of $\lambda_{\underline{k}}$, the electron-phonon mass enhancement parameter, over the FS. $\lambda_{\underline{k}}$ is given by (Leavens and Carbotte 1972; Carbotte, Dynes, and Trofimenkoff 1969)

$$\lambda_{\underline{k}} = 2\int_0^\infty d\omega \frac{\alpha^2 F(\omega)}{\omega} \qquad (4.3.3)$$

The electron-phonon contribution to the electron effective mass m* is related to $\lambda_{\underline{k}}$ through

$$m^*/m = 1 + \langle \lambda_{\underline{k}} \rangle_{F.S.} \qquad (4.3.4)$$

For comparison, we also show the results of a one OPW calculation, using the HA potential, performed by Leavens (1970). The dotted line indicates the regions of the FS for which the divergence in $g_{\underline{k}\underline{k}'}\lambda$ becomes crucial. This is where the free electron FS intersects zone boundaries. In these regions Leavens employs a renormalization technique which consists of arbitrarily changing the functional dependence of the $\alpha^2_{\underline{k}}F(\omega)$ function for low ω so that $\alpha^2_{\underline{k}}(\omega)$ no longer diverges. Of course for the

Fig. 4.3.6 The variation of $\lambda_{\underline{k}}$, the electron-phonon mass enhancement parameter, over the $1/48^{th}$ of the FS in Al. ----- the unrenormalized calculations of Leavens (1970). The notation for the different Φ directions is the same as in Fig. 4.3.3.

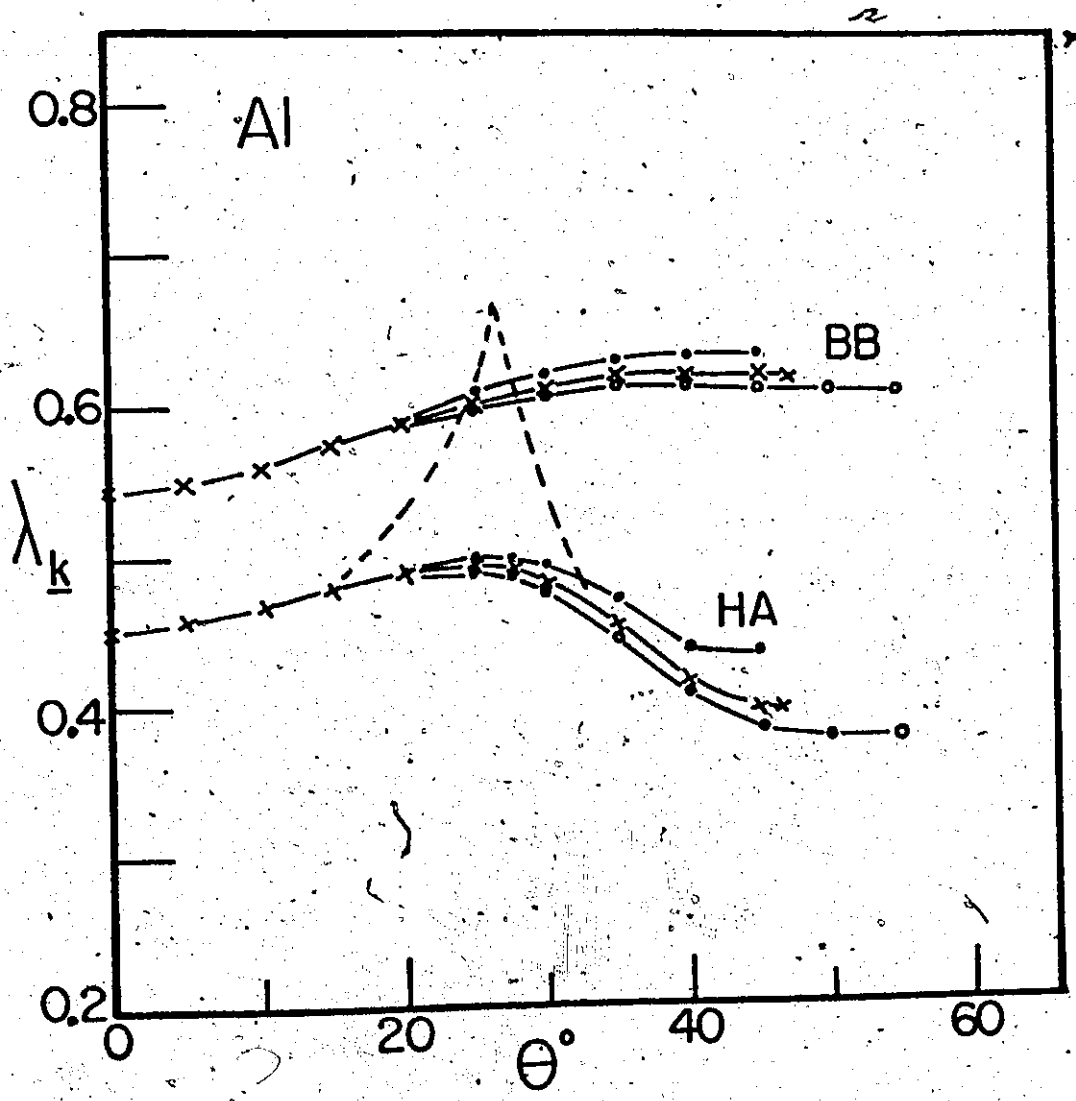
Al
BB
HA
0.8
0.6
0.4
0.2
λ_k
0
20
40
60
θ°

BB potential we have employed, this problem does not occur.

One notes that the BB potential gives somewhat less anisotropy and higher values of $\lambda_{\underline{k}}$, than the HA potential. The larger values for $\lambda_{\underline{k}}$ occur because for most $\underline{q}$ the BB potential form factors are larger than the HA form factors.

Having presented some of the results obtained with the BB potential in Al, we would like to conclude this section by noting that this potential offers an interesting and very economic way of dealing with the divergence in the one OPW matrix elements for a FS that intersects zone boundaries and, in addition, illustrates that when a reasonably correct approach to anisotropy is employed in polyvalent metals, essentially the same behaviour as monovalent metals is obtained. However, it suffers from some fairly serious defects. Since it is essentially a Bardeen pseudo-potential, it has the same shortcomings as the original. The major weakness (Sham and Ziman 1963) is the assumption that the field of the ion can be represented by a sharp-edged square-well effective potential, and a sharply defined volume of charge (the atomic polyhedron) for the valence electrons. Also, the behaviour of the form factors around $2k_f$ is rigidly determined by the function $G'(q)$ and the parameter U_o is relatively ineffective in altering the shape of the pseudo-potential. It is somewhat of a happy coincidence that in Al, the BB potential turns out to be quite similar in shape to the HA potential, which is based on somewhat firmer physical grounds. However, in other metals, it is not clear that the BB potential would not be radically different from other empirical potentials. Another major criticism that can be made is that, in a rather fundamental sense, it is not really a pseudo-potential at all.

Elementary pseudo-potential theory tells us that, in the nearly free electron approximation, the energy gaps in the conduction band at the appropriate reciprocal lattice points $\underline{G}$, are equal to $2|V(\underline{G})|$, where $V(\underline{G})$ is the pseudo-potential form factor for $\underline{q} = \underline{G}$. By the very nature of the BB potential these gaps would all be zero! However, one could counter with the argument that in setting $V(\underline{G}) = 0$, the BB potential is attempting to simulate the effects of a multiple OPW calculation where the entire matrix element for scattering from $|k\rangle$ to $|k+G\rangle$ should go to zero, and, as such, is attempting to incorporate very complicated effects in an exceedingly simple way. It is perhaps not unreasonable that some contradictions develop.

The objective in this Chapter has been to investigate the BB potential as an interesting device designed to overcome the difficulties encountered in the one OPW approximation in a very economical way. It has also hopefully demonstrated that the consequences of anisotropy in a polyvalent metal are essentially the same as those encountered in the alkali metals — one expects to see the anisotropy vanish at high and low temperatures and reach a maximum in some intermediate temperature region. In regard to the electrical resistivity, we have also shown that a conventional one OPW calculation leads to serious discrepancies at low temperature which can be resolved by treating the divergence of the one OPW matrix elements. There is no doubt, however, that a completely reliable and detailed multiple OPW calculation is necessary to discuss all the details of the above effects. We do feel, however, that in a qualitative sense, the above calculation demonstrates the essential features of the problem.

CHAPTER V

CONCLUSIONS

The main effort in this thesis has been to investigate some aspects of the transport properties of simple metals, in particular, the alkalis. The investigation has been carried out in two major areas: (a) Working within the framework of the conventional first order variational solutions to the Boltzmann transport equations and in the approximation of a spherical FS, we have attempted to provide a consistent description of the following properties:

(i) The ideal electrical resistivity.

(ii) The pressure dependence of the ideal electrical resistivity.

(iii) The ideal thermal resistivity.

(iv) The room temperature electron diffusion thermopower (magnitude and volume derivative).

(v) The low temperature phonon drag contribution to the thermopower.

The conventional theoretical expressions have been reformulated in terms of relevant "transport frequency distributions". This results in a considerable saving of computational time and also allows for a somewhat clearer picture of the role of Normal and Umklapp processes. The information on the phonons has been taken from Born-von Kármán force constant fits to experimentally determined dispersion curves and the electron-ion scattering has been treated using pseudo-potential theory.

The main conclusions that can be drawn for this section are as follows.

It is possible to provide a quantitatively accurate description of the pressure dependence of the electrical resistivity of the metals considered while remaining within the approximations mentioned. In particular, it is not necessary to resort to a distorted FS in order to explain the experimental data. We have succeeded in describing the anomalous behaviour of Li (relative to the other alkalis Na, K, and Rb) in terms of a simple pseudo-potential and a spherical FS. A particular improvement on previous work in this field is the fact that our calculations extend over a wide temperature range as opposed to a single temperature (usually room temperature or 0°C). The only adjustable parameter that occurs in our calculations is a "core radius" which occurs in the pseudo-potential. This was fixed once and for all by fitting a given experimental resistivity, and all other calculations were carried out with no further adjustments. It was encouraging to note that the pseudo-potentials so obtained were in close agreement with the AW pseudo-potentials (Appapillai and Williams 1973), which are generally considered to be the best potentials (calculated essentially from first principles) available to-day. If more complex forms of screening were used, we feel that our fitted potentials would agree even more closely with the AW potential. We feel that this lends considerable support to the idea of using pseudo-potentials which are obtained by a fit to the resistivity, at least in the metals considered here. Because of our fitting procedure, it would be somewhat facetious to claim good agreement in the case of the constant (zero temperature)

volume electrical resistivity. However, our main effort was directed towards accounting for the differences between the constant (atmospheric) pressure and constant volume resistivities and in this we have been quite successful.

For the ideal thermal resistivity the agreement with experiment while quite reasonable was not as good as for the electrical resistivity and our feeling is that this is mainly due to the well known inadequacy of the first order variational solution of the Boltzmann equation in this case.

We approached the calculation of the thermopowers with some concern as these properties are known to be very sensitive to the details of the electron-ion interaction. We were very gratified to find that with no further adjustments, we were able to reproduce the essential features of the experimental results. In the section which deals with the thermopowers we have clearly demonstrated the sensitivity of the calculations to the form of pseudo-potential used. It was, therefore, particularly encouraging, especially in the case of the phonon drag contribution to the low temperature thermopower where Na and K are observed to have a similar behaviour while Rb and Li are distinctly different and also differ from one another, to obtain good qualitative agreement with experiment. The only significant failure in regard to the thermopowers was the inability to completely account for the volume coefficient of the electron diffusion component. We were able to predict the correct sign for this coefficient in two of the four alkalis. We have indicated this could in part be due to the use of a very elementary form of screening and that if more sophisticated

dielectric functions are used, this problem could perhaps be overcome. We have, however, been able to reproduce the correct sign and reasonably correct magnitudes for the electron diffusion component itself. Here again, Li is anomalous in comparison with the other alkalis and we were able to account for this.

We consider it significant that a wide range of fairly sensitive properties have been accounted for using the same pseudo-potentials and also retaining the simplicity and economy of a spherical FS.

(b) Our second major effort was to carry out detailed calculations of the effects of anisotropy on the electrical resistivity and related properties such as the Hall constant. To do this, a scattering time solution to the Boltzmann equation was utilized and cast in a form which uses a directionally dependent "transport frequency distribution" $\alpha^2_{tr} F_{\underline{k}}(\omega)$. Once again this allows temperature effects to be looked at much more economically than if one had retained the traditional formulation. Also, the role of Normal and Umklapp processes is presented in a more physically transparent way. The major results and conclusions obtained in this section are as follows.

The anisotropy in the scattering times is very definitely temperature dependent and displays the same general features in each metal. It is least at high and very low temperatures and passes through a maximum at some intermediate temperature. The degree of anisotropy is directly related to the strength of the Umklapp scattering processes and is thus a sensitive function of the size of the pseudo-potential form factors for momentum transfers with $q \sim 2k_f$. The anisotropy is

determined in most part by zone geometry and the role of Umklapp processes and to a much lesser extent by the inherent anisotropy of the phonon spectrum. The anisotropy is most severe in Li, somewhat less in Rb, and considerably less in Na and K. However, we emphasize that this conclusion depends on what pseudo-potential is employed in the particular metal.

One of the more significant results of this thesis was our ability to use these anisotropic scattering times to carry out what we believe to be the first theoretical calculation which clearly demonstrates the variation of the low field Hall coefficient with temperature. The ratio n*/n (where n* is the effective number of carriers per unit volume and n is the free electron carrier density) falls with decreasing temperature, passes through a well-defined minimum and rises again. This is precisely the behaviour observed experimentally. We should note here, however, that the position of the experimental minimum is at somewhat higher temperatures than what we observe theoretically. We demonstrate that our theoretical minimum is due to the onset of Umklapp processes and feel that the lack of better agreement with experiment in this regard is due to the non-applicability of the low field approximations to the experimental conditions in the low temperature range.

It is important here to emphasize that our conclusions are based on calculations in the ideally pure metal and, as the recent calculations of Kus and Carbotte (1973) show, the smallest amounts of impurities severely reduce the anisotropy. This effect, combined with the fact that obtaining true low field experimental conditions ($\omega_c\tau \ll 1$) at very low temperatures with present technology is extremely difficult if not

almost impossible (Hurd 1972), would indicate that the minimum we predict is at present of theoretical interest only. However, we feel that any further theoretical efforts in this direction (perhaps an effort to solve the transport problem more accurately in the intermediate field regime; $\omega_c\tau \sim 1$) should take into account the peculiar role of Umklapp processes in this temperature range.

We have also looked at the effect of anisotropy in the scattering times on calculations of the electrical resistivity. To do this, we compare resistivities obtained in the "scattering time" and "first order variational" solutions to the Boltzmann equation. The differences in the two solutions arise from the different averaging of the scattering times in the two cases. The "scattering time" resistivity ρ_{ST} is proportional to $\frac{1}{\langle\tau_k\rangle_{FS}}$, whereas the "first order variational" resistivity ρ_V is proportional to $\left\langle\frac{1}{\tau_k}\right\rangle_{FS}$. In all cases and at all temperatures $\rho_{ST} < \rho_V$. The major conclusions in this area are the following:

(i) in Na, K, and Rb, anisotropy is unimportant at high temperatures ($T > 30°K$); however,

(ii) any calculations at low temperatures in these metals should include the effects of anisotropy and,

(iii) in the case of Li, anisotropy is important over the entire temperature range and ignoring it can lead to significant discrepancies.

We have also considered the effect of the pseudo-potential in determining the differences between ρ_{ST} and ρ_V and, as one would expect, the extent to which ρ_{ST} is less than ρ_V is related to the amount of Umklapp

scattering introduced by the pseudo-potential. An interesting observation here was that the differences between the ρ_{ST} obtained using the different potentials were much less than the differences in the ρ_V.

We would like to again emphasize that the above conclusions apply in detail to the ideally pure metals only. However, one could also point out at this stage that the calculations of Kus and Carbotte on deviations from Mathieson's Rule were not only made possible but were also rather physically transparent because of the neatness of the scattering time solution to the Boltzmann equation and its reformulation in terms of the functions $\alpha^2_{tr} F_{\underline{k}}(\omega)$. In fact the functional form of the deviations are in large part determined by the behaviour of the anisotropy in the pure metals.

Chapter V of this thesis was concerned with a simple device to eliminate the divergence of the one OPW matrix elements which occur in a system where the FS intersects zone boundaries. We have demonstrated the failure and its rectification in the case of Al and after carrying out similar calculations as were performed in the alkalis, have reached the following conclusions:

(a) The effects of anisotropy in a polyvalent metal are essentially the same as in the alkalis. We present simple arguments to indicate that the same behaviours would be present even if detailed calculations including distorted Fermi surfaces were undertaken, and,

(b) the breakdown of the one OPW approximation causes severe discrepancies at low temperatures and any efforts to reproduce the low temperature behaviour of the ideal electrical resistivity must include a scheme to deal with this problem.

REFERENCES

Alderson, J.E. and Farrell, T. (1969), Phys. Rev. 185, 876.

Animalu, A.O.E. (1965), Phil. Mag. 11, 379.

Appapillai, M. and Williams, Anthony R. (1973), J. Phys. F: Metal Phys., Vol. 3, 759.

Ashcroft, N.W. and Guild, L.J. (1965), Phys. Lett. 14, 23.

Ashcroft, N.W. and Lekner, J. (1966), Phys. Rev. 145, 83.

Ashcroft, N.W. (1966), Phys. Lett. 23, 48.

Ashcroft, N.W. and Langreth, D.C. (1967), Phys. Rev. 159, 500.

Bailyn, M. (1960), Phys. Rev. 120, 381.

Bardeen, J. (1937), Phys. Rev. 52, 688.

Baym, G. (1964), Phys. Rev. 135, A1691.

Bloch, F. (1928), Z. Physik. 52, 555.

Bross, H. and Holz, A. (1963), Phys. Stat. Sol. 3, 1141.

Bross, H. and Bohn, G. (1967), Phys. Stat. Sol. 20, 277.

Carbotte, J.P. and Dynes, R.C. (1968), Phys. Rev. 172, 476.

Carbotte, J.P., Dynes, R.C. and Trofimenkoff, P.N. (1969), Can. J. Phys. 47, 1107.

Cohen, M.L. and Heine, V. (1970), Solid State Physics: Advances in Research and Applications, Vol. 24 (Academic Press, Inc., New York).

Collins, J.G. and Ziman, J.M. (1961), Proc. Roy. Soc. A, 264, 60.

Copley, J.R.D. (1970), Ph.D. Thesis, McMaster University, Hamilton, Ontario, Canada.

Cowley, R.A., Woods, A.D.B. and Dolling, G. (1966), Phys. Rev. 150, 489.

Deutsch, T., Paul, W. and Brooks, H. (1961), Phys. Rev. 124, 753.

Dickey, J.M., Meyer, A. and Young, W.H. (1967), Proc. Phys. Soc. 92, 460.

Dugdale, J.S. and Gugan, D. (1960), Proc. Roy. Soc. A, 254, 184.

Dugdale, J.S. (1961), Science, N.Y. 134, 77.

Dugdale, J.S. and Gugan, D. (1962), Proc. Roy. Soc. A, 270, 186.

Dugdale, J.S. and Phillips, D. (1965), Proc. Roy. Soc. A, 287, 381.

Dynes, R.C. and Carbotte, J.P. (1963), Phys. Rev. 137, A913.

Dynes, R.C. (1968), Ph.D. Thesis, McMaster University, Hamilton, Ontario, Canada.

Ekin, J.W. and Bringer, A. (1973), Phys. Rev. B, 7, 4468.

Gilat, G. and Nicklow, R.M. (1966), Phys. Rev. 143, 487.

Gilat, G. and Raubenheimer, L.J. (1966), Phys. Rev. 144, 390.

Greene, N.P. and Kohn, W. (1965), Phys. Rev. 137, A513.

Gugan, D. (1971), Proc. Roy. Soc. A325, 223.

Hayman, B. and Carbotte, J.P. (1971a), Can. J. Phys. 49, 1952.

Hayman, B. and Carbotte, J.P. (1971b), J. Phys. F: Metal Phys. 1, 828.

Hayman, B. and Carbotte, J.P. (1972a), Phys. Rev. B, 6, 1154.

Hayman, B. and Carbotte, J.P. (1972b), J. Phys. F: Metal Phys. 2, 915.

Harrison, W.A. (1966), Pseudopotentials in the Theory of Metals (W.A. Benjamin Inc., New York).

Hasegawa, A. (1964), J. Phys. Soc. Japan, 19, 504.

Heine, V. and Abarenkov, I. (1964), Phil. Mag. 9, 451.

Heine, V. (1970), Solid State Phys. 24, 1.

Hurd, C.M. (1972), The Hall Effect in Metals and Alloys (Plenum Press, New York - London).

Kaveh, M. and Wiser, N. (1972a), Phys. Rev. Lett. 29, 1374.

Kaveh, M. and Wiser, N. (1972b), Phys. Rev. B, 6, 3648.

Kittel, C. (1966), Introduction to Solid State Physics (John Wiley and Sons, Inc., New York).

Kohler, M. (1949), Z. Physik. 125, 679.

Kus, F. and Carbotte, J.P. (1973), J. Phys. F.: Metal Phys. 3, No. 10, 1828.

Leavens, C.R. (1970), Ph.D. Thesis, McMaster University, Hamilton, Ontario, Canada.

Leavens, C.R. and Carbotte, J.P. (1972), Annals of Physics 70(2), 338.

Lee, M.J.G. and Falicov, L.M. (1968), Proc. Roy. Soc (London) A304, 319.

MacDonald, D.K.C., White, G.K. and Woods, S.B. (1956), Proc. Roy. Soc. A, 235, 358.

MacDonald, D.K.C., Pearson, W.B. and Templeton, I.M. (1958), Proc. Roy. Soc. A, 248, 107.

Martin, D.L. (1965), Phys. Rev. 139, A150.

Mott, N.F. and Jones, H. (1936), The Theory of the Properties of Metals and Alloys (Oxford University Press).

Price, D.L., Singwi, K.S. and Tosi, M.P. (1970), Phys. Rev. B, 2(8), 2983.

Robinson, J.E. and Dow, J.D. (1963), Phys. Rev. 171, 815.

Segall, B. (1961), Phys. Rev. 124, 1797.

Seth, R.S. and Woods, S.B. (1970), Phys. Rev. B, 2, 2961.

Sham, L.J. and Ziman, J.M. (1963), Solid State Phys. 15, 221.

Shaw, R.W., Jr. and Pynn, R. (1969), J. Phys. C: Solid State Phys. 2, 2071.

Smith, H.G. et. al. (1968), Neutron Inelastic Scattering, Proceedings of a Symposium, Copenhagen, Vol. 1, (Vienna IAWA), p. 149.

Sondheimer, E.H. (1950), Proc. Roy. Soc. (London) 75, A203.

Sundström, L.J. (1965), Phil. Mag. 11, 657.

Trofimenkoff, P.N. and Carbotte, J.P. (1970), Phys. Rev. B, 1, 1136.

Truant, P.T. (1972), Ph.D. Thesis, McMaster University, Hamilton, Ontario, Canada.

Tsuji, M. (1958), J. Phys. Soc. Japan, 13, 979.

Van Hove, L. (1954), Phys. Rev. 95, 249.

Woods, A.D.B., Brockhouse, B.N., March, R.H., Stewart, A.T. and Bowers, R. (1962), Phys. Rev. 128, 1112.

Ziman, J.M. (1960), Electrons and Phonons (Oxford: Clarendon Press).

Ziman, J.M. (1961), Phil. Mag. 6, 1013.

Ziman, J.M. (1964a), Advan. Phys. 13, 89.

Ziman, J.M. (1964b), Principles of the Theory of Solids (Cambridge University Press).